

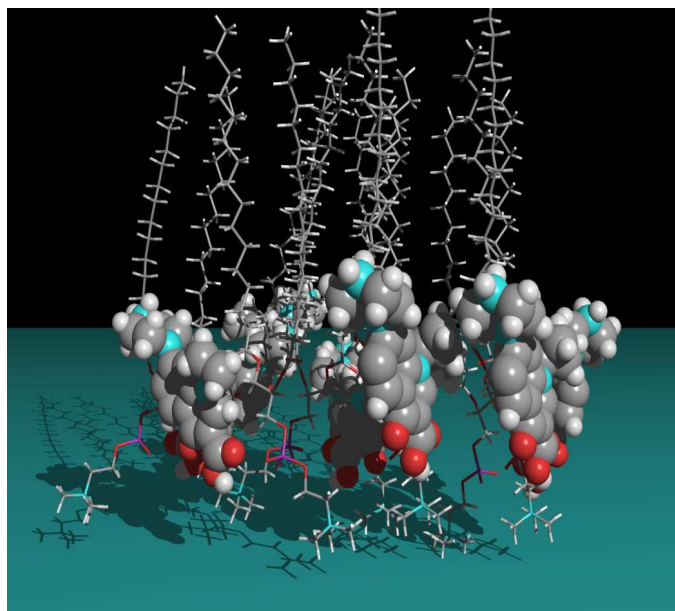
UCL

Université Catholique de Louvain

Louvain Drug Research Institute
Cellular and Molecular Pharmacology



**INTERACTIONS BETWEEN FLUOROQUINOLONES AND LIPIDS:
BIOPHYSICAL STUDIES**



HAYET BENSIKADDOUR

Dissertation for the acquisition of a Doctoral Degree in
Biomedical and Pharmaceutical Sciences

Orientation: Pharmaceutical Sciences

Promoter. Prof. Marie-Paule Mingeot-Leclercq

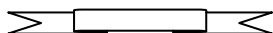
May 2011

À la lumière de ma vie

Mon Cher Papa

Remerciements

Avant tout, je tiens à remercier mon Cher Papa Mr Omar Bensikaddour pour les sacrifices interminables qu'il m'a faits, depuis mon enfance afin de m'assurer une excellente éducation. L'homme qui a illuminé mon chemin, et qui a suivi de près chaque instant passé dans la réalisation de cette thèse jusqu'à la phase de la rédaction. Grâce à son amour, son courage et sa force qui circulent dans mes veines, j'ai pu achever la rédaction de ce manuscrit. Papa, je te serai éternellement redevable pour tout. Repose en Paix et que Dieu le Tout Puissant t'accueille dans son vaste Paradis...Amin...



Ce travail de thèse a été réalisé au laboratoire de Pharmacologie Cellulaire et Moléculaire, dirigé par le Prof. M-P Mingeot-Leclercq à la Faculté de Pharmacie et Sciences Biomédicales de l'Université catholique de Louvain (UCL) que je remercie de m'avoir accueillie dans son unité, de m'avoir accordé sa confiance et de m'avoir suivie pendant ces quatre années de recherches.

Je voudrai remercier particulièrement le Professeur P-M. Tulkens, sans qui une grande partie de ce manuscrit n'aurait probablement jamais pu avoir sa forme finale. Merci pour son aide précieuse, son pragmatisme et son dynamisme ont notamment marqué mon esprit.

Mes remerciements vont aux membres de mon comité d'encadrement, les Professeurs B. Gallez, V. Préat, L. Lins, P. Courtoy et qui m'ont fait l'honneur d'évaluer ce travail de thèse. Je les remercie également pour leurs remarques et commentaires qui ont contribué à l'amélioration de ce manuscrit.

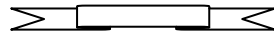
J'exprime mes sincères reconnaissances au Prof. Erik Goormaghtigh de m'avoir accueillie dans son unité « Structure et Fonctions des membranes biologiques» pendant plus qu'un an, de m'avoir guidée dans mes premiers pas en spectroscopie de l'infrarouge et de m'avoir transmis l'art d'interprétation des spectres. Mes remerciements s'adressent aussi au Prof. Fabrice Homble.

I would like to acknowledge Professor Jordi Hernandez-Borell, chairman of Bioelectrochemistry and Nanobiotechnology Group, faculty of pharmacy (university of Barcelona, Spain), for kindly providing me a scientific document (Muchas gracias!), and to accept our invitation to judge this thesis work.

Je suis reconnaissante à tous les Professeurs qui ont contribué à ma formation doctorale et à l'avancement de mon sujet de recherche. Je cite Professeur Karim Snoussi pour son apport scientifique et ses invitations sympathiques à une tasse de café !, et Professeur Fred Opperdoes pour sa disponibilité et sa bonne humeur auprès de tous les étudiants ! Sans oublier Professeur Marianne Fillet pour sa collaboration dans ce travail de recherche.

Finally, my thanks would not be complete without mentioning all the members of the FACM unit, the old and the new, as well as my colleagues Aliou Emmanuel and Mohamed.

Thank you Françoise for the bibliographic help you brought me, to Olga for your morning smile, to Marie-Claire for not only the cells but all these moments spent together, to Oscar for your advice, to Els for our discussions, always scientific, to Sébastien for your moral support... and to everyone who encouraged me during the writing of this thesis.



The objective of a thematic in scientific research cannot be achieved, especially in the presence of people who surround us. They have contributed largely to the accomplishment of this work by their support, their encouragement and their patience, especially in the most vulnerable moments and the most critical periods of my life. I think of my family, my parents, my brothers and my little nephews and nieces... and to all the people who are dear to my heart.

To you all, I say THANK YOU !

Ota ou Huita !

« Cherchez le savoir, du berceau jusqu'au tombeau »

Le prophète Mohamed (SAW) (Hadith Nabawi)

Abstract

Probing fluoroquinolones/lipid interactions at the molecular level represents an important challenge in both membrane biophysics and pharmaceutical research. As the pharmacological target of these antibiotics is intracellular, they must pass across the bacterial membranes. Likewise, fluoroquinolones enter eukaryotic cells, which imply their ability of interacting with lipids membranes. In this context, the aim of my Thesis has been to characterize the effect of two closely related fluoroquinolones, ciprofloxacin and moxifloxacin, on physicochemical properties of the major phospholipids DPPG and DOPC/DPPC that are mimicking the prokaryotic and eukaryotic lipid membranes, respectively, by means of biophysical methods.

First, I have studied the effect of these drugs on domains lipids erosion, lipids packing and their ability of modifying the conformation and orientation of the acyl chain(s) of phospholipids.

Second, I have determined the binding affinities of ciprofloxacin to different model lipid membranes (DPPG, DPPC) and its effects on head group mobility and on thermotropic profile of these two phospholipids.

The data reported in this Thesis point to different effects of ciprofloxacin and moxifloxacin on the phospholipids tested. Indeed, moxifloxacin induces more changes in the acyl chain conformation of phospholipids and has more lipid packing effects than ciprofloxacin. The latter interacts primarily with the head groups of lipids, and thereby modifies the orientation of the acyl chain. Thus, the first step in the interaction of ciprofloxacin with lipid membranes relates to its binding to these headgroups, which is stronger with negatively charged (DPPG) than with zwitterionic phospholipids (DPPC). Conversely, our results suggest that moxifloxacin is located in a more hydrophobic environment of the membranes, probably by creating a pocket in the interior of the lipid bilayer. These contrasting behaviors may be related to the fact that ciprofloxacin is, globally speaking, a more hydrophilic drug than moxifloxacin.

Our work may help in shedding more light on the role played by lipids in the transport of fluoroquinolones in both prokaryotic and eukaryotic cells.

Overview of the Thesis

This thesis is devoted to the characterization at the molecular level of the interactions of fluoroquinolone antibiotics with lipid model membranes using biophysical tools. Two molecules have been selected: ciprofloxacin (CIP) and moxifloxacin (MXF), that show distinct physicochemical properties but share a common general mechanism of antibacterial action.

Our thesis is divided into three main parts: Introduction, Results, General Discussion and Perspectives.

- The Introduction starts with a general overview of the pharmacology of fluoroquinolones. Next, we describe the models of lipid membranes and the biophysical methods (*Atomic force microscopy, Langmuir-Blodgett technique, as well as fluorescence, infra-red, nuclear magnetic resonance spectroscopies*) used to investigate changes in the biophysical properties of the membranes while interacting with fluoroquinolones.

The Aims of the thesis are given at the end of the Introduction.

- The Results section comprises two scientific articles. The first one, published in *Biophysical Journal*, reports the differential effects observed with CIP and MXF on the conformation, orientation and lipid packing of zwitterionic lipids found in eukaryotic membranes.

The second article, published in *Biochimica Biophysica Acta: Biomembranes*, analyzes into more details the binding parameters and effects of CIP on the thermotropic behavior of eukaryotic and prokaryotic lipid model membranes.

- A General Discussion, based on the data of these two articles is presented after the results section.

Finally, we present the perspectives of our work.

The references to all articles mentioned in the Thesis are listed at the end, but the two published papers shown in the Results section have their own reference lists.



INDEX



INDEX	1
ABBREVIATION LIST	5
INTRODUCTION	9
I. Fluoroquinolones	11
I.1. Pharmacology of fluoroquinolone antibiotics	11
I.1.1. <i>Definition</i>	11
I.1.2. <i>Chemical structure and fluoroquinolones generations</i>	11
I.1.3. <i>Mode of action of fluoroquinolones and their targets</i>	14
I.1.4. <i>Pharmacokinetic and pharmacodynamic parameters</i>	15
I.1.5. <i>Mechanism of fluoroquinolones resistance</i>	17
I.2. Pharmacology of selected fluoroquinolones (Ciprofloxacin and Moxifloxacin)	20
I.2.1. <i>Chemical structures</i>	20
I.2.2. <i>Mode of action and indications</i>	21
I.2.3. <i>Pharmacokinetic and pharmacodynamic parameters</i>	22
I.2.4. <i>Resistance</i>	22
II. Cell and Models membrane	24
II. 1. Cell membranes	24
II. 2. Classification and chemistry of lipids: Membrane composition (Eukaryotic and prokaryotic cells)	27
II. 2. .1 <i>Glycerophospholipids</i>	27
II. 2. 2. <i>Sphingolipids</i>	31
II. 2. 3. <i>Sterols</i>	32
II. 3. Models of lipid membranes	33
II. 3.1. <i>Monolayer</i>	34
II. 3.2. <i>Supported Bilayer (SB)</i>	34
II. 3.3. <i>Liposomes: from MLV to GUV</i>	34
III. Biophysical methods for studying fluoroquinolones-lipids interactions	37
III. 1. Atomic Force Microscopy (AFM)	37
III.1.1. <i>Introduction</i>	37
III.1.2. <i>Physical principles</i>	37
III.1.3. <i>The operating modes in AFM</i>	38
III.1.4. <i>Applications of AFM to study lipid membranes and drug-lipid interactions</i>	40
III.1.5. <i>Advantages and limitations</i>	41
III. 2. Langmuir-Blodgett technology (LB)	42
III.2.1. <i>Introduction</i>	42
III.2.2. <i>Langmuir monolayer formation</i>	42
III.2.3. <i>Langmuir monolayer characterization</i>	43
III.2.4. <i>Application of LB for characterization of lipid membranes interacting with drugs</i>	44
III.2.5. <i>Advantages and limitations</i>	45

III. 3. Spectroscopic methods	46
III.3.1. UV/Vis spectroscopy	47
III.3.1.1. <i>Introduction</i>	47
III.3.1.2. <i>Physical and chemical principles</i>	47
III.3.1.3. <i>Application of UV/Vis spectroscopy in fluoroquinolones-lipids interactions</i>	50
III.3.1.4. <i>Advantages and limitations</i>	58
III. 3. 2. Fourier Transform Infrared Spectroscopy (FTIR)	59
III. 3. 2. 1. <i>Introduction</i>	59
III. 3. 2. 2. <i>Physical and chemical principles</i>	59
III. 3. 2. 3. <i>Fourier Transform spectrometer</i>	61
III. 3. 2. 4. <i>Attenuated Total Reflection (ATR)</i>	61
III. 3. 2. 5. <i>Properties of ATR-FTIR spectra</i>	62
III. 3. 2. 6. <i>Applications of ATR-FTIR spectroscopy to drug-lipids interactions</i>	65
III. 3. 2. 7. <i>Advantages and limitations</i>	66
III. 3. 3. Nuclear Magnetic Resonant spectroscopy (NMR)	68
III. 3. 3. 1. <i>Introduction</i>	68
III. 3. 3. 2. <i>Physical and chemical principles</i>	68
III. 3. 3. 3. <i>The NMR spectrometer</i>	71
III. 3. 3. 4. <i>Properties of NMR spectra</i>	73
III.3.3. 5. <i>Applications of NMR spectroscopy to study lipid state behavior and to characterize fluoroquinolones-lipids interactions</i>	75
III. 3. 3. 6. <i>Advantages and limitations</i>	78
AIM OF THE THESIS	81
RESULTS	85
Chapter 1: Investigation of interaction of fluoroquinolones (CIP vs MXF) with model membranes at molecular level	87
Chapter 2: Characterization of the interactions between fluoroquinolones (CIP with eukaryotic and prokaryotic model lipids membrane (DPPC vs DPPG)	103
GENERAL DISCUSSION	117
PERSPECTIVES	127
REFERENCES	131



ABBREVIATION LIST



ABC	ATP-Binding Cassette
AFM	Atomic Force Microscopy
ANS	8-Anilin-1-Naphtalene Sulfonic acid
ATP	Adenosine TriPhosphate
ATR	Attenuated Total Reflection
FTIR	Fourier Transform Infra Red
AUC	Area Under Curve
Cer	Ceramides
Chol	Cholesterol
CIP	Ciprofloxacin
CL	Cardiolipin
Cmax	Maximum Concentration
CSA	Chemical Shift Anisotropy
DMPC	Dimyristoylphosphatidylcholine
DMPG	Dimyristoylphosphatidylglycerol
DNA	Desoxyribonucleic acid
DOPC	Dioleoylphosphatidylcholine
DPH	Diphenylhexatriene
DPPC	Dipalmitoylphosphatidylcholine
DPPG	Dipalmitoylphosphatidylglycerol
FID	Free Induction Decay
FQs	Fluoroquinolones
GluCer	Glucosylceramides
GPL	Glycerophospholipids
GUV	Giant Unilamellar Vesicle
IRE	Internal Reflection Element
LB	Langmuir-Blodgett
LUV	Large Unilamellar Vesicle
MDR	Multidrug resistance
MFP	Member of the facilitator super family protein
MIC	Minimum Inhibition Concentration
MLV	Multilamellar Vesicle
MRP	Multidrug Resistance Protein
MXF	Moxifloxacin
NMR	Nuclear Magnetic Resonance
NOE	Nuclear Overhauser Effect
PA	Phosphatidic acid
PB	Planer Bilayer
PC	Phosphatidylcholine
PD	Pharmacodynamics

PE	Phosphatidylethanolamine
PG	Phosphatidylglycerol
PI	Phosphatidylinositol
PK	Pharmacokinetics
PLs	Phospholipids
PS	Phosphatidylserine
RNA	Ribonucleic acid
RND	Restriction Nodulation Division
SM	Sphingomyelin
SPB	Supported Planar Bilayer
SUV	Small Unilamellar Vesicle
TMA-DPH	Trimethylammonium-diphenyl-hexatriene
Try	Tryptophan
UV-Vis	Ultraviolet-Visible



INTRODUCTION



I. Fluoroquinolones

I- 1- Pharmacology of fluoroquinolones antibiotics

I.1.1. Definition

Fluoroquinolones are the first wide spectrum antibiotic class of totally synthetic origin. Starting from nalidixic acid (Figure 1) that was introduced in the clinics in the early 1960's but was limited in its use due to its narrow spectrum (Gram-negative organisms only, and fast development of resistance), the medicinal chemists have developed more potent compounds by fluorination at the 6-position of the quinoline ring, giving rise to the class of fluoroquinolones.

I.1.2. Chemical structure and fluoroquinolone generations

Fluoroquinolones have been developed through side-chain modification from 1,8-naphthyridine molecules to more active compounds notably by substitution of the 7 position by a piperazine or other mono or bi-cyclic moieties, the fluorination of the 6 position, as well as other modifications at various sites (Figure 1). This led to improved potency, broadened spectrum and reduced side effects.

Based on their chemical structure and their spectrum of antibacterial activity, the fluoroquinolones have been classified into three generations. The first generation (I) agent, flumequine, displayed anti-pseudomonal activity as a result of the addition of a piperazine substituent at position 7 of the naphthyridine core. Due to its ocular toxicity, flumequine was quickly replaced by the second generation agents (IIa), such as ciprofloxacin, that are more active against most Gram-negative pathogens. Then, in the aim to improve the anti-Gram positive activity and mainly *Streptococcus pneumoniae* (to treat respiratory infections), new molecules were developed such as grepafloxacin and sparfloxacin (generation IIb). Despite their globally satisfactory results in treating the target infections, these molecules were quickly withdrawn because of a globally non-favorable risk/benefit ratio due mainly to major cardiac (dysrhythmia) and skin (rash and photosensitization) toxicities. This led to the development of the so-called third generation. The IIIa compounds, moxifloxacin and trovafloxacin, both have 7-azabicyclo modifications. These markedly enhance their activity against Gram-positive pathogens and add significant activity against anaerobe organisms. Trovafloxacin, however, was withdrawn because of rare but severe hepatotoxic reactions.

A more recent fluoroquinolone is gemifloxacin (generation IIIb), which has a marked activity against pneumococci making it useful against strains resistant to other fluoroquinolones. Gemifloxacin, however, is not approved for clinical use in Europe (mainly because of clastogenic effects observed *in vitro*) and sparingly used elsewhere because of frequent cutaneous reactions (rash).

The first representative fluoroquinolones of the fourth generation is garenoxacin. This molecule was developed by removing the fluorine at position 6 (thought to cause genotoxicity) but adding a difluoromethoxy substituent in position 8). Garenoxacin has been brought to clinical studies (Van Bambeke et al., 2005), and is currently marketed in Japan, but its future in Europe and in the USA remains so far undetermined (the applications for registration have been withdrawn in 2006 and 2007).

Many other fluoroquinolones have been clinically developed and the structures of the main ones are shown in Figure 1 (Ball, 2000;Ball, 2003;Van Bambeke et al., 2005). Yet, today, ciprofloxacin, levofloxacin and moxifloxacin account for most of the clinical use of fluoroquinolones in Europe and North America.

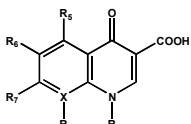
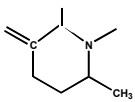
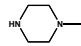
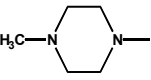
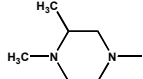

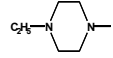

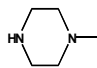
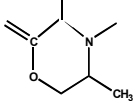
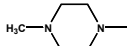
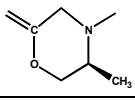
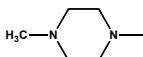

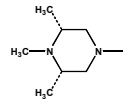

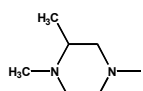

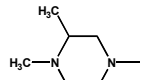
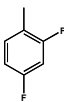
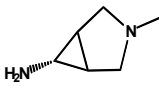

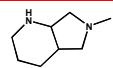

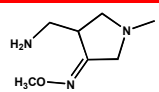

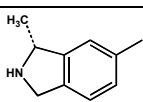
							
generation	drug	X	R ₈	R ₁	R ₅	R ₆	R ₇
I	nalidixic acid	N		-CH ₂ -CH ₃	H	H	-CH ₃
IIa	flumequine				H	F	H
	norfloxacin	C	H	-CH ₂ -CH ₃	H	F	
	pefloxacin	C	H	-CH ₂ -CH ₃	H	F	
	lomefloxacin	C	F	-CH ₂ -CH ₃	H	F	
	enrofloxacin	C	H		H	F	
	ciprofloxacin	C	H		H	F	
	ofloxacin				H	F	
	levofloxacin				H	F	
IIb	sparfloxacin	C	F		-NH ₂	F	
	grepafloxacin	C	H		-CH ₃	F	
IIIa	gatifloxacin	C	-O-CH ₃		H	F	
	trovafloxacin	N			H	F	
	moxifloxacin	C	-O-CH ₃		H	F	
IIIb	gemifloxacin	N			H	F	
IV	garenoxacin	C	-O-CHF ₂		H	H	

Figure 1. Pharmacophore and structures of the main quinolones
Ciprofloxacin and moxifloxacin are framed in red (Van Bambeke et al., 2005)

I.1.3. Mode of action of fluoroquinolones and their targets

Fluoroquinolone are very effective to treat infections caused by their target organisms. This is due to their intense bactericidal activity associated with a generally good bioavailability.

The bacterial targets of fluoroquinolones are the DNA gyrase and DNA topoisomerase IV (Figure 2). These two enzymes are required for condensation and segregation of DNA molecules before and after replication.

DNA gyrase is made of 4 subunits: two subunits A (*gyrA*, 97 kDa) and two subunits B (*gyrB*, 90kDa). *GyrA* plays a role in DNA-strand breakage, and *gyrB* mediates the ATPase activity of the enzyme. The DNA gyrase is involved in the introduction of negative supercoils needed for binding of initiation proteins to replication origins and in the relaxation of positive supercoils arising from DNA strand unwinding during replication. It also facilitates RNA polymerases movement, DNA repair and recombination (Reece and Maxwell, 1991).

Topoisomerase IV is also composed of 4 subunits: two subunits C (*ParC*, 75 kDa) and two subunits E (*ParE*, 70 kDa). *ParC* and *ParE* display about 40% homology with *gyrA* and *gyrB*, respectively. The role of topoisomerase IV is to relax negative and positive supercoils. Thus, topoisomerase IV contributes to the control of supercoiling by opposing the activity of gyrase and exhibits a potent decatenating activity (Kato et al., 1990; McNairn et al., 1995). Since gyrase and topoisomerase are conserved enzymes, fluoroquinolones exhibit activity against a broad spectrum of bacterial species.

Depending to their targets, bacteria can be classified into three groups. One group composed of mycobacterial species, have only gyrase as target. Most other bacteria contain both gyrase and topoisomerase IV. In Gram-positive bacteria (group 2), gyrases are less susceptible to impairment by fluoroquinolones than in Gram-negative bacteria (group 3). Topoisomerase IV seems to have the same susceptibility in both types of microorganisms (Jacoby, 2005). DNA gyrase is nevertheless considered as the primary target of fluoroquinolones, probably due to the larger cytotoxicity of the complexes they form with this enzyme compared to topoisomerase IV (Fournier et al., 2000; Khodursky and Cozzarelli, 1998).

The action of fluoroquinolones consists in the trapping of gyrase and topoisomerase IV on DNA by blocking religation of DNA around gyrase and reducing the ATPase activity of topoisomerase IV. Therefore, the drug breaks DNA replication leading to cell death (Hiasa and Shea, 2000).

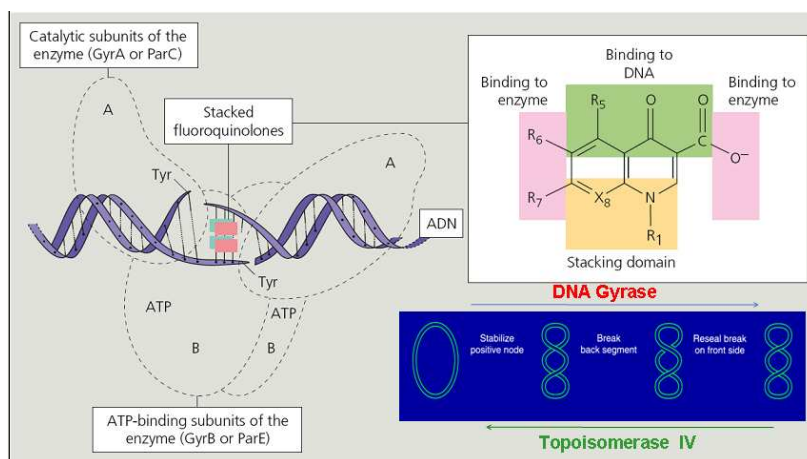


Figure 2. Ternary complex formed between DNA, DNA-gyrase or Topoisomerase IV and stacked fluoroquinolones. *Adapted from Shen (Shen et al., 1989)*

I.1.4. Pharmacokinetic and pharmacodynamic parameters

I.1.4.1. Pharmacokinetics of fluoroquinolones

Absorption Fluoroquinolones are well absorbed after oral administration. Indeed, bioavailability level exceeds 75% for most drugs. Studies *in vitro* (Caco-2 cells) and *in vivo* (rats) show that fluoroquinolones are mainly absorbed by passive diffusion (Rabbaa et al., 1997). However, the absorption of fluoroquinolones drugs by an active process could be also take place in certain regions of the gastrointestinal tract (Harder et al., 1990) The absorption of drugs is affected by:

- i) the dose administered. The maximum concentration of drug in serum (C_{max}) and Area Under the Curve (AUC) values are observed with a low dose (less than 500 mg for levofloxacin; (Chien et al., 1997a;Chien et al., 1997b) suggesting saturation of a transporter.
- ii) the composition of the food and other substances co-administrated with the fluoroquinolones. Food containing carbohydrate or high fat content can delay the absorption of fluoroquinolones, but do not modify their overall bioavailability (Allen et al., 2000;Rabbaa et al., 1997). In contrast, all fluoroquinolones form complexes with di-

and trivalent cations, such Mg^{2+} , Al^{3+} , and Ca^{2+} that are present in antacids and other pharmaceutical formulations. This drastically reduces their oral absorption (Ofoefule and Okonta, 1999).

Distribution Fluoroquinolones traverse cell membranes by passive and/or active process, and accumulate in tissues. This make them potentially suited to fight bacteria present not only in blood and in the interstitial spaces but also in the intracellular compartments.

However, drug distribution is not the same in all tissues. While accumulation of drug is larger in excretory organs (liver, kidney), or prostate (when active urinary infection is present), there is less accumulation in the cerebrospinal fluid or in the lung (even in patients with inflammation of the bronchial tree such as in bronchitis) (Fischman et al., 1996a;Fischman et al., 1996b;Fischman et al., 1998;Tamai et al., 2000).

The serum protein binding of fluoroquinolones is variable, being generally low for more hydrophilic compounds such as ciprofloxacin and fair to important for more lipophilic compounds, such as moxifloxacin or gemifloxacin (Wise et al., 1986).

Metabolism The major site for biotransformation of most fluoroquinolones is the piperazine ring at C-7. The rate and extent of biotransformation can be modulated by substitutions of this ring (Bryskier and Chantot, 1995).

Excretion Several fluoroquinolones are excreted as unchanged drug in the bile and urine (Chow et al., 2001;North et al., 1998). For liver excretion, this is due to their zwitterionic nature that makes them possible candidates for transport by both anion and cation transport systems (Okano et al., 1990). Depending to the drug, the half time of fluoroquinolones varies between 5 h (e.g. ciprofloxacin) to 12 h (e.g. moxifloxacin) (Lubasch et al., 2000).

1.1.4. 2. *Pharmacodynamics of fluoroquinolones*

Pharmacodynamics (PD) describes the relationship between measures of pharmacokinetics parameters (PK) (drug level in serum and tissue) and the antimicrobial and toxicological effects of drugs (Andes and Craig, 2002a). The potency of antibiotics *in vitro*, based on most commonly accepted standards for susceptibility testing, is assessed by the determination of the so-called "minimum inhibition concentration" (MIC), i.e. the lowest concentration at which the antibiotic inhibits the growth of bacteria in a standard inoculum (10^5 colony forming units/mL). The AUC represents the drug exposure over a

given period and is directly proportional to the dose of the drug (assuming a 100 % bioavailability) and inversely proportional to its clearance. A number of *in vitro*, animal, and clinical studies have shown that 24h-AUC/MIC ratio is the major PK/PD parameter determining the global efficacy of fluoroquinolones against bacteria (disregarding whether dealing with Gram-negative [e.g. *Pseudomonas aeruginosa*] or Gram-positive [e.g. *Streptococcus pneumoniae*] organisms). Its value to obtain a static effect *in vitro*, survival in animal models, and a clear success in clinical studies varies from 10-30 for Gram-positive to 70-125 for Gram-negative bacteria (Andes and Craig, 2002a; Lacy et al., 1999; Marchbanks et al., 1993).

Time course of antimicrobial activity: is determined using three types of analysis, namely (i) the measure of the time needed to obtain to a defined magnitude of organism reduction, (ii) the magnitude of inoculum reduction at a specific time, or (iii) the changes in bacterial numbers over time (Firsov et al., 1998). Most studies have shown that the ratio between the concentration and the MIC is the main driving parameter in this context. Several *in vitro* and *in vivo* studies have also demonstrated that fluoroquinolones have a postantibiotic effect (delay in organism regrowth after short periods of drug exposure) (Andes and Craig, 2002b) but the clinical impact of this observation remains debatable.

I.1.5. Mechanisms of fluoroquinolones resistance

The large clinical use of fluoroquinolones has been quickly associated with the emergence of resistance. Resistance occurs through three main mechanisms, namely target mutation, decreased access to the target, and the expression of a protective protein.

I.1.5.1. Resistance due to target enzymes mutation

As described in the section dealing with their mechanism of action, fluoroquinolones block DNA replication by interacting with either DNA gyrase or topoisomerase IV or both. Mutations in the gene encoding any subunit of one target enzyme may, therefore, reduce not only the susceptibility of the organism to the drug but also indirectly affect the sensitivity of the other target enzyme (Pan and Fisher, 1998; Pan et al., 2001). Alteration in DNA gyrase (composed of two gyrA and two gyrB subunits) is primarily responsible for resistance in Gram-negative bacteria. Mutations associated with resistance usually cluster in the amino terminus of gyrA between amino acid positions 67 and 106, with a critical region at amino acid positions 83 and 87 (Yoshida et al.,

1990;Jacoby, 2005). Alteration in topoisomerase IV (composed of two ParC and two ParE subunits) can contribute to resistance in Gram-positive species, and also clustered around specific regions. Thus, in *Staphylococcus aureus*, the first-step drug resistance mutations are in either ParC (at or around position 154) or ParE (at or around position 60) subunits of topoisomerase IV (Ferrero et al., 1995;Hori et al., 1993;Eliopoulos, 2004).

I.1.5.2. Resistance due to altered access of drug to target enzymes

To reach their target which is present in the bacterial cytoplasm, fluoroquinolones must cross the bacterial membranes (outer and inner membrane in Gram-negative organisms, or the single pericellular membrane in Gram-positive organisms). Since all conventional fluoroquinolones have a negatively charged carboxyl group at position 3, and a positively charged group at position 7 (piperazinyl or pyrrolidinyl ring derivatives), they exist as four species in solution: positively charged, negatively charged, zwitterionic and uncharged. The proportion of these species varies with pH and it seems that only the zwitterionic species easily diffuse through the membranes (Nikaido and Thanassi, 1993). Partition of drug species is affected by differences in the pH between the medium and the cytoplasm and thus can modify the proportion of zwitterionic vs. the positively or negatively species.

In Gram-negative bacteria, the outer membrane is not easily crossed by fluoroquinolones, and these antibiotics actually gain access to the periplasmic space by passage through porins (water-filled canals that play a critical role in bacterial nutrition by allowing the passage of polar molecules such as sugars and amino acids). Resistance to fluoroquinolones may result from a decreased influx correlated with a reduction in expression of these porins, such as, for instance, ompF one of two major porins in *E. coli* (Andersen et al., 1987;Cohen et al., 1989).

Efflux system in Gram-negative bacteria: Fluoroquinolones are also subject to efflux, i.e. outward transport system(s) through protein that pump the drug out of the bacteria and, accordingly, reduce their intracytosolic concentration. While efflux often causes only a modest decrease in susceptibility, it may cooperate with other mechanism to cause full resistance. Most efflux pumps acting on fluoroquinolones are multidrug (MDR) native to bacteria and are not specific to these drugs (Poole, 2000b;Putman et al., 2000).

The most important efflux pumps in common Gram-negative bacteria are member of the restriction nodulation division RND (e.g. AcrAB) or member of the facilitator super family MFP (e.g. EmrAB and MdfA) (Edgar and Bibi, 1997;Lomovskaya and Lewis, 1992;Okusu et al., 1996). In *Pseudomonas aeruginosa*, the main efflux systems are the so-called Mex-transporters and, most notably, the MexAB-OprM, MexCD-OprJ, MexEF-OprN, and MexXY-OprM, which can be overexpressed in strains with decreased susceptibility to ciprofloxacin (Poole et al., 1993;Robillard and Scarpa, 1988;Mesaros et al., 2007).

Efflux system in Gram-positive bacteria: The major efflux pumps in Gram-positive bacteria are member of the facilitator super family MFP (e.g. NorA of *Staphylococcus aureus*, Bmr of *Bacillus subtilis*). The activity of fluoroquinolones against these organisms is reduced when the expression of these transporters is upregulated (Neyfakh et al., 1993;Ohki and Murata, 1997). In *S. pneumoniae*, the first transporter described has been PmrA, but recent studies show that another (probably dimeric) transporter of the ABC group, PatA/PatB, may be the main one (Marrer et al., 2006;El Garch et al., 2010).

I.1.5.3. Resistance due to a protective mechanism

Resistance to fluoroquinolones could be induced via plasmid coded for the gene, called “qnr”. Plasmid-mediated quinolone resistance was identified in clinical strains of *Klebsiella pneumoniae*, and transferable to other Gram-negative bacteria by conjugation (Martinez-Martinez et al., 1998). The qnr gene was found to produce a 219 amino acid protein belonging to the pentapeptide repeat family. The resistance is occurred when qnr protein binds to and protects both DNA gyrase and topoisomerase IV from inhibition by fluoroquinolone drugs (e.g. Ciprofloxacin) (Tran and Jacoby, 2002;Tran et al., 2005;Wang et al., 2003;Li, 2005).

Other plasmid-mediated resistance to hydrophilic quinolones (e.g. ciprofloxacin and norfloxacin) has recently identified “qepA” to encode a drug efflux pump belonging to the major facilitator superfamily (MFS) (Perichon et al., 2007).

In addition, inactivation of ciprofloxacin by a variant of an aminoglycoside-degrading enzyme has been described (Robicsek et al., 2006).

I.2. Pharmacology of selected fluoroquinolones: Ciprofloxacin and Moxifloxacin

I.2.1. Chemical structures

Ciprofloxacin (CIP) [1-cyclopropyl-6-fluoro-1,4-dihydro-4-oxo-7-(1piperazinyl)-3-quinolinecarboxylic acid], (MW = 331.34 g/mol) and moxifloxacin (MXF) [1-cyclopropyl-7-(2,8-diazabicyclo [4.3.0] nonane)-6-fluoro-8-methoxy-1,4-di-hydro-4-oxo-3-quinoline carboxylic acid], (MW = 401.4 g/mol), (Figure 3), are two typical members of the so-called second and third generation fluoroquinolones. Most notably, MXF differs from CIP by the presence of a C-8 methoxy group and a bulkier C-7 (octahydropyrrolo [3.4]-pyridinyl vs piperazinyl for CIP) substituent (Dalhoff et al., 1996).

These changes in chemical structure between MXF and CIP were introduced in order (i) for the bulkier C-7 octahydropyrrolo [3.4]-pyridinyl, to expand the spectrum of ciprofloxacin towards *S. pneumoniae* (against which ciprofloxacin is poorly active, hence limiting its potential indications in respiratory tract infections); (ii) for the C-8 methoxy, to increase the potency without risks of phototoxicity associated with the presence of a C-8 halogen such as in sparfloxacin. This modification (compared to ciprofloxacin) also increases the activity against anaerobes and decreases the frequency at which resistant mutants can be selected *in vitro*.

Regarding CIP and MXF, these structural changes, guided by microbiological and toxicological considerations, have resulted in modification of biophysical properties (see p 48-52) (e.g. hydrophobicity, difference in partition of drug species), and differences in pharmacokinetics (Klopman et al., 1987) while maintaining the basic mode of action of the drug.

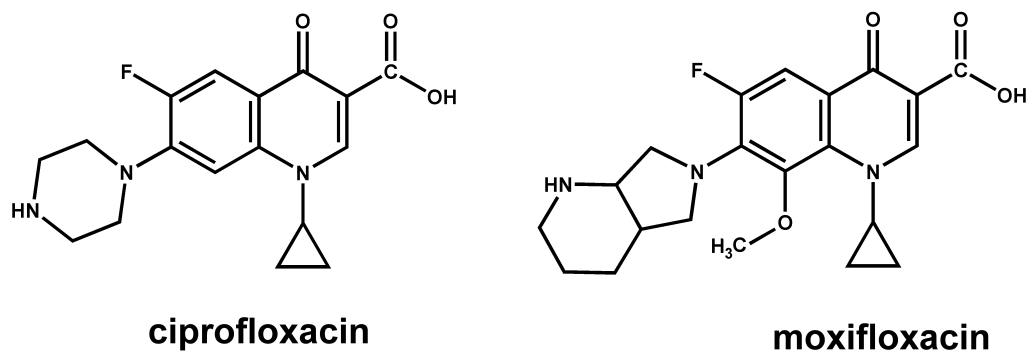


Figure 3. (a) Chemical structure of CIP [(1-cyclopropyl-6-fluoro-1,4-dihydro-4-oxo-7-(1-piperazinyl)-3-quinolinecarboxylic acid)] and (b) MXF [1-cyclopropyl-7-(2,8-diazabicyclo [4.3.0] nonane)-6-fluoro-8-methoxy-1,4-di-hydro-4-oxo-3-quinoline carboxylic acid]

I.2.2. Mode of action and indications

As for all fluoroquinolones, the mechanism of action of both MXF and CIP results from blocking the bacterial DNA replication through inhibition of DNA gyrase and topoisomerase IV. The structures of these drugs, however, have an influence on the bacterial targets. Indeed, MXF, with its C-8 methoxy group, prefers gyrase (*gyrA*), while CIP, with a hydrogen as C-8 substituent, has topoisomerase IV (*ParC*) as preferred target (Fukuda and Hiramatsu, 1999; Pan et al., 1996; Pestova et al., 2000).

Moxifloxacin is a broad-spectrum antibiotic that is active against both Gram-positive and Gram-negative bacteria (but not *P. aeruginosa*). It is indicated for the treatment of respiratory tract infections such as acute sinusitis, acute exacerbations of chronic bronchitis, and community acquired pneumonia (Ball et al., 2004; Van Bambeke and Tulkens, 2009), and, as its intravenous form, for skin and skin structure infections as well as for abdominal infections (due to its activity against methicillin-susceptible *S. aureus* and anaerobes, respectively).

Ciprofloxacin, due to its activity against members of *Enterobacteriaceae* and non-fermenters Gram-negative organisms, is an appropriate drug to treat the urinary tract infections (Naber et al., 2000; Warren et al., 1999), and other major infections caused by Gram-negative infections even when *P. aeruginosa* is suspected to be the causative organism.

I.2.3. Pharmacokinetic and pharmacodynamic parameters

The pharmacokinetic properties of CIP and MXF, give them a highly bactericidal effect *in vivo*, an appropriate penetration in body fluid and tissues, and an easy scheme of administration (Table 1) (Van Bambeke and Tulkens, 2009;Mandell et al., 2007).

Compared with other antibiotics, such as the macrolides, CIP and MXF cause few pharmacokinetic drug-drug interactions. They do not interact with most foods or with many commonly prescribed medications with which macrolides cannot be administered without caution (such as oral contraceptives, anticoagulants, morphine, or digoxin) (Allen et al., 2000;Ball et al., 2004;Stass and Kubitza, 2001b). However, the coadministration of CIP and MXF, like all other quinolones, with preparations containing di- or trivalent cations (such as typically found in antacids or iron preparations) must be avoided due to the formation of non-absorbable complexes (Nix et al., 1989;Polk et al., 1989;Stass and Kubitza, 2001a).

Table 1. Summary of the Pharmacokinetic of CIP and MXF in normal human volunteers

Drug	Dose (mg/ml)	Route	Protein Binding (%)	C _{max} (µg/ml)	V _d (L/kg)	AUC (mg,h/L)	Clearance (ml/min)	Bioavailability	t _{1/2} (h)	Reference
CIP	400	i.v.	30	3.4-6.7	1.9	8.1-14.2	417-568		3-4	(Dudley et al., 1987)
	500	p.o.	30	1.5-2.9	2.1-5.0	9.0-11.0	700-902	55-70	3-5	(Davis et al., 1996)
MXF	400	i.v.	39-52	3.7-5.0	2.0	23-45	147-194		8.2-15.4	(Stass and Kubitza, 1999;Wise et al., 1999)
	400	p.o.	39-52	2.5-5.0	3.1-3.6	20-45		86-100	8.3-15.6	(Sullivan et al., 1999)

Abbreviation: i.v intravenous, p.o: per orally, V_d: volume of distribution, AUC area under curve, t_{1/2} half time

I.2.4. Resistance

✓ Resistance due to target enzymes mutation

Specifically, mutations in topoisomerase IV (ParC or ParE subunits), affect CIP activity, and result in resistance of Gram-positive species such as *Streptococcus pneumoniae*, *Staphylococcus aureus* (Pan and Fisher, 1996;Perichon et al., 1997). Similar data have been reported for MXF, when *Streptococcus pneumoniae* have mutations in DNA gyrase (gyrA or gyrB) (Nagai et al., 2001).

For Gram-negative bacteria, alterations in DNA gyrase (*gyrA*) are more often responsible to both drugs (CIP and MXF) resistance (Bachoual et al., 2000).

✓ *Resistance due to the efflux pumps in bacteria*

In addition to mutations in drug target enzymes, multidrug resistance (MDR) efflux pumps expressed in Gram-negative and Gram-positive bacteria (e.g. AcrAB-TolC of *E.coli*, NorA of *Staphylococcus aureus*) contribute to decrease susceptibility to CIP leading to clinically meaningful resistance to this drug (Neyfakh et al., 1993; Sulavik et al., 2001; Wang et al., 2001; Poole, 2005).

In contrast, MXF is not a poor substrate of the NorA efflux pump of *Staphylococcus aureus* (Schmitz et al., 1998). Likewise, another efflux-pump plasmid-mediated, encoded by the QepA gene, has been reported to induce resistance to CIP, but not to MXF (Luzzaro, 2008). Yet, overexpression of MexAB-OprM pumps of *Pseudomonas aeruginosa*, decrease activity to both CIP and MXF (Dupont et al., 2005; Zhang et al., 2001). It should be noted that MXF is used primarily against Gram-positive bacteria and its relatively poor activity against *P. aeruginosa* could be related to a limited ability to penetrate the outer membrane barrier (Poole, 2000a).

✓ *Resistance due to the efflux pumps in eukaryotic cells*

In eukaryotic cells, efflux transporters members of the ABC transporters family (which utilize ATP hydrolysis as a source of energy) appear to reduce the accumulation of CIP but not that of MXF. Thus, CIP accumulates five times less than MXF in J774 macrophages cells, where its accumulation is subject to efflux pumps through the activity of MRP2 and MRP4 transporters (Marquez et al., 2009; Michot et al., 2004; Michot et al., 2005; Michot et al., 2006).

A similar behavior has been observed in human intestinal epithelial (Caco-2) cells, in which the intestinal secretion of CIP is primarily mediated by MRP2 efflux pump protein (Cavet et al., 1997; Alvarez et al., 2008). Moxifloxacin can also be subject to efflux mediated by P-glycoprotein in Calu-3 cells (Brillault et al., 2009). Yet, globally speaking, the effect of multidrug efflux pumps is less pronounced with MXF than with the CIP.

II. Cell and Models membrane

II. 1. Cell membranes

Biomembranes are essential for the compartmentalization that defines cells and organisms. In addition to this function, membranes provide cells with energy, have a critical role in several cell signalisation pathways and enzymatic activities and facilitate the signal transduction (Abankwa et al., 2008; Gorfe and McCammon, 2008; Brannigan et al., 2008).

The variety of membranes is depending on the organisms. In fact, prokaryotes either have one cell membrane (Gram-positive) or have inner and outer membranes (Gram-negative). In addition to their plasma membrane, eukaryotes have membranes surrounding the nucleus and organelles. In spite of this variety, the structure and organization of biomembranes can be generalized to the Fluid Mosaic Model as proposed by Singer and Nicolson (Singer and Nicolson, 1972). This paradigm consists of an assembly of amphiphilic lipids organized in two layers with their polar headgroups along two opposite surfaces and their acyl chains forming the nonpolar domain in between. The lipid bilayer is loaded with peripheral proteins that associate at the surface of the membrane or integral proteins with one or more transmembrane (TM) segments (Figure 4).

The fluid mosaic model does not exclude the possibility of heterogeneity like that encountered in epithelial cells, which have different lipid (and protein) composition in their apical and basolateral domains. Moreover, regarding the lateral organization of lipids, there is evidence of the existence of small membrane domains called “lipids rafts”. Lipid rafts are defined as a preferential association between sphingolipids, sterols, and specific proteins bestowing to the membrane a lateral organization (Lingwood and Simons, 2010). They are formed in the plasma membrane of many cell types as well as in many intracellular membranes. These domains are distinguished from the bulk lipid of the bilayer, and are involved in lipid trafficking as well as protein targeting and other important biological functions. Although there is no direct evidence for co-localized rafts formation in the inner and outer leaflets of the bilayer, the two leaflets may be coupled by interdigitation of the longer chains to sustain bilayer rafts organization (Nelson and Cox, 2005). Lipids rafts are diverse in terms of their composition and their size, which vary from 50 nm to up to 700 nm. The small raft domains are limited by bilayer curvature, and large rafts appear to encompass smaller heterogeneous domains. This is probably

stimulated by particular proteins called “rafts protein”. These data support the hypothesis about the existence of biological membrane heterogeneities that could also be modulated by lipid-protein as well as lipid-lipid interactions (Lingwood and Simons, 2010).

The lipids present in rafts have physical properties that differ from those of the bulk lipids. Rafts are several angstroms thicker than the rest of bilayer, with a predominance of saturated acyl chains in the liquid ordered state. In addition, the coexistence of liquid ordered and liquid-disordered states has been demonstrated in rafts-mimicking model membranes consisting of cholesterol, sphingomyelin, and POPC in a 1:1:1 molar ratio (Simons and Vaz, 2004), and also in vesicles derived from cells (GUVs) (Baumgart et al., 2007). Although of large interest, rafts have not been studied in our Thesis given our main objectives and will, therefore, not be further discussed in the remaining of our work.

The structural complexity of biological membranes is the result of the physicochemical properties of the individual membrane components (lipids and proteins), which is governed by its composition and chemical environment (Simons and Ikonen, 1997). The structural variation of lipids yields a multitude of molecules with diverse physical properties, which in concert with membrane proteins; regulate membrane properties such as permeability, domain organization and trafficking (Simons and Vaz, 2004).

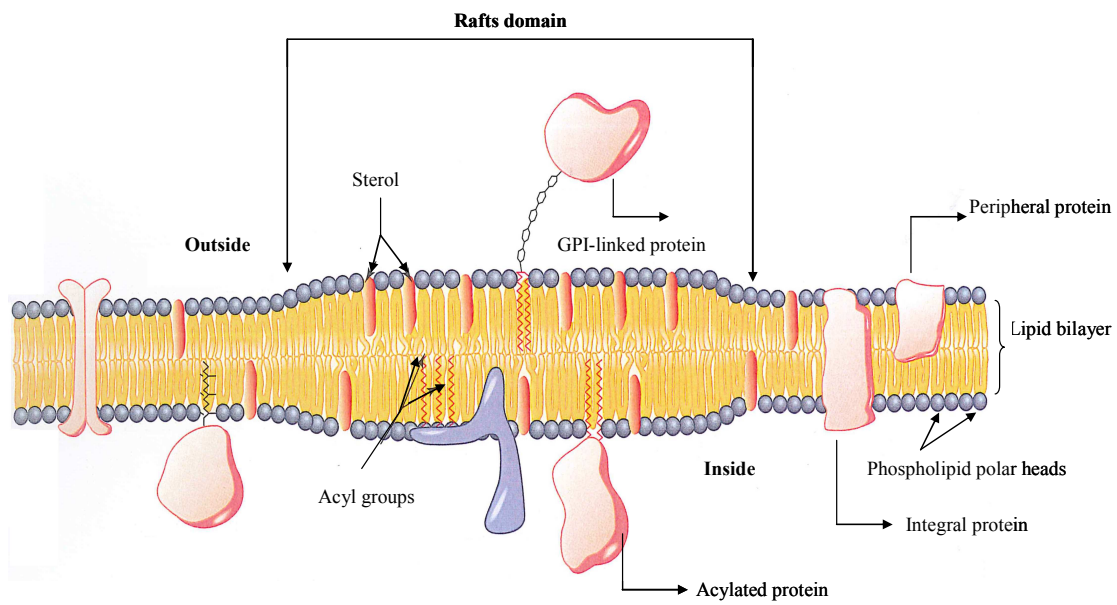


Figure 4. Eukaryotic plasma membrane components.
 Membranes have microdomains that are enriched in cholesterol and sphingolipids.
(Luckey, 2008) reprinted from (Nelson and Cox, 2005)

II. 2. Classification and chemistry of lipids: Membrane composition (eukaryotic and prokaryotic cells)

Lipids are major compounds of biological membranes and they have a crucial role in membrane compartmentalization, cell signaling, and are essential for energy production and storage. A typical biomembrane contains more than a hundred different species of lipids (van Meer, 2005), for which structural diversity originates through variability of the polar head groups and the apolar hydrocarbon chains (e.g. length, degree of saturation, hydroxylation).

A comprehensive classification of lipids molecules is essential to the understanding their role in the pharmacokinetics, pharmacodynamics and toxicodynamics of several drugs at both molecular and cellular level. Lipids can be classified into eight categories based on their chemical structure and driven by the distinct hydrophobic and hydrophilic elements: fatty acyls, glycerolipids, glycerophospholipids, sphingolipids, sterols lipids, prenol lipids, saccharolipids, and polyketides) (Fahy et al., 2005). The three mainly classes of membranes lipids are glycerophospholipids (GPL), sphingolipids, and sterols.

II. 2.1 *Glycerophospholipids (GPL)*

Glycerophospholipids, called simply as phospholipids (PLs), are the main constituents of biological membranes, and are built on a glycerol backbone with a head group attached at the *sn*-3 position, and fatty acid chains attached via ester linkage at the *sn*-1 and/or *sn*-2 position. Depending to the chemical structure of the head group, seven classes of glycerophospholipids are therefore recognized: phosphatidic acid (PA), phosphatidylcholine (PC), phosphatidylethanolamine (PE), phosphatidylserine (PS), phosphatidylglycerol (PG), diphosphatidylglycerol (cardiolipin, CL), and phosphatidylinositol (PI) (Figure 5).

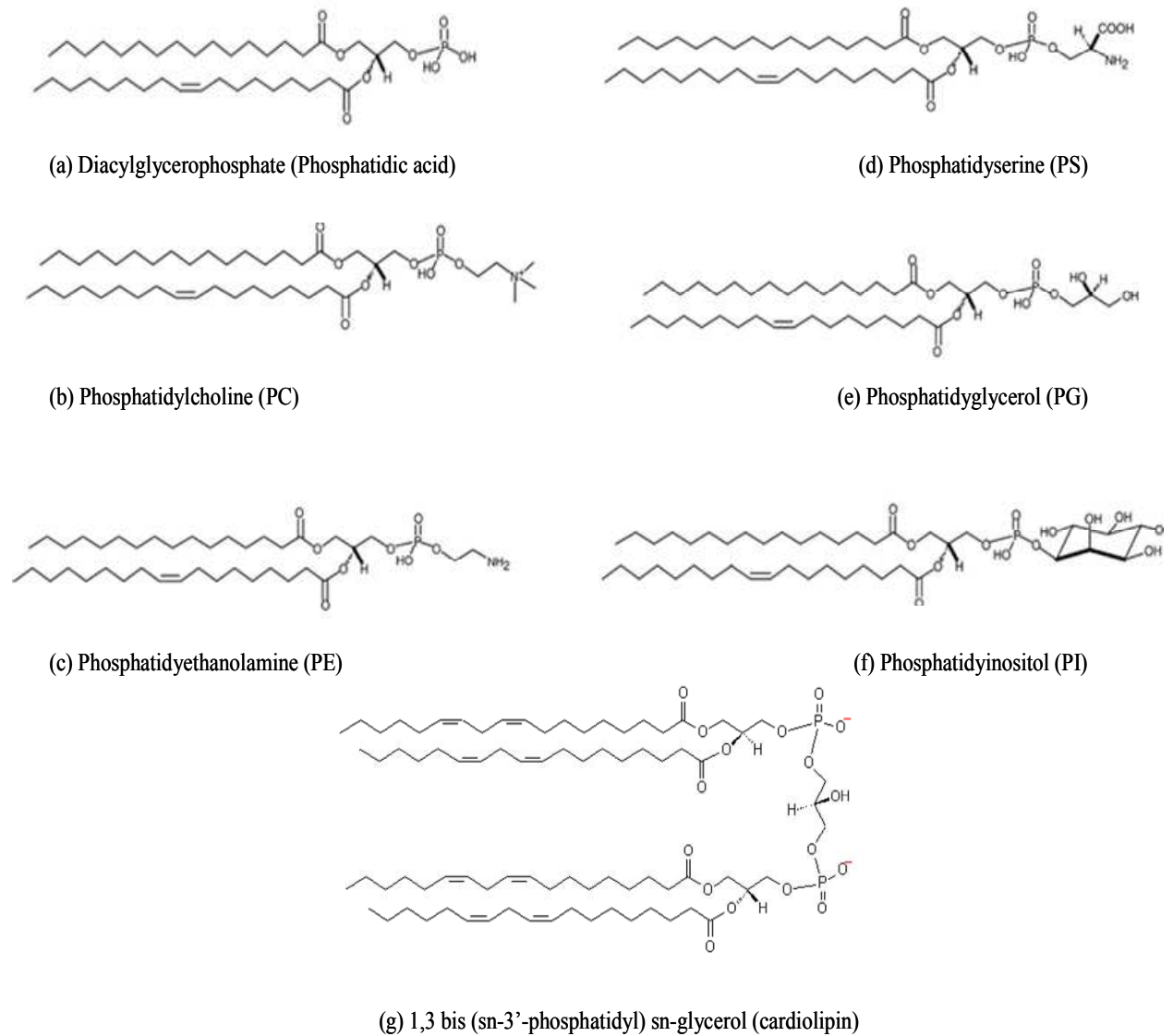


Figure 5. Chemical structures of the common glycerophospholipids present in biological membranes. *Adapted from (Fahy et al., 2005).*

Although all phospholipids are amphiphilic molecules and define the polar (headgroups) and nonpolar domains (acyl chains) of the bilayer, they also have important chemical, biological and physical properties. In fact, the anionic phospholipids (PS, PI, PG and CL) have a net negative charge at physiological pH, while the zwitterionic PLs (PE and PC) are neutral. Moreover, the acyl chain on C1 of most phospholipids of biological membranes is saturated with 16 or 18 carbons long, while that on C2 is often longer and unsaturated. Naturally occurring unsaturated fatty acids have *cis* double bond that makes a 30° bend, or a kink in the acyl chain as shown in Figure 6. (e.g. saturated and unsaturated fatty acid (stearate, oleate)). The degree of unsaturation of the fatty acid contributes to the elasticity of the membrane which influences insertion and packaging of proteins and also drug transport (Fa et al., 2007).

The composition of membrane is very different between eukaryotic and prokaryotic cells (Table 2), and this is due, particularly, to a variation in phospholipids content. Zwitterionic phospholipids (e.g. PC and PE) are abundant in eukaryotic membranes, while negatively charged phospholipids (e.g. PG and CL) are dominant in prokaryotic membranes, notably in the Gram-positive bacteria such as *Staphylococcus aureus* (lipid percentage of 58% and 42% for PG and CL, respectively). The proportion of these negatively charged lipids is lower in Gram-negative bacteria such as *E.coli*, where their percentage is only about 20% (Lohner and Prenner, 1999; Epand et al., 2007).

In addition, differences in phospholipids composition are also observed between the inner and the outer leaflets (monolayer) of mammalian membrane cells, resulting in membrane asymmetry. A typical example is the erythrocyte membrane, the outer leaflet of which is enriched in SM and PC, while the inner leaflet contains most of the PE, PS and nearly the entire PI found in the membrane (Table 3). Furthermore, the same phospholipid species may have acyl chains different in the outer leaflet from those in the inner leaflet. The consequences of lipid asymmetry are a variation in the thickness of the lipid bilayer and domain formation (Renooij et al., 1976; Lohner and Prenner, 1999; Nelson and Cox, 2005).

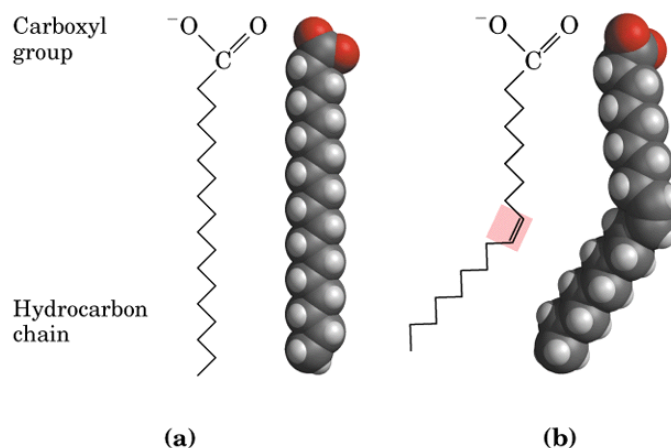


Figure 6. Saturated and unsaturated fatty acids with 18-carbon chains. In (a) stearic acid (no double bonds) and in (b) oleic acid with one cis double bond introduces a kink (rigid bend) in the hydrocarbon tail chain (Nelson and Cox, 2000).

Table 2. Approximate lipid compositions of different cell membranes (Eukaryotic and Prokaryotic cells) Percentage of total lipid

Lipid	Eukaryotic cells			Prokaryotic cells			
	Chinese hamster ovary (CHO cell) (phospholipids)	Human alveolar macrophages	Human Erythrocyte membrane	<i>E. coli</i>	<i>Pseudomonas aeruginosa</i>	<i>Staphylococcus aureus</i>	<i>Staphylococcus pneumoniae</i>
PE	16.4	20.6	6.2+2.7	82	60	-	-
PC	55	31	24.2+0.4	-	-	-	-
PS	6.7	20.7	2.6+0.2	traces	21+11	58+42	50+50
PG+CL	13			6+12			
PI+PA						-	-
SM	8.9	6.6	18.9+0.3	-	-	-	-
Chol	ND	7.9	48.1+2.2	-	-	-	-
Others		13.2					
References	(Hanada et al., 1990)	(Sahu and Lynn, 1977)	(Lohner and Prenner, 1999) (Wolkers et al., 2002)	(Erand et al., 2007)			

Table 3. The asymmetric distribution of lipids in erythrocyte membranes. The content of each lipid is expressed as % mol in the inner and outer leaflets (Nelson and Cox, 2005)

Membrane phospholipid	Percent of total membrane phospholipid	Distribution in membrane	
		Inner monolayer	Outer monolayer
PE	30	80	20
PC	27	30	70
SM	23	20	80
PS	15	95	05
PI	05	70	30
PI 4-phosphate		100	-
PI 4-5 biphosphate		80	20
PA		80	20

II. 2.2. Sphingolipids

Sphingolipids are built on sphingosine, a long chain amino alcohol to which a fatty acyl chain is attached by an amide linkage. The most common sphingolipids found in eukaryotic cell membranes are phosphosphingolipids (sphingomyelin, SM), neutral glycosphingolipids (glucosylceramides, GluCer) and ceramides (Cer) (Figure 7).

Sphingolipids are located mainly in the outer leaflet of membranes (Lohner and Prenner, 1999) and play a central role in membrane organization, cell recognition, and signal transduction. Sphingomyelin and glycosphingolipids interacting with sterols contribute to the formation of membrane microdomains (called lipid rafts) (Simons and Vaz, 2004; Huwiler et al., 2000). Ceramides serve as messengers in signal transduction cascades (Futerman and Hannun, 2004).

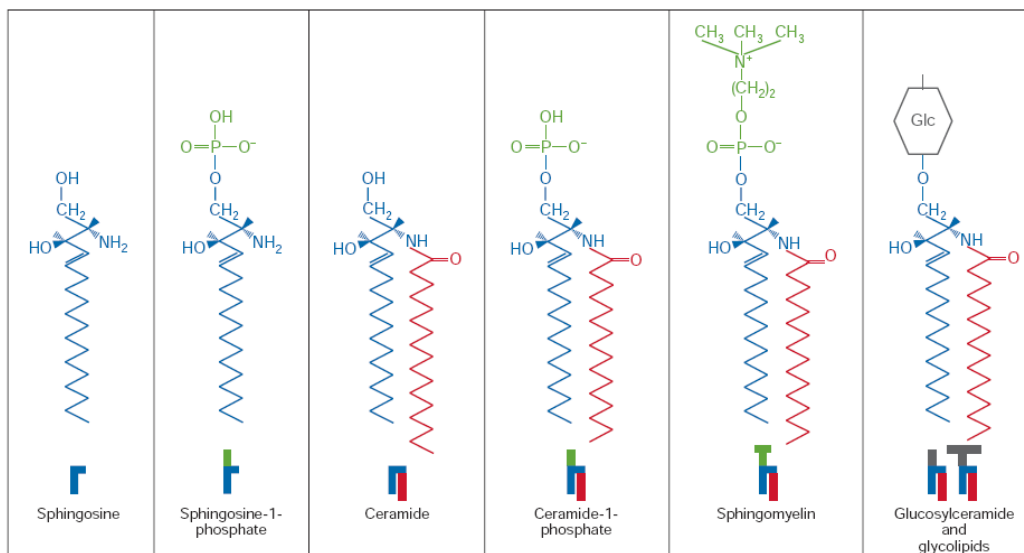


Figure 7. Chemical structure of common sphingolipids

Sphingoid base (in blue) and only one kind of fatty acid (palmitic acid, in red) is N-acylated are shown (Futerman and Hannun, 2004)

II. 2.3. Sterols

A third major class of biological lipids are sterols (cholesterol in mammalian membrane cells), which are derived from cyclic polyisoprene precursors (Figure 8). The cholesterol content of various eukaryotic cell membranes varies from 0 % to 25 % (Jain and Wagner, 1988), and around 90 % of total cholesterol is located in plasma membrane. Different sterols are found in other eukaryotic cells (e.g. stigmasterol in plants, and ergosterol in yeast and fungi), while prokaryotic cells are completely devoid of cholesterol. The presence of cholesterol in membranes increases bilayer thickness, tight packing of saturated acyl chains, and compressibility (Pan et al., 2009; Zhang et al., 2010).

In addition to its structural role, cholesterol is the precursor of numerous hormones and of bile acids, and thereby is critical in several biological processes including tissues development (Haines, 2001).

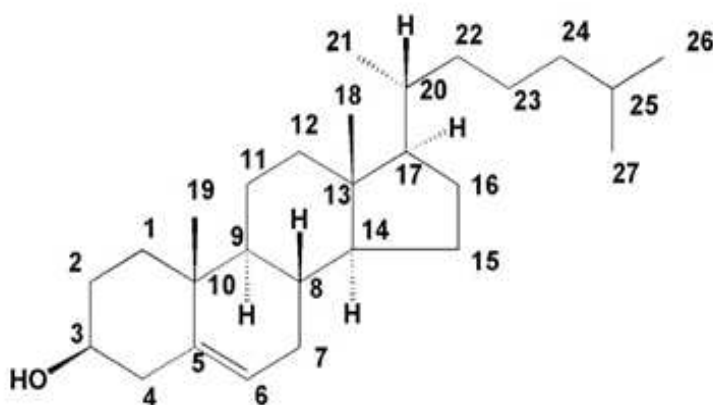


Figure 8. Chemical structure of cholesterol, a major component of mammalian membranes (Futerman and Hannun, 2004; Fahy et al., 2005)

II. 3. Models of lipid membranes

Progress in the knowledge in structure-activity of biological membranes and their relation with drug transport requires purified samples. Due to the complexity of the constituents of the biological membranes, and the difficulty to purify them, models membranes made of a limited number of defined lipids are suitable tools to characterize *in vitro* drug-lipid interactions. These models allow the application of spectroscopic techniques that can provide useful informations about drug insertion in membrane. Depending on the method of preparation, a variety of model lipid membranes can be used (Figure 9):

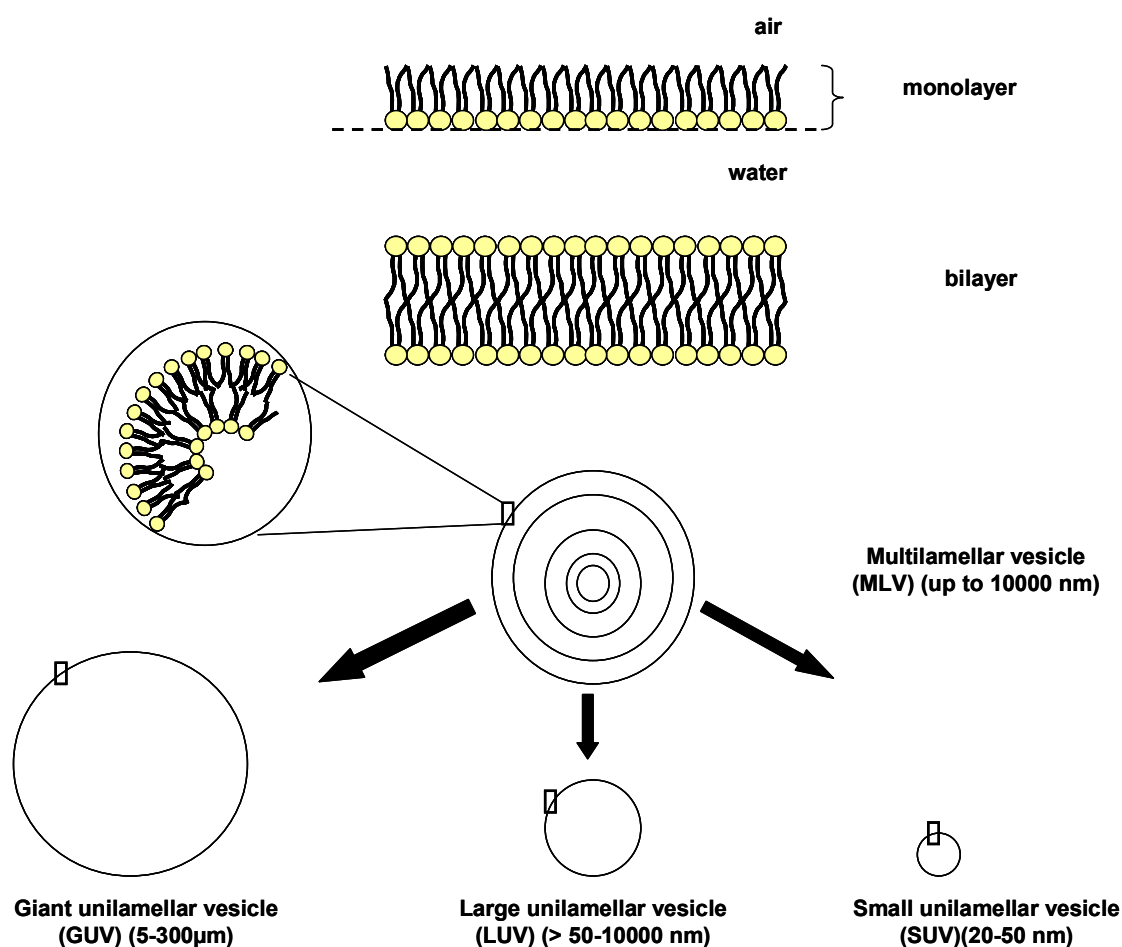


Figure 9. Schematic drawing of model membrane: monolayer, bilayer and liposomes. *Multilamellar liposomes (MLVs) have many bilayers as indicated. Small unilamellar liposomes (SUVs), large unilamellar liposomes (LUVs) and giant unilamellar liposomes (GUVs) have only one bilayer, but they display a difference in their size.*

II. 3.1. Monolayers

Amphipathic lipid molecules can spontaneously assemble as a monolayer, in which the lipid molecules line up at air-water interface with their hydrophobic tails in the air and hydrophilic head groups in the water. Such unilamellar phase is formed in Langmuir-Blodgett trough container, with a movable barrier that allows control of the area occupied per lipid molecule and measurement of the pressure of the monolayer. The surface pressure (π) is created by the difference between the surface tension of the monolayer and the pure water interface. Thus, a monolayer reveals pressure effects of membrane constituents (Deleu et al., 2005). The monolayers are considered as suitable model membranes to study layer structure and intra-layer molecular organization by infrared spectroscopy (Oliveira, 1992).

II. 3.2. Planar Bilayers (PBs)

Planar bilayers previously called “Black films” are one of the most suitable models to mimic biological membranes. The lipid is dissolved in organic solvent and is deposited over a tiny orifice in a Teflon sheet, which is then inserted between two aqueous compartments. This model membrane is mostly used to study protein-lipid interactions and electrical properties of membrane because it offers access for electrodes on both side of the membrane (Henkart and Blumenthal, 1975; Benz et al., 1978; Benz and Gisin, 1978).

Recently, supported lipid bilayers (SPB) have been used in nanobiotechnology, and notably in atomic force microscopy, which allows direct observation of the lipid membrane surface and domain formation in lipid mixtures (e.g. DOPC+DPPC) (Mingeot-Leclercq et al., 2008). The common method for forming SPB is the fusion of lipid vesicles (SUV) on a flat support such as mica sheet. The fusion is achieved by heating and cooling the vesicles in contact with the solid support (Jass et al., 2000; Reviakine and Brisson, 2000).

II. 3.3. Liposomes: from MLV to GUV

In contrast to planar lipid bilayers, liposomes are closed bilayer vesicles. They spontaneously form when lipid bilayers are dispersed within aqueous environment due to their amphiphilic nature. The polar headgroups are oriented towards the inner and the

outer aqueous media protecting the hydrophobic region (acyl chain) of the polar environment. Depending to the method of preparation, liposomes could be multilamellar or unilamellar (a single bilayer), and according to their size, are classified as Small Unilamellar Vesicles (SUV), Large Unilamellar Vesicles (LUV) or Giant Unilamellar Vesicles (GUV).

i) *Multilamellar Vesicles (MLV)*

These liposomes, which contain concentric spheres of lamellae with aqueous media between consecutive bilayers, are simply made by shaking through dried lipid film into an aqueous solution. They are polydisperse, with diameters varying from 0.4 to 50 μm . MLV are often used to study protein-lipid binding and to determine lipid state transition by NMR (Linseisen et al., 1997; Luckey, 2008).

ii) *Small Unilamellar Vesicles (SUV)*

Disruption of MLVs suspensions by sonication produces small unilamellar vesicles with diameters in the range of 20 to 50 nm. Since the acyl chains are less tightly packed in the small vesicles than in the larger vesicles, they have less lateral tension, which is related to membrane elasticity. They are very asymmetric due to their high degree of curvature, which makes incorporating proteins with difficulty. Nevertheless, SUV liposomes are employed in binding studies with small peptides by using spectroscopic methods (Beschiaschvili and Seelig, 1992).

iii) *Large Unilamellar Vesicles (LUV)*

Large Unilamellar Vesicles, with diameters from 0.1 to 1 μm , can be obtained by several freeze-thaw cycles of MLVs liposomes, following by lipid extrusion. This technique consists in forcing the liposomes under nitrogen pressure to pass through polycarbonate filters of defined pore size. LUVs have the advantage of size distribution homogeneity and large encapsulated volume. These liposomes are the most used model membranes for drug delivery (Allen and Cullis, 2004), and to characterize membrane protein (e.g. protein incorporation, protein variants activity) by forming proteoliposomes (Costello et al., 1984).

iv) *Giant Unilamellar Vesicles (GUV)*

These giant liposomes have a diameter varies from 5 to 300 μm . They can be obtained by slowly hydrating lipids at low ionic strength and high lipid concentration, following by sedimentation through sucrose solutions to eliminate MLV. Homogenous vesicles can be improved by electro-formation applying a voltage to the solution of lipids (Akashi et al., 1998a; Akashi et al., 1998b) These giant liposomes reach the size of living cell and are large enough to allow insertion of a microelectrode or to visualize their surface sections by optical microscopy. They can be manipulated by micropipettes to test their elastic compressibility (Akashi et al., 1998a; Fa et al., 2007). GUVs are not appropriate model membrane for characterization of membrane protein due to the fragility of the corresponding proteoliposomes.

Amongst the models of lipid membranes presented in this section, GUV vesicles are probably the most relevant model of biological membranes, since their curvature radius is similar to that of eucaryotic cells. A typical exemple of their usefulness is the characterization of membrane heterogenities by using GUVs derived from mast cells (Baumgart et al., 2007).

III. Biophysical methods for studying fluoroquinolones-lipids interactions

Since the activity of fluoroquinolone antibiotics results from inhibition of DNA gyrase and DNA topoisomerase IV, two enzymes that are intracellular (Pestova et al., 2000), the membranes of the bacteria are the first barrier for fluoroquinolones to access to these target. Likewise, the fast accumulation of fluoroquinolones in eukaryotic cells implies their crossing of the eukaryotic plasma membrane. In order to gain insights into the molecular interactions between lipids of model membranes and fluoroquinolones, the application of biophysical tools, able to establish a relation between physico-chemical properties of these drugs and their passage across the membrane, is required. In this section, we describe the main biophysical methods used in this Thesis. An overview of these methods will be presented in a summary Table 7 at the end of the chapter.

III. 1. Atomic Force Microscopy (AFM)

III. 1. 1. *Introduction*

The atomic force microscopy is a scanning probe microscope which has been invented by (Binnig et al., 1986). The AFM can provide informations about surface properties of biological samples (e.g. lipid bilayer). From the three dimensional topographical analysis, roughness and adhesion forces measurements, AFM represent an essential tool to study the model membrane domains and the effect of drugs (e.g. fluoroquinolones) on the membrane organization (Giocondi et al., 2010).

III. 1. 2. *Physical principles*

The principal of AFM is based on the interaction between a tip, which is attached to a cantilever and the sample surface deposited on a flat support such as mica sheet. The physical parameter measured is the sum of the forces resulting from different interactions. Attractive or repulsive forces resulting from these interactions, (e.g. ionic repulsion, and van der Waals and electrostatic attraction) cause a positive or a negative bending of the cantilever, respectively. This bending is detected by a laser beam reflected from the back side of the cantilever and collected in a photodiode (Figure 10). If the tip is scanning over the sample surface, the deflection of the cantilever can be recorded as an image which represents the three dimensional shape of the sample surface.

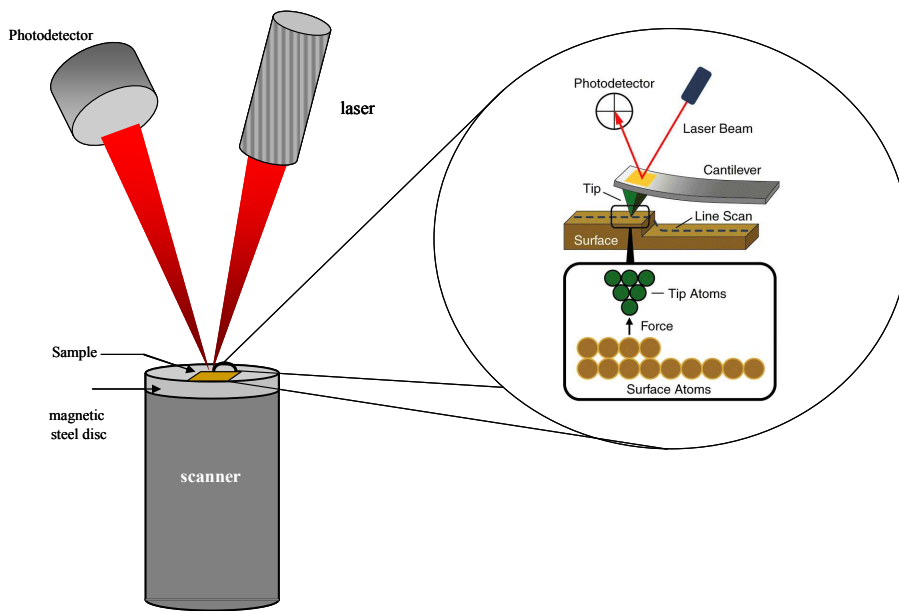


Figure 10. Principle of Atomic Force Microscopy

III. 1. 3. *The operating modes in AFM*

In AFM, we distinguished three main scanning modes: i) contact mode, ii) non contact mode and iii) tapping mode (intermittent contact mode) (Dorobantu and Gray, 2010) (Figure 11).

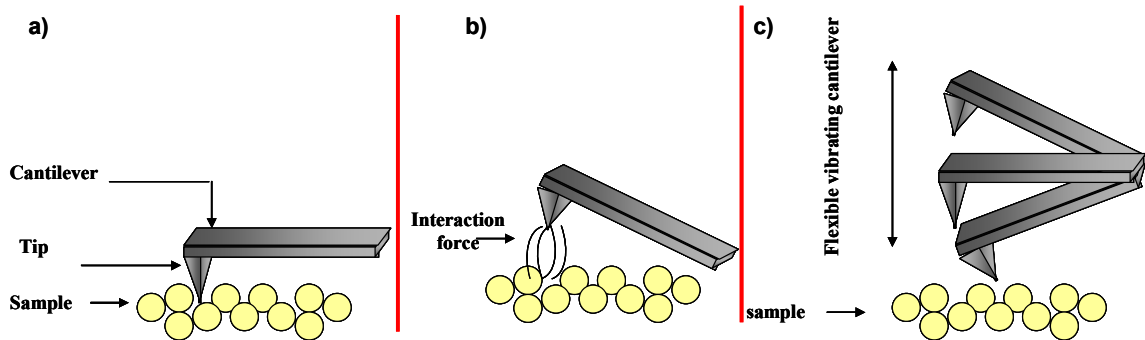


Figure 11. Schematic representation of AFM scanning modes

a) contact mode, b) non-contact mode and c) tapping mode

i) Contact mode

In contact mode, the tip makes soft physical contact with the surface of the sample and the main interacting force (F (N)) between tip and surface is repulsive, and can be calculated via Hook's law:

$$F = K \cdot Z \quad [\text{Eq. 1}]$$

where K (N/m) and Z (m) are spring constant and the deflection of the cantilever, respectively.

Two contact modes can be applied: the constant height mode, where the sample height is maintained constant relative to the tip, and the cantilever deflection is recorded. This mode is limited to the flat sample, and used to obtain topographic information. The second mode is the constant force mode, where the deflection of the cantilever is fixed and the motion of the scanner in z-direction is recorded. The image contrast is due to the variations of the scanner position delivering the topographic information. The contact mode allows a good resolution, but the adhesion forces can induce damage of both tip and soft sample.

ii) Non contact mode

In this mode, the tip operates in the attractive force (Van der Waals) region, without having a contact with the sample surface (Martin et al., 1987). The use of a cantilever with a spring constant of 20-100 N/m and a silicon tip are needed for scanning soft biological samples. Topographic images of this mode can be affected by the detection of a liquid drop as a part of the sample surface.

iii) Tapping mode (intermittent contact mode)

In tapping mode, the cantilever oscillates on the surface sample at a frequency close to its resonance frequency with high amplitude (above 20 nm) (Zhong et al., 1993). An electronic feedback system ensures that the oscillation amplitude remains constant, such that a constant tip-sample interaction is maintained during scanning. Forces that act between the sample and the tip will not only cause a change in the oscillation amplitude, but also changes in the resonant frequency and phase of the cantilever. The intermittent contact cause less damage to the sample surface by eliminating of a large part of shearing forces.

III. 1. 4. *Applications of AFM to study lipid membranes and drug-lipids interactions*

The AFM provides informations on the structure of biological samples like lipid membranes, and allows exploring in real time changes induced when interacting with drugs.

i) *Characterization and organization of domains in model membrane*: most studies on SPB model have demonstrated the formation of domains. As a typical example, the topographic image obtained for mixed of (DOPC:DPPC) (1:1, mol:mol). The AFM image reveals that DPPC molecules are in gel phase, forming domains surrounded by a fluid matrix of DOPC. The height difference between the two phases is due to differences in thickness and of the acyl chains length of DOPC vs. DPPC films (El Kirat et al., 2010).

The membrane asymmetry and the size of gel domains in (DOPC:DPPC) mixture have been observed by real time AFM by decreasing the temperature from 60°C to 23°C. The growth rates of the DPPC gel domains being dependent on the coupling between the two leaflets of the bilayer (Giocondi et al., 2001).

These membrane domains and the dynamic remodeling of bilayer can be affected by the presence of drugs. As a typical example, azithromycin, a macrolide antibiotic, was found to induce progressive erosion and disappearance of DPPC gel domains of (DOPC:DPPC) bilayer. By contrast, SM and (SM:Chol) domains surrounded by a fluid matrix of DOPC, and mimicking lipid rafts were not modified by this antibiotic. The higher membrane stability was suggested to reflect stronger intermolecular interactions between SM and Chol molecules (Berquand et al., 2004).

Another example used SPB of *E.coli* lipid extracts to study the interaction of fluoroquinolones antibiotics such as CIP and its two derivatives. The AFM images have shown the formation of pores and adsorption of CIP on the top of the SPB (Montero et al., 2006).

ii) *Characterization of the phase behavior and thermotropic properties of lipids*: a phase transition process involves a cooperative rearrangement of the individual phospholipids molecule that composes the bilayer. Such phase transition implies changes in the packing properties of the bilayer, which can be observed by using a combination of temperature-controlled AFM imaging mode with force spectroscopy (Garcia-Manyes and Sanz, 2010b). The experiments conducted on DPPC and DMPC bilayers showed that the force

needed to pierce the lipid bilayer is temperature dependent. In fact, the solid-like phase exhibits a much higher force than its liquid-like counterpart and the phospholipids exhibit changes in elastic constants (e.g. compressibility, bending, and elasticity).

AFM contact mode image was used to study the stability of a DMPC supported bilayer by heating the sample from 19°C to 60°C. At low temperature, the bilayer is in the gel phase. Upon increasing the temperature, the bilayer undergoes two distinct phase transition at 30.3°C and 37.5°C, respectively. The low temperature transition was related to the melting of the leaflet that is far from the surface, whereas the second transition was involved the phase transition of the leaflet in contact with mica surface (Garcia-Manyes and Sanz, 2010a; Giocondi et al., 2010).

III. 1. 5. *Advantages and limitations*

AFM is capable to image surface topography from nano to the micro scale, in air and under liquid of lipid model membranes. It offers the possibility to follow *in situ* membrane modification upon addition of drugs, and provides direct structural information (e.g. lipid asymmetry, lipid domains) (Giocondi et al., 2010).

However some disadvantages of AFM must be noted. Contact and tapping modes can cause damage of soft sample due to the lateral forces of tip-sample interaction. In addition, non-contact mode is limited to the hydrophobic sample with a minimal fluid layer. Moreover, thermotropic properties of lipids investigated by AFM are dependent on the nature of support, the thickness and composition of the proximal and distal leaflet layer. Hence, an increase of the transition temperature of lipids is a common observation to all AFM determination (e.g. the melting transition of DPPC was reported to be 52°C by AFM and 42°C by DSC) (Garcia-Manyes et al., 2005).

III. 2. Langmuir-Blodgett technology (LB)

III. 2. 1. Introduction

The Langmuir-Blodgett technique offers the possibility to prepare ultrathin layer suitable for biomolecular immobilization at molecular level. The development of biomimetic membrane, which is based on LB technology, corresponds to highly organized molecular assemblies that can be analyzed through the insertion of drugs in an oriented position (Girard-Egrot et al., 2005).

III. 2. 2. Langmuir monolayer formation

The LB technology is based on the property of lipids to orient themselves at an air/water interface between the gaseous and the liquid phase, and, thereby, to form an insoluble monolayer. The equipment used for the production of Langmuir monolayer is shown in Figure 12. Briefly, it consists of Teflon's container holding a liquid subphase, a compressing system constituted with mobile barriers, and a measuring apparatus for monolayer characterization. Included in these are a surface pressure sensor and a position detector attached to the barriers to measure the surface area of the film. The dipper controls the immersion and withdrawal of the solid substrate for monolayer deposition (Oliveira, 1992).

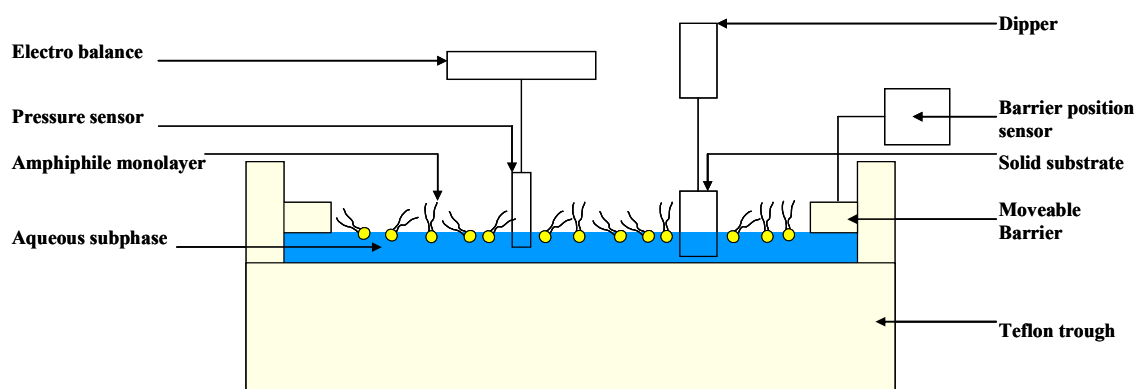


Figure 12. A schematic representation of a Langmuir Blodgett trough

The sample is dissolved in an organic volatile solvent (e.g. chloroform) and is spread on the surface of an aqueous subphase. After solvent evaporation, the interfacial film results in a monomolecular layer, with the headgroups immersed in the water and tail groups (acyl chain) remaining outside. When the Langmuir monolayer is compressed, the intermolecular distance decreases, and the surface tension diminishes. The force exerted by the film per unit length called surface pressure (π (N/m)) and is given by:

$$\pi = \gamma_0 - \gamma \dots [\text{Eq. 2}]$$

where γ_0 and γ are the surface tensions of the liquid in the absence and in the presence of a monolayer, respectively.

III. 2. 3. Langmuir monolayer characterization

During the compression, the molecules self-organized and the monolayer undergoes several states transformations analogous to the gaseous, liquid and solid state to finally form a floating monolayer ordered at the surface. The monitoring of the surface pressure π as a function of the area available to each molecule (area per molecule expressed in \AA^2) allows determining a surface pressure/area (π -A) isotherm.

Figure 13 shows a typical pressure/area (π -A) isotherm curve for a phospholipid monolayer. The shape of the isotherm depends on temperature, hydrocarbon chain length and on the presence of unsaturated acyl chains.

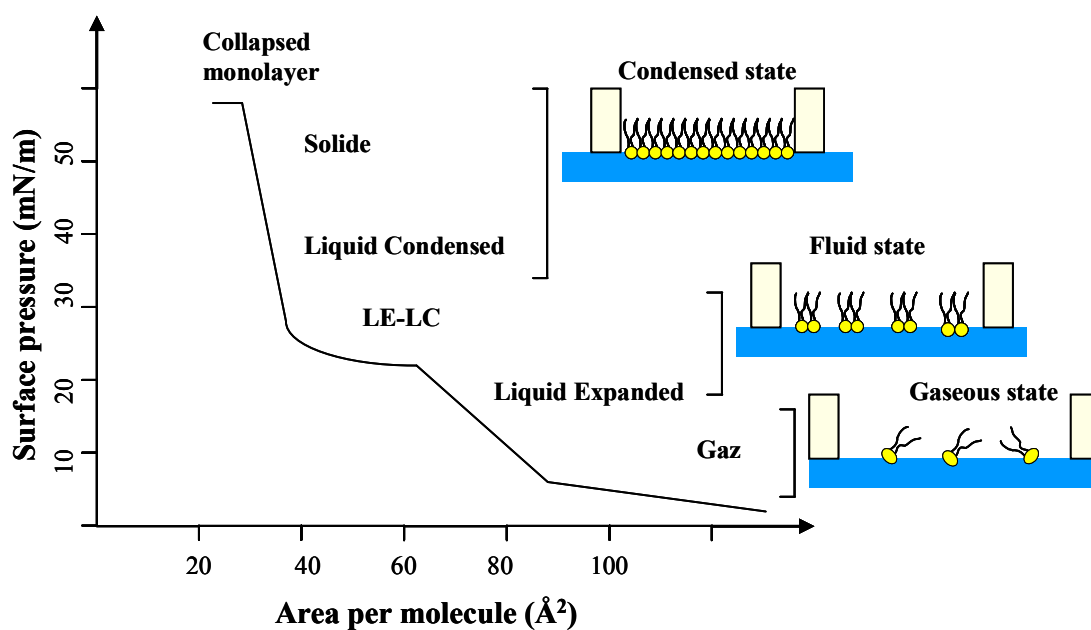


Figure 13. A schematic (π -A) isotherm of a phospholipids monolayer

(Adapted from (Girard-Egrot et al., 2005))

Five main stages in (π -A) isotherm can be observed when the lateral compression of the monolayer is performed:

Stage 1: the intermolecular interaction is weak. Thus, the surface pressure is low and the monolayer is in the gaseous state.

Stage 2: the intermolecular interaction enhances. Thus, the surface pressure increases linearly with decreasing area, and the monolayer is in the fluid state (Liquid expanded).

Stage 3: a transition from liquid expanded (LE) to liquid condensed (LC) of the monolayer is observed. The area per molecule is reduced without significant increase of surface pressure.

Stage 4: the liquid condensed state is compacted. The intermolecular interaction increases to make the film more ordered. Thus, the surface pressure is higher and the monolayer is well organized.

Stage 5: lateral pressure is too high for monolayer stability, and it is called collapse surface pressure. The collapsed monolayer is sent out to form bilayers.

III. 2. 4. *Applications of LB for characterization of lipid membranes interacting with drugs*

Langmuir-Blodgett films are used as a model system for biomimetic studies. The effect of temperature on the state of the DPPC monolayer is revealed in the pressure-area isotherms. Two fluid states, liquid expanded and liquid condensed are evident in the surface pressure versus area isotherm curve of DPPC (Philips and Chapman, 1968).

LB has also been used to characterize the lipid packing of a lipid monolayer upon addition of a drug. Monolayer compression isotherms were measured to study the incorporation of CIP and its pentyl derivative in DPPC. The pressure/area (π -A) isotherms curves of DPPC in the presence of different molar ratio of drugs showed a shift of the curve to the lower area in the presence of CIP, and an expansion of the area in the presence of pentyl-CIP. These data suggest that the drugs perturb the packing of DPPC monolayer (Montero et al., 1997; Hernandez-Borrell and Montero, 2003; Montero et al., 1998).

III. 2. 5. *Advantages and limitations*

The Langmuir-Blodgett technique is an appropriate method for preparing well-organized ultrathin films. These LB films can be used in AFM or ATR-FTIR for the characterization of biological models membranes (e.g surface topography, hydrocarbon chain conformation).

However, the structure and the loss of the integrity of the monolayer, including inhomogeneous crystalline domains, local collapse, trans-bilayers and lateral heterogeneities, can occur during the time elapsed between the spreading and dipping of the monolayer (Rinia and de Kruijff, 2001). Additionally, the interface changes from an air/water to an air/solid interface can induce attractive interactions between the lipids molecules and the substrate, which can modify the molecular arrangement. The integrity of the monolayer depends on the deposition speed, and the transfer surface pressure (Steiner, 1991; Spratte and Riegler, 1994; Steitz et al., 1991). In addition, a lack of thermal stability can also be observed (Oliveira, 1992).

III. 3. Spectroscopic methods

Spectroscopy methods are based on the measurement of electromagnetic radiations emitted or absorbed by a particular sample. The electromagnetic radiation is characterized by an electric and magnetic field component which oscillate in phase perpendicular to each other and to the direction of energy propagation intensity. According to the frequency of the wave, electromagnetic radiations are classified into radio waves, microwaves, infrared, visible light, ultraviolet, X-rays and γ -rays (Figure 14). Radiations produced after the absorption result in electronic transition such in UV-Vis spectroscopy, vibrational and rotational transition such in Infrared spectroscopy or nuclear such in Nuclear Magnetic Resonance.

Spectrophotometry, Fluorescence, Infra-red and Nuclear Magnetic Resonance are mainly used for drug-lipid interaction studies. These methodologies have a high sensitivity and specificity, and they are less time consuming comparing to others analytical methods.

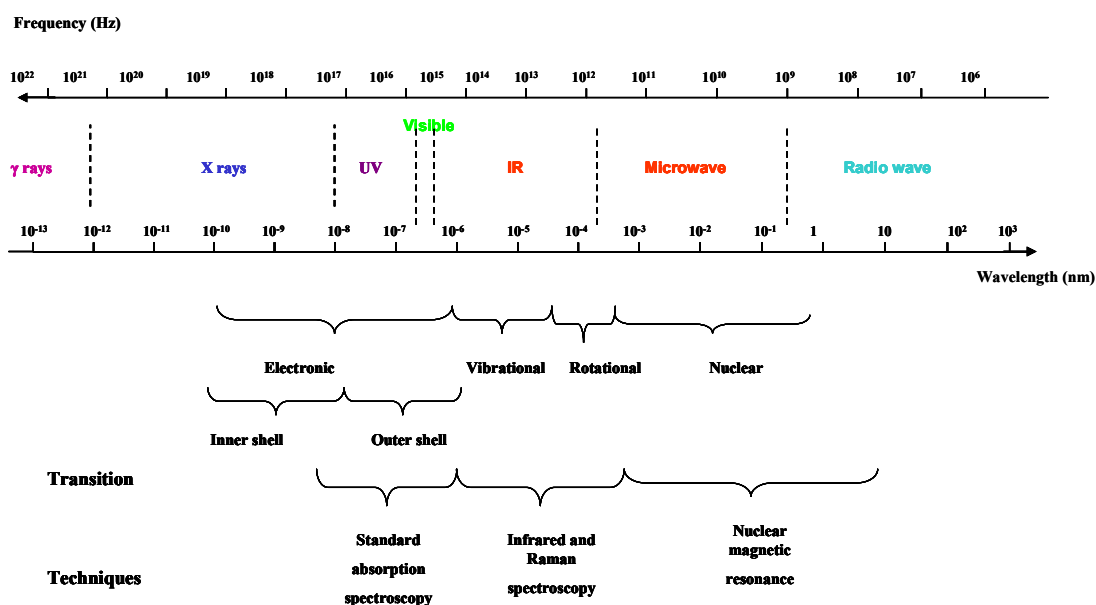


Figure 14. *Electromagnetic spectrum with the characteristic transitions and the relevant spectroscopic techniques*

III. 3. 1. UV/Vis-spectroscopy

III. 3. 1.1. Introduction

Absorption and fluorescence spectra are sensitive molecular methods that can be used for studying the physicochemical properties of drugs and lipids.

The UV absorption spectra, the fluorescence emission spectra, polarization and their time dependence are important parameters that one can use for the characterization of drugs-lipids complexes. To limit ourselves to the topic of our Thesis, we will focus on the interactions of fluoroquinolones with lipids.

III. 3. 1. 2. Physical and chemical principles

Absorption spectroscopy is the measurement of the attenuation of a beam of light after it passes through a sample. The fundamental relationship in quantitative absorption (A) spectrometry is given by Beer Lambert's law:

$$A = \epsilon c l = \log (I_0/I) \quad [\text{Eq. 3}]$$

where ϵ is the molar absorptivity of the fluorophore, l is the optical pathlength, c is the concentration of the sample, and I_0 and I are the intensity of photons incident and transmitted by the sample, respectively.

Fluorescence occurs when a molecule has been promoted to an electronically excited singlet state by absorption, and then decays back to the ground singlet state by emission of photons following the radiative decay process.

The fluorescence provides informations about energy (wavelength), time decay, polarization and intensity (number of photons) at a given wavelength.

The mechanisms by which electronically excited molecules come back to ground state are given by the Jablonski diagram as shown in Figure 15. The absorption of a photon takes the molecule from ground state (singlet state, S_0) to either a first excited state (singlet state S_1) or to a second excited state (S_2). Then the excited molecule relaxes to the lowest vibronic level of the first excited state through internal conversion. It can then relax from the singlet excited state to the ground state via three mechanisms: first, by emitting a photon (radiative process); second, without emitting a photon (nonradiative mechanism), and third by going to a triplet state (T_1) by intersystem crossing, which is also a nonradiative process. The transition from triplet (T_1) to ground singlet state is forbidden and hence is a very slow process relative to fluorescence. Emission from T_1 is called phosphorescence, and generally is shifted to longer wavelengths relative to the

fluorescence. Also the excited state S_1 can be deactivated by a quenching reaction, a process that decreases the fluorescence intensity (Lakowicz, 1999).

The fluorescence emission spectrum is generally a mirror image of the absorption spectrum (S_0 to S_1 transition)

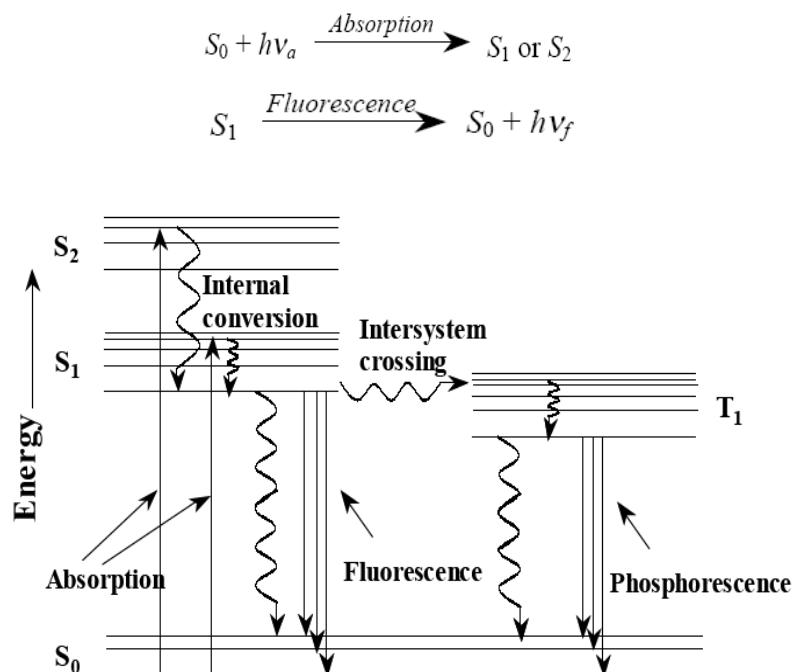


Figure 15. Jablonski diagram showing the energy levels and various processes in an electronically excited molecule. From (Lakowicz, 1999).

The fluorescence intensity of a molecule is characterized by four parameters:

- *The fluorescence quantum yield (Φ)* which defines the fraction of electronically excited molecules that decays to the ground state (S_0) through radiative mechanism, as shown in equation 4:

$$\phi = \frac{k_r}{k_r + k_{nr}} \quad [\text{Eq. 4}]$$

where k_r and k_{nr} , are the radiative and nonradiative rate of the fluorescence, respectively.

- *The Stokes shift ($\Delta\nu$)* in (nm), is the difference between the absorption and fluorescence maxima wavelengths.

- *The fluorescence lifetime (τ)* in (ns), represents the average time spent by the molecule fluorescent (fluorophore) in the excited state (S_1) before coming to the ground state (S_0).

The typical fluorescence intensity decay is a plot of fluorescence intensity as a function of time. For a single fluorophore, the fluorescence intensity decay $I(t)$ is a single exponential as :

$$I(t) = I_0 e^{-t/\tau} \quad [\text{Eq. 5}]$$

where I_0 is the initial intensity and τ is the fluorescence lifetime. This parameter (τ) is related to the radiative (k_r) and the nonradiative (k_{nr}) rates, following equation (6):

$$\tau = \frac{1}{k_r + k_{nr}} = \frac{\phi}{k_r} \quad [\text{Eq. 6}]$$

- *The fluorescence polarization (anisotropy)* defines the fluorescence emission emitted from the samples excited with polarized light. This polarization is due to the photoselection of the fluorophore according to its orientation relative to the direction of the polarized excitation, and can be considered as a competition between the molecular motion (rotational correlation time θ) and the lifetime τ of fluorophore in solution. If the fluorescence lifetime of the fluorophore is much shorter than the rotational correlation time θ (a parameter that describes how fast a molecule tumbles in solution) ($\tau \ll \theta$), the excited molecules will stay aligned during the process of emission and, as a result the emission, will be polarized. In a typical experiment the sample containing the fluorescent molecule is excited with linear polarized light and the vertical (I_v) and horizontal (I_h) components of the intensity of the emitted light are measured. The polarization (P) and anisotropy (r) are calculated using the following equations (7, 8), respectively:

$$P = \frac{I_v - I_h}{I_v + I_h} \quad [\text{Eq. 7}]$$

$$r = \frac{I_v - I_h}{I_v + 2I_h} \quad [\text{Eq. 8}]$$

The fluorescence polarization (or anisotropy) is a measure of the average depolarization during the lifetime of the excited fluorophore under steady state conditions.

III. 3. 1. 3. *Applications of UV/Vis-spectroscopy in fluoroquinolones-lipids interactions*

Generally speaking, UV/Vis-spectroscopy provides informations on photochemical properties of drugs such as polarity, ionization constant, Stokes shifts, fluorescence quantum yield and fluorescence lifetime. It also allows the evaluation of the binding parameters of drugs to lipids (e.g stoichiometry, affinity, cooperativity and number of electrostatic interaction). These data are useful for analyzing the conformational changes (e.g. orientation, mobility, fluidity...etc) resulting from the interaction of drugs with lipids, and to evaluate the biological impact of the considered interaction.

Regarding fluoroquinolones, the major applications of absorption spectrophotometry and fluorometry can be classified into two main groups:

i) *The spectroscopic properties of fluoroquinolones*

Fluorescence properties of fluoroquinolones antibiotics make them optimal molecules for *in vitro* experimental studies. The spectroscopic properties of these drugs are interesting to study those properties that may have an effect on their *in vivo* activity (Takacs-Novak et al., 1990; Yu et al., 1994).

As previously described, fluoroquinolones have two proton-binding sites (the piperazinyl in the 7 position, and the carboxyl in the 3 position). They exist in four microspecies in aqueous solution, namely positive H_2Q^+ , negative Q^- , neutral HQ^0 and zwitterionic HQ^{+-} .

✓ *Fluorescence spectra of fluoroquinolones are dependent on the solvent properties*

This has been studied with three fluoroquinolones, ofloxacin (OFL) and norfloxacin (NOR), on the hand, and flumequine (FLU) on the other hand.

- OFL and NOR exist mainly in neutral zwitterionic forms in water, and in other microspecies forms in organic solvents. In aqueous solution, the fluorescence quantum yield of OFL and NOR is high. In organic solvents, the internal conversion rate of $S_1 \rightarrow S_0$ for OFL and NOR is very fast, owing to the similar geometrical structures and dipole moments between these states, the fluorescence quantum yield becomes weak and the lifetimes are long (Anstead et al., 1993). The fluorescence properties of FLU are relatively insensitive to the solvent nature, as indicated in the Table 4 (Park et al., 2000; Park et al., 2002; Park et al., 2004).

Table 4. The fluorescence spectral data of ofloxacin, norfloxacin and flumequine.

Fluorescence emission (E), Stokes' shifts ($\Delta\nu$), fluorescence quantum yield (Φ) and fluorescence lifetime (τ)
(Park et al., 2002)

Drug	Solvent	λ_{em} (nm)	$\Delta\nu$ (cm ⁻¹)	Φ	τ (ns)
Ofloxacin (OFL)	H ₂ O	475	8984	0.199	5.86
	CH ₃ OH	482	9931	0.006	12.5
	CHCl ₃	455	9535	0.004	14.2
Norfloxacin (NOR)	H ₂ O	436	7160	0.160	2.30
	CH ₃ OH	448	7901	0.020	2.56
	CHCl ₃	419	7409	0.008	3.27
Flumequine (FLU)	H ₂ O	375	3987	0.034	0.73
	CH ₃ OH	371	3761	0.034	0.82
	CHCl ₃	372	3652	0.036	0.71

✓ *Fluoroquinolones are more photochemically active in an environment that is both protic and polar*

- The photochemical and photophysical properties of NOR have been studied in aqueous solutions at pH between 7.4 and 12. It was found that the fluorescence quantum yield decreased with pH (from 0.12 at pH 7.4 to less than 0.001 at pH12), suggesting a different intrinsic radiative constants of the fluoroquinolone anion and the zwitterionic form (Bilski et al., 1996;Huang et al., 1997;Bilski et al., 1998;Cuquerella et al., 2004).

- A similar behavior has been reported for CIP (Vazquez et al., 2001a). Indeed, the fluorimetric titration of CIP as a function of pH was investigated to determine the ionization constants of this antibiotic in solution and in the presence of liposomes. The maximum emission spectra of CIP were observed in acidic to neutral media, pH between 4.2 and 7.4, and almost no fluorescence was observed in alkaline media (pH10.4). A similar pattern was observed in the presence of either DPPC or DPPC: DPPG (0.9:0.1, M:M) liposomes. The interpretation of these data was that the N-7 of the piperazinyl substituent could act as an electron-releasing group for the quinolone ring (electron acceptor), resulting in an intramolecular quenching phenomenon.

- The absorption spectra of MXF at different pH show also important changes in the peak position and emission intensity of the drug with acidity (Langlois et al., 2005).

This effect of pH on photochemical properties of fluoroquinolones allows determining the protonation equilibrium between the four microspecies: positive H₂Q⁺, negative Q⁻,

neutral HQ^0 and zwitterionic HQ^+ as shown in Figure 16. Microconstants values of these microspecies were determined by absorption spectroscopy at different pH of the medium and represented in the Table 5 (HernandezBorrell and Montero, 1997;Vazquez et al., 2001a;Langlois et al., 2005). The distribution diagram of these four microspecies shows a predominance of neutral and zwitterionic forms at neutral pH and the majority of positively forms at acidic pH (Hernandez-Borrell and Montero, 2003). The UV absorption spectroscopy was also used to estimate the degree of partitioning of CIP into *Escherichia coli* lipid membrane extract and to measure protonation equilibrium of CIP and MXF (Vazquez et al., 2001b;Sun et al., 2002;Langlois et al., 2005).

- The measure of the respective abundance of the different microspecies can be used to determine the distribution coefficient of CIP and MXF at different pH ($\log D_{\text{octanol/water}}$). By comparing their $\log D$ at pH 7.4, values (-0.79 vs -0.28), CIP is considered to be more hydrophilic than MXF (Takacs-Novak et al., 1990;Sun et al., 2002;Langlois et al., 2005).

Table 5. Protonation of CIP and MXF

(k_{11} , k_{12} , k_{21} and k_{22} are microconstants values of the microspecies as shown in Figure 16)

Drug	pKa ₁	pKa ₂	k ₁₁	k ₁₂	k ₂₁	k ₂₂	Reference
CIP	6.08±0.11	8.58±0.55	6.61	8.04	6.23	8.43	(Vazquez et al., 2001b)
	6.18	8.73	6.19	8.72	7.04	7.86	(Sun et al., 2002)
MXF	6.25	9.29	7.46	8.08	6.29	9.25	(Langlois et al., 2005)

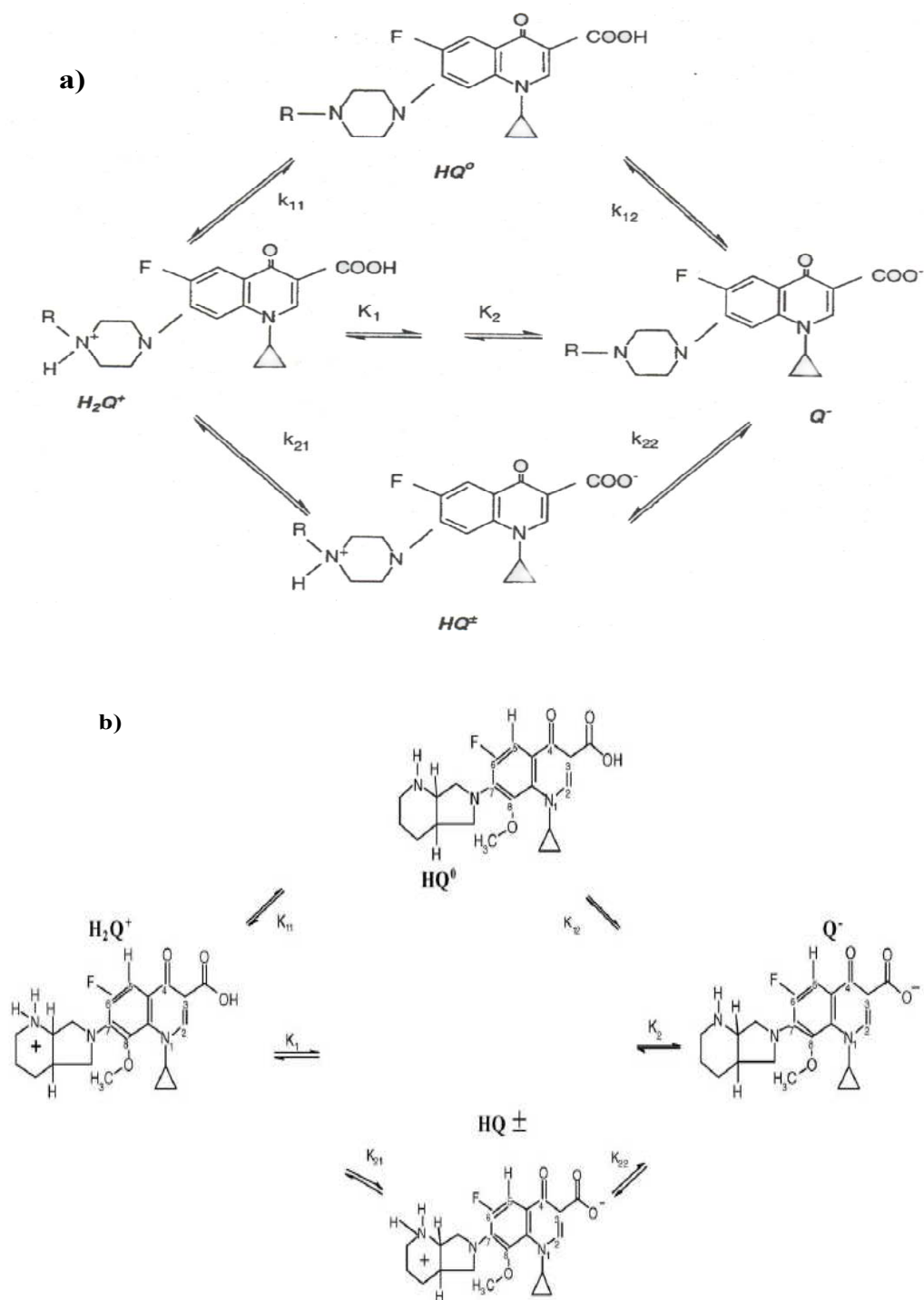


Figure 16. Protonation equilibrium of CIP (a) and MXF (b) (R=H)
 (HernandezBorrell and Montero, 1997;Huang et al., 1997;Merino et al., 2002;Langlois et al., 2005)

✓ *Fluorescence spectra of fluoroquinolones is dependent on the presence of trivalent metal ions*

Spectrophotometry was employed to investigate the complex formation between moxifloxacin or fleroxacin and metal ions (e.g. Al^{+3}) (Djurdjevic et al., 2007). In their presence, the maximum absorption peaks of these fluoroquinolones are shifted toward higher wavelengths. In conjunction with potentiometric studies, the authors indicate a formation of a stable aluminum-fluoroquinolone complex, favored by the presence of a sodium dodecylsulfate (SDS) in which the drug is protonated.

ii) *The binding properties and effect of fluoroquinolones on the lipids*

Fluorescence probes are frequently used to determine binding parameters of drugs to lipids, and to study the changes in membrane organization and membrane fluidity induced by these agents.

✓ *Localization of fluoroquinolones in the phospholipids bilayer and their effect on the membrane fluidity using DPH and TMA-DPH probes*

- Amongst the various physical states of lipids, we must distinguish two major ones called liquid crystalline (L_{α}) and solid-like gel (L_{β}), respectively, (Figure 17). The melting transition temperature (T_m) of lipids reflects the change from the gel state (solid) along the chains to the liquid crystalline state (fluid) as the temperature is increased (Keough and Davis, 1979; Davis et al., 1981).

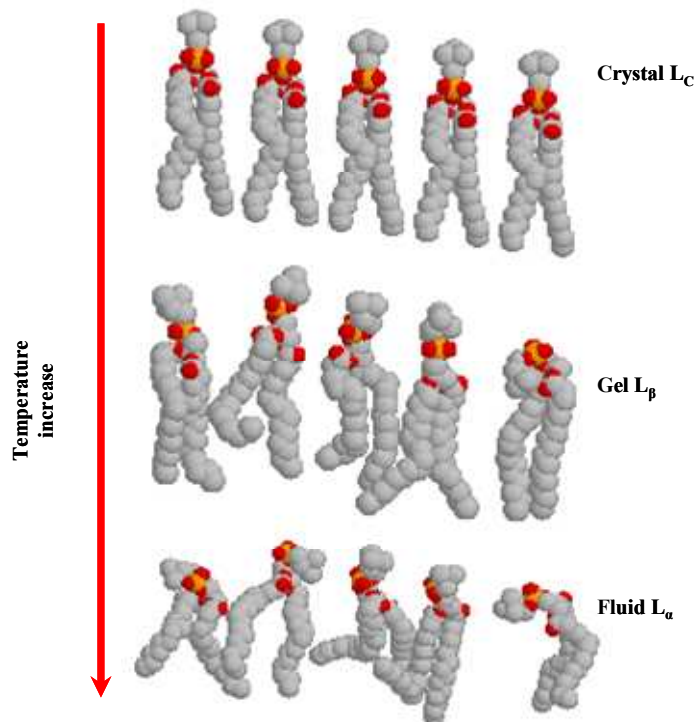


Figure 17. The versatility of lipids is a function of the temperature, resulting in the crystalline, gel and fluid states. Phosphatidylcholine is taken as model lipid.

(Adapted from: <http://www.umass.edu/microbio/rasmol/3x5w.gif>)

Heller et al., (1993); *J.Phys.Chem.* 97:8343 (Eric Martz)

Two probes are frequently used to investigate the drug localization into the lipid bilayer and its effect on the membrane fluidity: 1-(4-trimethylammoniumphenyl)-6-phenyl-1,3,5-hexatriene (TMA-DPH), a probe, which according to Illinger et al (Illinger et al., 1995) is distributed preferentially at the surface of the bilayer, and 1,6-diphenyl-1,3,5-hexatriene (DPH), a probe known to be located in the hydrophobic core of the bilayer (Figure 18) (Illinger et al., 1995;Saldanha et al., 2002).

With fluorescence anisotropy, membrane fluidity is interpreted in terms of hindrance to rotational motion of the probe, since it is embedded in the constraining phospholipidic membrane array (Kinosita, Jr. et al., 1977). The anisotropy value (r) is high in the gel crystalline state of the lipid and low in the fluid state. Therefore, thermotropic variations allow determining transition temperature (T_m) from the gel to its fluid state.

The localization of CIP in the DPPC phospholipids bilayer and its effect on membrane fluidity was investigated using steady-state anisotropy of TMA-DPH and DPH (Merino et al., 2002;Hernandez-Borrell and Montero, 2003). In the presence of CIP, a slight decrease of the transition profile of TMA-DPH and DPH, and a fluidification effect in the fluid state of DPPC, were observed at acidic pH (4.7). Since the positive microspecies (H_2Q^+) are predominant at this pH, the authors suggested that the main force involved in the interaction between CIP and DPPC is hydrophobic.

✓ *Binding of fluoroquinolones to the lipids and their effect on the surface potential of liposomes using ANS probe*

- The 8-anilin-1-naphtalene sulfonic acid (ANS) (Figure 18) is an anionic hydrophobic fluorescent label. ANS is not fluorescent in water but becomes fluorescent when it is bound to a membrane (lipophilic environment). This property makes it a sensitive indicator of membrane potential (Ma et al., 1985).

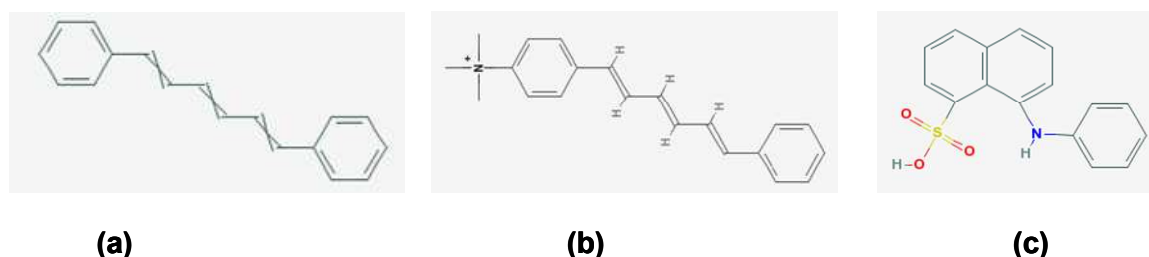


Figure 18. Chemical structural of some fluorescence probes
 (a) diphenylhexatriene, (b) Trimethylammonium-diphenylhexatriene (TMA-DPH) and
 (c) 8-anilin-1-naphtalene sulfonic acid (ANS).

To determine the association constant (K_a) (M^{-1}) of ANS to lipids, fluorescence titration curve of liposomes with various concentrations of ANS are analyzed using equation 9.

$$[ANS]_{bound} = C_{max} \frac{(K_a [ANS]_{free})^b}{1 + (K_a [ANS]_{free})^b} \quad [\text{Eq. 9}]$$

where C_{max} is the maximum concentration of ANS bound to lipids, b is a cooperativity parameter, and $[ANS]_{bound}$ and $[ANS]_{free}$ are the concentrations of bound and free ANS at equilibrium, respectively.

The fraction of ANS bound is calculated from equation 10:

$$[ANS]_{bound} = \frac{F_b - F_0}{A_b - A_0} \quad [\text{Eq. 10}]$$

and the amount of ANS free is deduced from equation 11:

$$[ANS]_{free} = [ANS]_{total} - [ANS]_{bound} \quad [\text{Eq. 11}]$$

where F_b , F_0 , A_b and A_0 are the fluorescence intensities and the emission coefficients of ANS in the presence and the absence of lipids, respectively.

The emission coefficients of ANS are determined as the slope of the fluorescence emission intensity at high sample concentration (1mM) as a function of low concentration of ANS (0.1-1.4 μ M).

To determine the variation of the surface potential (mV) in the two different samples (liposomes), the values of the different association constants (K_a) obtained from equation 9 are used in equation 11.

$$\Delta \psi = \frac{RT}{F} \ln \left[\frac{K_{a1}}{K_{a2}} \right] \quad [\text{Eq. 12}]$$

where R , T and F are the universal constant of gases, the temperature and the Faraday constant, respectively. K_{a1} and K_{a2} are the association constants of ANS to the two types of sample (Ma et al., 1985).

- ANS has been used to examine the binding of CIP to lipids and its effect on the surface potential of liposomes. In these studies, several LUVs liposomes were used: zwitterionic (DPPC), DPPC negatively charged with 10 M% of DPPG, and *Escherichia coli* lipid

membrane extract liposomes (Vazquez et al., 2001b; Vazquez et al., 2001c; Montero et al., 2006). It was found that CIP quenched the fluorescence of ANS bound to liposomes in competition experiments, and the displacement of ANS was greater for liposomes with DPPG, due to the repulsive electrostatic forces between headgroup of DPPG and negative charge of the probe (Ma et al., 1985). The results indicate that the binding of ANS to liposomes surface is dependent on the presence of the drug (CIP) and the lipid composition.

III.3.1. 4. *Advantages and limitations*

The simple and relatively inexpensive technique of UV/Vis-spectroscopy has made it to become a universal and accurate method for estimating the degree of partition of fluorescent drugs into a lipid membrane. Several parameters, such as pH, polarity of the medium and temperature can affect the absorption and/or fluorescence spectra, from which the partition and other properties of drugs can be inferred.

In addition, fluorescence measurement is widely used to obtain information regarding the nature and accessibility of binding site of drugs to the lipid.

Although the measurement of absorption and fluorescence spectra (at micromolar range) can be very sensitive, the positions of spectral bands are not sensitive to the finer detail of the molecular structure, such as the presence of specific functional groups. Hence, fluorometry is not useful for molecular identification.

It should also be noted that a good interpretation of UV-Vis spectra requires three important conditions: the absence of significant noise background, a drug with a high fluorescence quantum yield, and the absence of perturbation of the signal by related (e.g. photobleaching, Raman effect) and unrelated (e.g. absorption of other compounds) phenomena.

III.3. 2. Fourier Transform Infrared Spectroscopy (FTIR)

III.3.2.1. Introduction

FTIR spectroscopy is one of the most used methods to study biological membranes. It provides information on the physicochemical behavior of phospholipids-drugs complex under various conditions (e.g. temperature, pressure, pH ...etc). In addition, information on the orientation and degree of organization of a drug molecule, within the phospholipid bilayer, can also be obtained by monitoring polarized spectra. Thus, infrared spectroscopy is an important tool for elucidation of membrane structure and for identification of drug effects.

III.3.2.2. Physical and chemical principles

Infrared (IR) absorption spectroscopy is the measurement of different IR radiation (frequencies) absorbed by a sample positioned in the path of an IR beam, as well as the intensities of these absorptions. Determination of these frequencies allows identification of the sample chemical structure, since chemical functional groups are known to absorb radiation at specific frequencies. The intensity of the absorption is related to the concentration of the sample. An IR spectrum is the plot of radiation absorption as a function of wavenumber, which is itself proportional to the frequency of the radiation. Wavenumber (ν) and wavelength (λ) can be interconverted (equation 13):

$$\nu(\text{cm}^{-1}) = \frac{1}{\lambda(\text{cm})} \quad [\text{Eq. 13}]$$

The IR radiation spans a section of the electromagnetic spectrum (Figure 14) having wavelengths (λ) from 0.78 to 1000 μm , or wavenumbers (ν) from roughly 13.000 to 10 cm^{-1} . The mid-infrared region from 4000 to 400 cm^{-1} is typically used for biological samples (Lee, 1997).

Understanding of IR spectroscopy theory requires the study of vibration mechanics. In a normal mode of vibration, each atom in a molecule executes a simple harmonic oscillation (vibration) about its equilibrium position. For a two atomic system consisting of two masses m_1 and m_2 connected by a bond, the vibrational frequency (ν) is related to the force constant (k) and the reduced mass (μ) by the following equation (14):

$$\nu = \frac{1}{2\pi} \sqrt{\frac{k}{\mu}} \quad \text{with} \quad \mu = \frac{m_1 m_2}{m_1 + m_2} \quad [\text{Eq. 14}]$$

From Equation 14, it is evident that the vibrational frequency is related to the rigidity or strength of the bond (force constant) and masses of the bonding atoms. Specifically, the vibrational frequency is higher for stronger bonds and for lighter atoms. For a polyatomic molecule, there is more than one fundamental frequency of vibration. The mathematical treatment of this vibration and rotation of a molecule is to set up the expression for the kinetic and potential energies of the molecule in terms of the coordinates of the atoms, and to obtain the wave equation for vibration, rotation, and translation. This procedure is not simple and utilizes quantum-mechanical treatments. It is found that for a molecule of n atoms, there are $(3n-6)$ modes of vibrations for a non linear molecule (e.g. H_2O) and $(3n-5)$ modes of vibrations for a linear molecule (e.g. CO_2). The number three corresponds to the degrees of freedom for each atom and the numbers 6 and 5 are conditions required to define the rotation and translation motions of the molecule. The condition which drops out in a linear molecule is the prohibition of rotation about the z axis, since a linear molecule cannot rotate about its axis unless it is distorted (Bright-Wilson et al., 1955).

Two types of vibrations, stretching (asymmetric or symmetric) and bending (scissoring, wagging, twisting or rocking) are responsible for the most important peaks used to identify organic compounds, in particular to provide information on the structure of the acyl chain of phospholipids. Figure 19 illustrates a few types of vibration for the CH_2 group. Bending motions require less energy and absorb at lower frequency (1400 cm^{-1}) than stretching motions (2800 cm^{-1}).

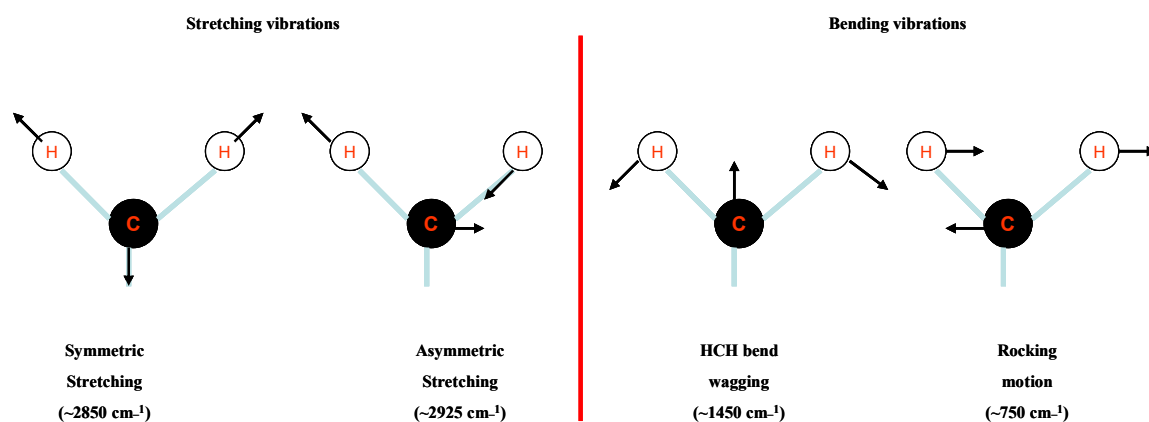


Figure 19. The type of normal vibration for a CH_2 group
Adapted from (Lee and Chapman, 1986; Lee, 1997)

III.3.2.3. Fourier Transform spectrometer

In Fourier Transform Infra-Red (FTIR) instrument, all IR wavelengths of the polychromatic source are measured at the same time. A typical FTIR spectrometer is composed of three basic elements: a radiation source, an interferometer, and a detector (Figure 20). The FTIR method splits the electromagnetic radiation into two beams. One beam travels over a longer path side of the spectrometer than the other beam. A recombination of the two beams creates an interference pattern or interferogram. Fourier Transformation is a computerized mathematical treatment of data from interferogram into the usual IR spectrum. FTIR has very high resolution ($<0.001\text{ cm}^{-1}$), and allows the acquisition of spectra from small samples.

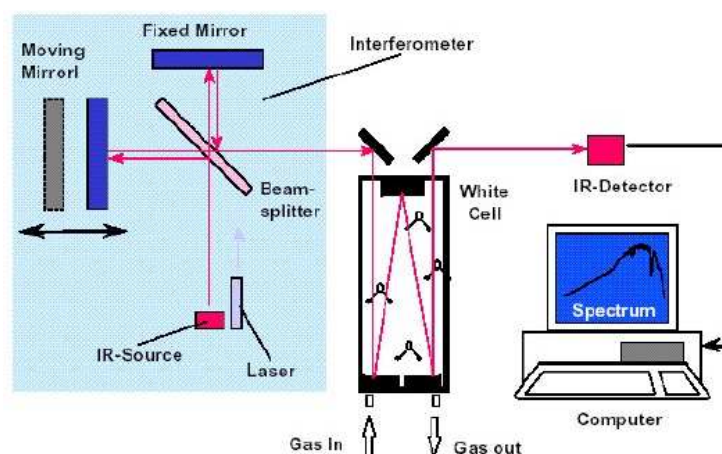


Figure 20. Schematic of a FTIR spectrometer, with Michelson interferometer composed of a moving mirror, a fixed mirror and a beamsplitter

III.3.2.4. Attenuated Total Reflection (ATR)

The principle of this method is based upon total reflection of IR radiation that occurs within a high refractive index of the internal reflection element (IRE) (Figure 21). Above a critical angle (θ_c), which depends on the refractive index of the IRE (n_1) and of external medium (n_2), the light beam is completely reflected when it impinges on the surface of the IRE and evanescent waves are formed (sinusoidal waves are internally reflected off an interface at an angle greater than the critical angle).

If an absorbing sample is placed in contact with the surface of the crystal at the point of the internal reflection, energy is absorbed by the sample. The reflected beam contains spectral information of the sample.

The penetration depth (d_p) of the evanescent wave is in the order of several micrometers depending on the angle of incidence of the beam (θ), the wavelength of the light (λ) and on the refractive indices of the sample (n_2) and ATR element (n_1) as given by the equation (15) (Fringeli and Gunthard, 1981):

$$d_p = \frac{\lambda}{2\pi n_1 \sqrt{\sin^2(\theta) - \left(\frac{n_2}{n_1}\right)^2}} \quad [\text{Eq. 15}]$$

Typical materials for ATR elements include germanium, silicon and diamond. The latter is excellent for its mechanical properties but is less used due its high cost. The most usual design is the trapezoidal plate which allows molecular orientation to be determined by means of linear dichroism for oriented membranes.

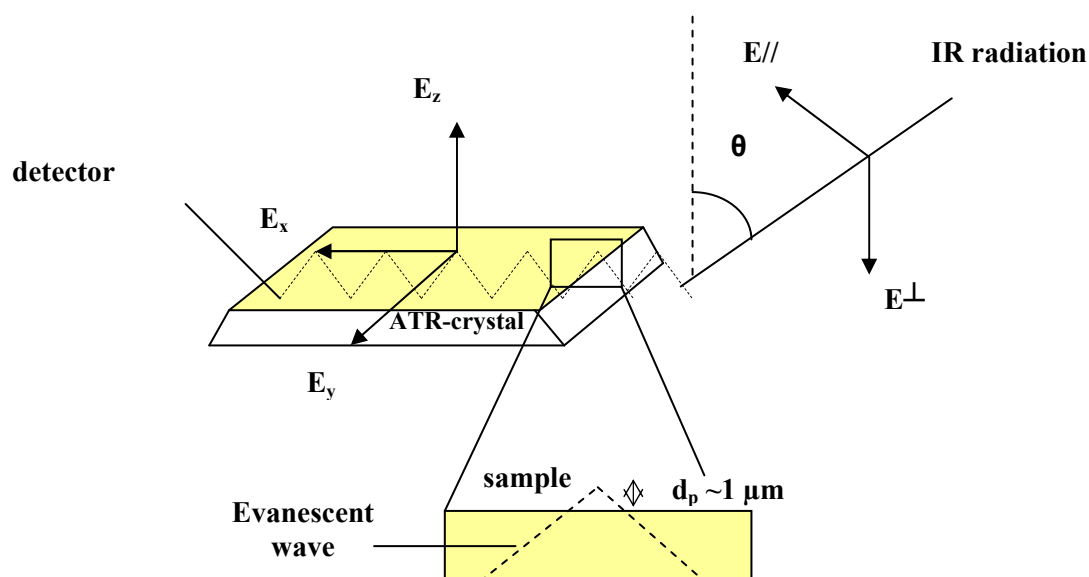


Figure 21. Schematic drawing of the ATR crystal

Adapted from (Goormaghtigh et al., 1999).

III.3.2.5. Properties of ATR-FTIR spectra

Several parameters can influence the band shape of ATR spectra: the wavelength of the incident radiation, the refractive indices of both IRE and the sample, the angle of incidence and the efficiency contact between the sample and the IRE (Goormaghtigh et al., 1999). In addition, the nature of the internal reflection element (IRE) and the thickness of the sample are two parameters which are particularly involved in the quality of dichroic spectra, from which the orientations of molecules are derived.

Non polarized spectra for state behavior and conformation determination of lipids

Information on the structure of the acyl chain and of the interfacial and head group regions of a membrane bilayer can be obtained by recording non polarized spectra.

The sharp main endothermic phase transition of aqueous phospholipid bilayers results in pronounced alterations in the methylene band parameters (Asher and Levin, 1977; Cameron and Mantsch, 1978; Cortijo and Chapman, 1981). The band maximum frequencies of the CH₂ asymmetric and symmetric stretching bands are sensitive to the static order of the acyl chains. In fact, in a phospholipid, an increase of temperature induces a rapid isomerization from *trans* (crystalline state) to *gauche* (fluid state). Thus, an increased proportion of *gauche* conformers above the phase transition causes a shift in stretching bands of CH₂ to higher frequencies (Casal et al., 1980). Consequently, the CH₂ bandwidths are sensitive to the degree of motional freedom of the CH₂ groups.

The band progression due to CH₂ wagging modes (1400 cm⁻¹) and CH₂ rocking band (720 cm⁻¹) of phosphatidylcholine are also sensitive to the lipid phase behavior, and determine changes in acyl chain packing (conformation) from hexagonal to orthorhombic (Chapman et al., 1967).

The structure of the interfacial region of lipid assemblies can be examined *via* the ester group vibrations. The most intense of these bands are the C=O stretching frequencies between 1750 cm⁻¹ and 1700 cm⁻¹, which are associated with the two ester groups in diacyl lipids: the carbonyl at the *sn-1* and the *sn-2* positions respectively. A shift in the C=O bands at the pre-transition temperature is a reflection of a decrease in the tilt of the acyl chains with respect to the bilayer normal (Bush, 1980; Casal et al., 1984; Levin, 1982; Mushayakarara, 1980).

The state of hydration of phospholipid bilayers can be evaluated *via* asymmetric (1250 cm⁻¹) and symmetric (1085 cm⁻¹) stretching modes of the PO₂⁻. Dehydration results in band shifts towards higher wavenumbers (Arrondo et al., 1984; Casal and Mantsch, 1984).

Polarized spectra for determination of lipids orientation

The possibility to obtain information on the orientation of different regions of the phospholipid molecules is a successful application of ATR-FTIR spectroscopy. The infrared light absorption is maximal if the dipole transition moment is parallel to the electric field component of the incident light. The orientation of the dipole is obtained by measuring the spectral intensity of polarized incident light.

The dichroic ratio, R^{ATR} , is the ratio of the integrated absorbance of a band measured with a parallel polarization of the incident light $A_{//}$ to the absorbance measured with a perpendicular polarization of the incident light A_{\perp} , as shown by equation (16):

$$R^{ATR} = \frac{A_{//}}{A_{\perp}} \quad [\text{Eq. 16}]$$

The dichroic ratio is used to determine the orientational order parameters of the drug relative to the lipid plane. It is related to an orientational order parameter, $S_{\text{experimental}}$, which can be expressed by equation (17):

$$S_{\text{experimental}} = S_{\text{membrane}} \cdot S_{\text{helix}} \cdot S_{\text{dipole}} \quad [\text{Eq. 17}]$$

where S_{membrane} describes the distribution function of the lipid membrane patch with respect to the internal reflection element, S_{helix} describes the orientation of the helices within the membrane plane (and assumed to be one, $S_{\text{helix}} = 1$) and S_{dipole} describes the dipole orientation within the helix axis (Figure 22) (Rothschild and Clark, 1979; Goormaghtigh et al., 1999).

From the dipole orientation with respect to the IRE normal, the dichroic ratio can be measured at various angles. Dichroism measurements of the CH_2 wagging band are often used to find the average special orientation of the membrane. Therefore, the orientation of drugs within lipid can be also evaluated (Fringeli and Gunthard, 1981).

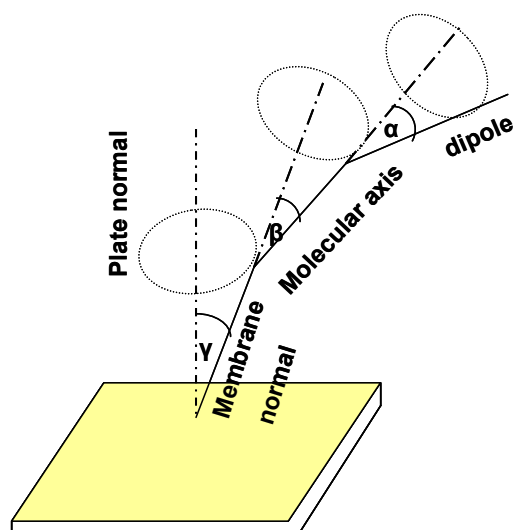


Figure 22. Set of axial symmetric distributions.

The dipole moment is distributed about the α -helix axis (angle α), which is distributed about the membrane normal (angle β) that has a mosaic spread distribution about the sample normal (angle γ). Adapted from (Rothschild and Clark, 1979).

III.3.2.6. Applications of ATR-FTIR spectroscopy to drug-lipids interactions

✓ *Changes of state transition profile of lipids induced by interaction with drug*

Analysis of the IR absorption spectra of the phospholipids in function of temperature provides information on the state transition temperature. Upon addition of drugs, changes in state transition profile and/or the appearance of new states can be observed.

A first example is the interaction of acetylsalicylic acid (ASA) with dipalmitoyl phosphatidylcholine (DPPC) (Casal et al., 1987). IR spectra of hydrated samples of DPPC were measured in the absence and presence of the ASA as a function of temperature and at different lipid–drug ratios. From the temperature dependence of the wavenumber of the CH₂ symmetric stretching vibrational mode (ν CH₂), the authors found that ASA decreases both the main and pre-transition temperatures, notably at drug-DPPC molar ratio of (1:1).

Another example is the interaction of D-propranolol (a beta-blocker agent) with dimyristoyl-phosphatidylcholine (DMPC) (Cao et al., 1991). The FTIR spectra of the symmetric CH₂ stretching mode of DMPC liposomes in the absence and presence of the drug indicated that, in addition to the shift in the transition temperature, the drug changed the gel state of the membrane and induced a second transition state.

The IR spectroscopy is also useful to study antibiotic-lipids interaction. A quantitative determination of acyl chain conformation in Gramicidin–DPPC mixtures has been investigated (Davies et al., 1990). The results show that the drug induced disorder of phospholipid gel state and order in liquid crystalline state.

✓ *Orientation of lipid bilayer in presence of drugs*

IR spectroscopy allows determination of the orientation and the degree of organization of phospholipid bilayer in the presence of drugs. Polarized IR spectra, were used to evaluate the localization of proteins within lipids bilayers (Rothschild and Clark, 1979; Rothschild et al., 1980). The application of IR spectroscopy to orientation of phospholipids in the presence of fluoroquinolones is discussed in this Thesis.

III.3.2.7. Advantages and limitations

IR spectroscopy has several advantages for membrane studies. The variations in frequency, line width, and intensity are sensitive to structural transitions of both lipid and drugs components.

The vibrations of individual groups provide structural information on highly localized regions of the bilayer. Thus, C-H stretching absorptions of the lipid acyl chains are distinguished from the carbonyl stretching of the interfacial region and the phosphate stretching of the polar headgroup.

The principal advantage of IR spectroscopy is the possibility of studying simultaneously the structure of lipids and drugs in intact biological membranes without addition of any external probe. The time-scale of the molecular vibrations is indeed very fast (in order of 10^{13} s^{-1}).

However, some factors can influence the IR spectroscopy. In particular, strongly distorted spectra may result from an unwise choice of the incident angle, the nature of the internal reflection element, or the thickness of the sample (Goormaghtigh et al., 1999).

The application of the IR is also limited to the molecules which are sufficiently transparent and active in the IR region. Complex molecules, such as lipids, (~ 130 atoms) have approximately 384 normal vibrations. This vibration number leads to an overlap of absorption bands, which complicates the identification and the interpretation of a single band, notably with aqueous samples. In fact, liquid water has strong and broad absorption bands, overlapping a considerable part of the IR spectral range (Fringeli and Gunthard,

1981). Therefore, the use of aqueous systems requires a thin film with a high concentration of the sample.

More recently, a combination of atomic force microscopy (AFM) and ATR-FTIR has been developed (Verity et al., 2009). This method provides conformational changes not resolvable by in situ AFM, with topographical details that are not identified by ATR-FTIR spectroscopy.

III. 3. 3. Nuclear Magnetic Resonance spectroscopy (NMR)

III. 3. 3. 1. Introduction

NMR technique has been applied to study the dynamics, the conformation, and the changes in membrane properties caused by addition of drugs. It provides detailed information about molecular conformation and ordering of lipids interacting with drugs. Additional information on molecular conformation can be obtained by two dimensional transfer, Nuclear Overhauser Effect (NOE) spectra, or 2-D homonuclear NMR Correlation Spectroscopy (COSY) used to measure the distance between nuclei. These two techniques have not been used in our Thesis and will, therefore, not be further detailed (more information is available in (Martin and Zektzer, 1988)).

III. 3. 3. 2. Physical and chemical principles

NMR is a spectroscopic method examining the absorption of radio frequency electromagnetic waves (Figure 14). From the analysis of the interaction between the magnetic moments of sample nuclei and an applied electromagnetic wave, NMR technique provides information about structure and dynamics properties of a sample.

✓ Nuclear magnetic moment (μ)

A nucleus is built up of protons and neutrons moving in a very small volume. Each of these particles is characterize by an orbital angular momentum associated with its motion and a spin angular momentum intrinsic to the particle. The sum of the orbital and spin angular moments of the particles, called “nuclear spin vector” (L), is given by equation (18):

$$L = \frac{h}{2\pi} \sqrt{I(I+1)} \quad [\text{Eq. 18}]$$

where h is the Planck's constant, and I is a nuclear spin number (taking one of the values 0, $\frac{1}{2}$, 1, $\frac{3}{2}$ and so one).

Nuclei with even numbers of protons and neutrons (like ^{12}C and ^{16}O) have a null spin. Nucleic with odd numbers of protons and/or neutrons (like ^1H , ^{13}C , ^{19}F , ^{31}P) have a magnetic (dipole) moment (μ) proportional to the spin vector (L) as expressed by equation (19):

$$\mu = \gamma L \quad [\text{Eq. 19}]$$

where the gyromagnetic ratio γ is a constant characteristic of each nuclide (Table 6).

Table 6. Gyromagnetic ratios (γ), NMR frequencies (ν), and natural abundances of some isotopes (Chang, 2005)

Isotope	I	γ ($10^7 \text{ T}^{-1} \text{ s}^{-1}$)	ν (MHz)	Natural abundance (%)
^1H	1/2	26.75	200	99.985
^{13}C	1/2	6.73	50.3	1.108
^{19}F	1/2	25.17	188.3	100
^{31}P	1/2	10.83	81.1	100

✓ Magnetic Resonance

The sum of the dipole moments of identical spins is called magnetization. In the absence of an external magnetic field, the nuclear magnetic moments of a sample are oriented at random giving a null resultant. When an external magnetic field B_0 is applied to the sample, the energy of interaction E between the magnetic moment μ of each nucleus and B_0 is given by equation (20):

$$E = h\nu = \mu B_0 \quad [\text{Eq. 20}]$$

Nuclei will tend to lose energy by orienting their magnetic moments in the direction of the field. However, a non-null resultant parallel to B_0 remains. This phenomenon is called “spin-polarization”.

Nuclear magnetic resonance reflects the transition from a nuclear spin energy level ($I = +\frac{1}{2}$), to the nuclear spin level ($I = -\frac{1}{2}$) (Figure 23) by varying either the frequency of the applied radiation or the intensity of the magnetic field, until the resonance condition is reached (the two magnetic moments wobble around the axis of the applied field). The resonance frequency (ω) or Larmor is given by equation (21):

$$\omega = \gamma B_0 \quad [\text{Eq. 21}]$$

Thus, magnetic resonance occurs when the protons in the spin state ($I = +\frac{1}{2}$) absorb energy of a specific frequency and change their spin state to ($I = -\frac{1}{2}$). The spectrometer records the NMR spectrum, as these nuclei return to equilibrium in a process called “relaxation”.

The NMR signal corresponding to a magnetization component as a function of time $I(t)$ is called the *free induction decay (FID)*, and the Fourier transformation is a convenient mathematical tool to give a frequency function $I(\nu)$ (Chang, 2005; Paniagua, 2005).

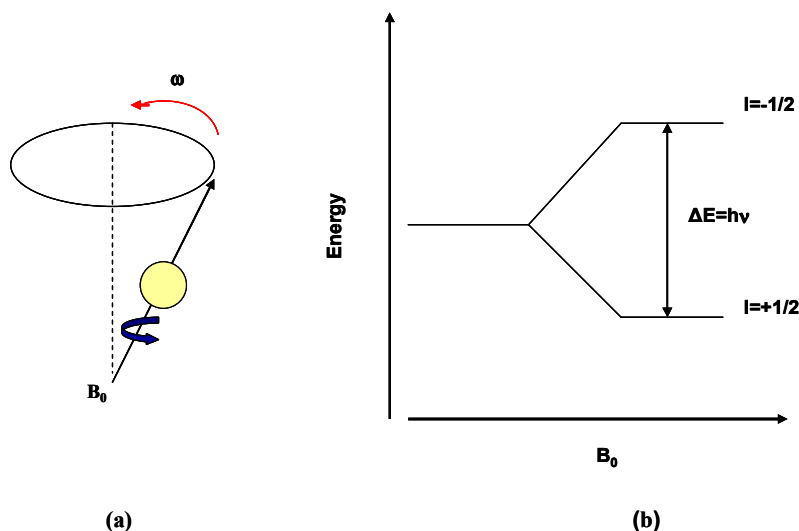


Figure 23. (a) Rotation of the nuclear magnetization along its own axis (blue) and along the magnetic field axis (red). (b) Difference in nuclear spin energy levels of $I = \pm \frac{1}{2}$ in an external magnetic field B_0 . Adapted from (Chang, 2005).

✓ Chemical shift

The particularity of NMR spectroscopy is that various protons absorb energy at slightly different frequencies for any given nucleus (ex ^1H) depending on its position in the molecule under study. These differential absorptions are displayed as different chemical shift. The chemical shift parameter (σ) is expressed in units of ppm (parts per million) and can be defined as the difference in resonance frequencies between a nucleus of a sample (ν_{sample}) and a reference nucleus (ν_{ref}), as deduced by equation (22):

$$\sigma = [(\nu - \nu_{\text{sample}}) / \nu_{\text{spec}}] 10^6 \quad [\text{Eq. 22}]$$

where ν_{spec} is the spectrometer frequency. By convention, NMR spectra are plotted with chemical shift (σ) increasing from right to left.

III. 3. 3. 3. *The NMR spectrometer*

The NMR instrument consists mainly of the following parts (Figure 24).

- ✓ *The magnet:* the magnetic field is generated by a superconducting magnet. The main coil that produces the field is placed in a liquid helium tub, which is surrounded by a liquid nitrogen Dewar flask.

- ✓ *The probe-head:* is introduced into the magnet from the bottom and connected to the radiofrequency source. Radiofrequency sources are electronic components that produce sine/cosine magnetic waves at appropriate frequencies. The sample dissolved in a deuterated solvent inside a glass tube, placed in the spinner and entered the probe-head from the top.

- ✓ *The lock system:* high resolution NMR measurements require a special field/frequency stabilization to allow accumulation of the signal, which may be separated by less than one Hz. This stabilization device is called 'lock' and is achieved with a deuterated solvent (e.g. ^2H). The deuterium lock measures the frequency of the deuterium line of the solvent and it is activated when the sample is placed in the magnet.

- ✓ *The shim system:* the precession frequencies are proportional to the magnetic field strength; which should be highly homogenous across the sample volume in order to be able to observe small frequency differences (small couplings). The process of optimization the magnetic field homogeneity for recording high resolution spectra is called 'shimming' a magnet. Therefore, the shim system is a device that corrects for locally slightly different magnetic fields.

- ✓ *The computer system:* the NMR spectrometers are controlled by a computer. The computing system has different tasks. The process controller must have on-line control of many spectrometer functions such as lock, generation and timing of resonance field pulses, digitization, accumulation of the NMR signal (FID, free induction decay) and must also apply a Fourier transformation to converted FID into an absorption peak (Conover, 1984).

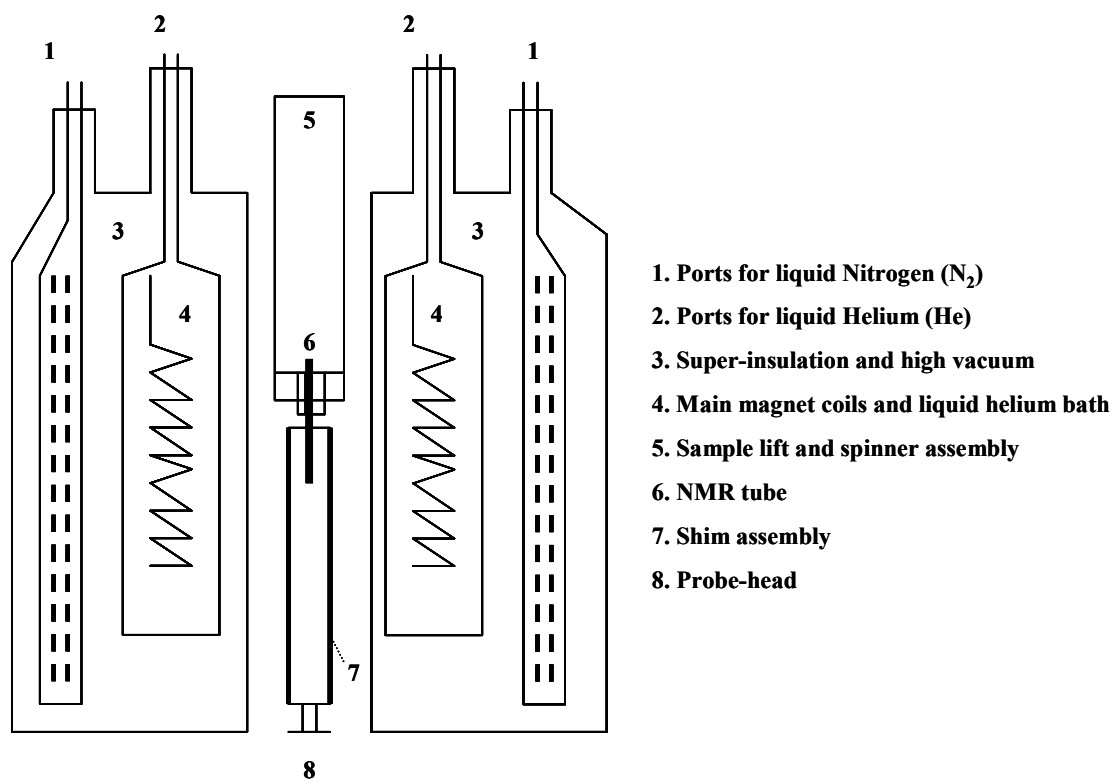


Figure 24. Main components of an NMR spectrometer

III. 3. 3. 4. *Properties of NMR spectra*

The three dimensional structures and the internal motions of drugs and lipids at atomic resolution can be extracted from NMR spectra. These are characterized by:

✓ *The degree of spin–spin coupling produced by neighboring effects.*

Each nucleus with $I \neq 0$ has a nuclear magnetic moment, and the magnetic field generated by this nucleus can affect the magnetic field experienced by a neighboring nucleus. Therefore, changes in the frequency will be observed in NMR absorption spectra. The direct nuclear spin-spin interaction is observed for two nuclei separated by no more than three bonds and is magnetically nonequivalent (Chang, 2005).

✓ *The relaxation.*

Magnetization does not proceed infinitely in the transverse plane but turns back to the equilibrium state, which is called the relaxation phenomenon. This is an exponential process, and is characterized by two different time-constants:

a) the time constant (T_1) known as spin-lattice (or longitudinal) relaxation time. It allows sampling the effect of very fast motions, occurring from picoseconds to the nanoseconds time scale.

b) the time constant (T_2) characterizing the spin-spin relaxation (or transverse relaxation time). It is related to the line-width of the signal (spectral line-shape) and it is sensitive to slower motional processes occurring at the microseconds to millisecond time scale.

The T_2 relaxation time of a spin $I=1/2$ nuclei, is affected by:

i) the homogeneity of the magnetic field (the "*shim*")

ii) the strength of the dipolar interaction (spin–spin coupling) with other $I=1/2$ nuclei.

iii) the tumbling time of the molecule this is related to its size (Dufourc, 2008;Larijani and Dufourc, 2006;Gadian, 1982).

✓ *The Chemical shift anisotropy:*

^{31}P NMR spectra are particularly useful for the study the structure and molecular motions of biological membranes. Indeed, the phospholipid head groups contain an isolated $I=1/2$ spin system that depends only on chemical shift anisotropy ($\Delta\sigma$) and dipolar proton-phosphorus interactions. The chemical shift of ^{31}P depends on the orientation of the group with respect of magnetic field of the spectrometer (Figure 25).

The principal chemical shift compounds, $(\sigma_{11}, \sigma_{22}, \sigma_{33})$, describe the interaction between the ^{31}P nucleus and the applied magnetic field along the three Cartesian directions (x, y, z). The ^{31}P NMR is the sum of spectra for all possible orientations of the axis system. The chemical shift expected when the field is parallel to the unique axis is indicated by $(\sigma_{\parallel} = \sigma_{11})$, whereas that expected for the field perpendicular to this axis is represented by $(\sigma_{\perp} = (\sigma_{22} + \sigma_{33})/2)$.

Both σ_{\parallel} and σ_{\perp} can be measured from ^{31}P spectrum, and the total chemical shift anisotropy, $\Delta\sigma$, is defined as the width of the resonance signal from the lower frequency “foot” (σ_{\perp}) at half height to the higher frequency (σ_{\parallel}) “shoulder” (Deslauriers et al., 1982; Seelig, 1978; Seelig, 1985; Seelig et al., 1985; Smith and Ekiel, 1984) as shown in equation 23 :

$$\Delta\sigma = \sigma_{\parallel} - \sigma_{\perp} \quad [\text{Eq. 23}]$$

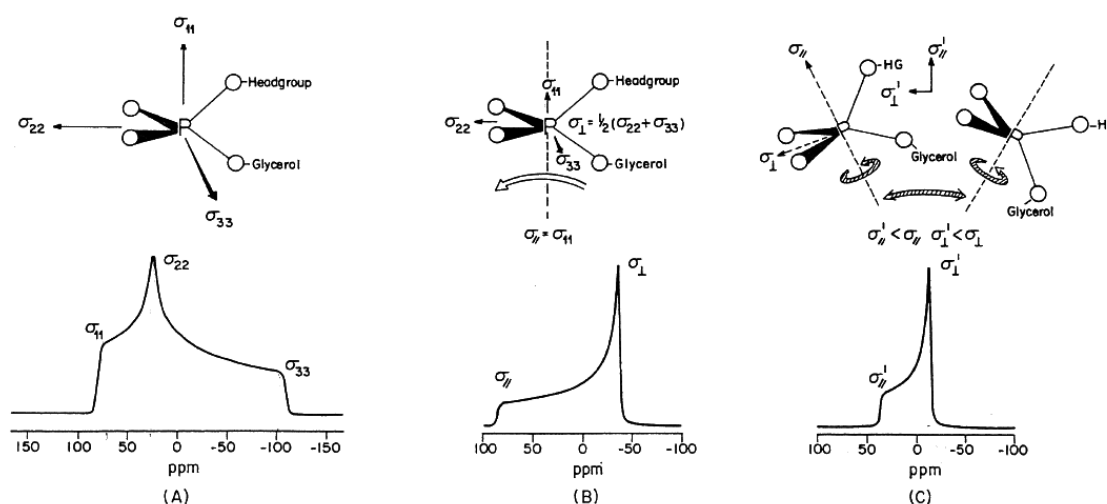


Figure 25. Possible motional states of the phosphodiester moiety of a membrane lipid and the expected ^{31}P - NMR spectra. (A) *Static phosphodiester*, (B) *ordered phosphodiester* (C) *disordered phosphodiester*. Taken from (Smith and Ekiel, 1984).

III.3.3.5. *Application of NMR spectroscopy to study lipid state behavior and to characterize fluoroquinolones-lipids interactions*

During the interaction between drugs and phospholipid molecules, one or several of NMR spectra parameters, cited above, may show important changes. We will focus our description on the interactions between fluoroquinolones and lipids.

i) *Membrane polymorphism and state transitions of lipids*

The analysis of the NMR spectrum of three nuclei namely ^1H , ^{13}C , and ^{31}P , is particularly instructive to study membrane organization and drug effects on the membranes. However, only limited information can be obtained on transformation of phospholipid states from ^1H and ^{13}C NMR due to the weak resolution of the corresponding signals. ^{13}C NMR can be applied to the study of lipid state transition if the phospholipid is enriched at the sn-2, carbonyl position (Wittebort et al., 1982).

^{31}P is more useful probe for the analysis of the structure and motion of the lipids that contain this atom (Kohler and Klein, 1976). In fact, ^{31}P NMR has been used to study phospholipid polymorphism, lateral diffusion, and transition from gel to liquid crystalline state as a function of temperature.

✓ ^{31}P NMR to study phospholipid polymorphism

A typical ^{31}P -NMR spectrum of polymorphic phases of phospholipid bilayers is represented at (Figure 26). In micelles, inverted micelles and SUV liposomes, a single narrow resonance signal is observed, reflecting an isotropic motion. If the lipid is incorporated into a bilayer, motion becomes more restricted (anisotropic) and a broad spectrum is observed. ^{31}P -NMR is also used to study the hexagonal phase of lipids which is characterized by a reduced residual shielding anisotropy and its sign is reversed (Watts and Spooner, 1991). To limit ourselves to the main objective of our Thesis, the spectra of hexagonal phase is not shown in the Figure 26.

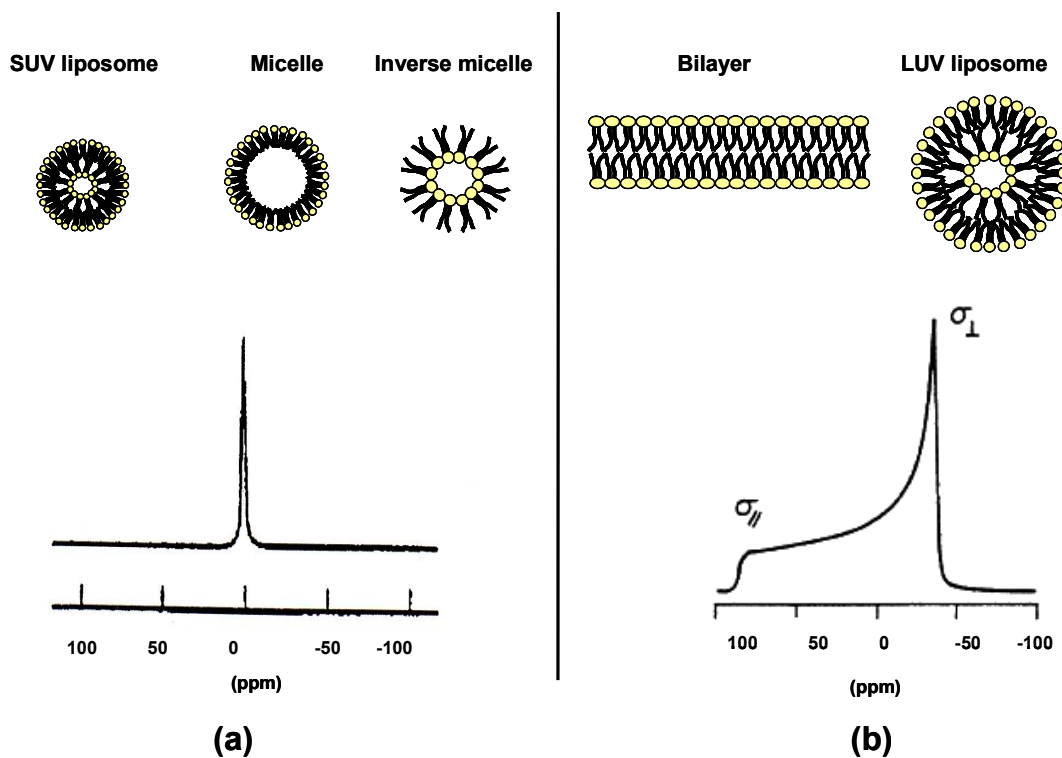


Figure 26. ^{31}P NMR spectra of polymorphic phases of phospholipids.

(a) In small vesicles, micelles or inverse micelle, (b) in bilayers, large unilamellar vesicles (LUV) Adapted from (Watts and Spooner, 1991).

✓ ^{31}P NMR to study the lipid state behavior

As the orientation of the phospholipids headgroups and the molecular motion of the lipid change from liquid crystalline to gel state when temperature increases, the chemical shift anisotropy ($\Delta\sigma$) is a sensitive parameter to detecting such changes (Zidovetzki et al., 1989).

The effect of the temperature on the effective chemical shift anisotropy ($\Delta\sigma$) of ^{31}P -NMR spectra of MLV liposomes composed of Chol:PC:SM:PI:PE has been investigated in our laboratory (Tyteca et al., 2003). As predicted, a decrease of $\Delta\sigma$ value was observed when the liposomes were warmed from 33°C to 70°C. A similar decrease of ($\Delta\sigma$) was noted for MLV liposomes mimicking the composition of the neuronal membrane, when the temperature was increased from 35°C to 65°C (Mingeot-Leclercq et al., 2002).

ii) Fluoroquinolones characterization and their effect on membrane lipids

✓ ^{19}F , ^1H NMR to study the drug metabolism and drug binding to biological compounds

Because of the presence of a Fluor atom, fluoroquinolones have been studied by NMR spectroscopy (Martino et al., 2005). ^{19}F -containing fluoroquinolones have been used to study the metabolism of these drugs (Park et al., 1997) and to measure the binding parameters between them and biological constituents. Thus, ^{19}F NMR has been applied to the study the interaction of lomefloxacin with hemoglobin in human erythrocytes. The fluorine signals of drug revealed a significant line broadening in the presence of oxyhemoglobin (HbO_2), hematin, globin and iron. The authors concluded that lomefloxacin interacts with all these compounds (Knaub et al., 1995).

Another example is the determination of the binding ability of fleroxacin to bacterial cells of *Micrococcus luteus* by ^1H and ^{19}F NMR relaxation measurements. From the spin-lattice relaxation rates and spin-spin relaxation measurement, the authors suggested that fleroxacin binds to the bacterial cells only by its isoquinoline moiety, whereas the piperazine and the fluoroethylene group showed no effect upon complexation (Waibel and Holzgrabe, 2007).

✓ ^1H and ^{13}C NMR to study the drug solubility and drug binding to iron

The interaction between fluoroquinolone and aluminum (Al^{3+}) has been investigated using ^1H and ^{13}C NMR spectra of fleroxacin and moxifloxacin. Addition of Al^{3+} into the drug solution induced changes in the ^{13}C and ^1H spectra. The changes were seen on carbonyls C2 and C4 signals of the fleroxacin, and on the carbonyls C4 and C11 of moxifloxacin. Thus, NMR data confirm the binding of Al^{3+} to the carbonyl and the adjacent keto group of these drugs (Djurdjevic et al., 2007).

The solubility of CIP encapsulated in LUV liposomes was investigated using ^1H -NMR. The ^1H NMR spectra of CIP loaded into DPPC/Chol (55:45, mol:mol) or POPC LUVs liposomes were recorded. As compared to free CIP, large shifts of the aromatic proton resonances (H_2 , H_5 , H_8), were observed. These data suggest that CIP molecules form stacks in aqueous solution by π - π interactions of aromatic molecules. The results indicate that CIP is located in the aqueous interior of the liposomes and does not precipitate.

Thus, CIP can respond quickly to changes in electrochemical equilibrium such as depletion of the pH gradient (Maurer et al., 1998).

✓ ³¹P NMR to study the drug effect on the orientation and mobility of phospholipids head groups

The effect of CIP and its derivative, N4-butypiperazinyl (BCIP), on the orientation of phospholipids head group was described using ³¹P-NMR spectroscopy.

³¹P-NMR powder spectra of multilamellar liposomes (DPPC) in the presence and absence of drugs, below (25°C) and above (50°C) to induce gel to liquid state transition, were recorded. From the second spectral moments, the authors noted that CIP and BCIP decreased slightly (~ 1 to 2°C) the melting temperature of DPPC, and that both fluoroquinolones induced a decrease in the second moment values. Therefore, these drugs (CIP and BCIP) may increase the local mobility of the phosphate groups or may change their average orientation with respect to the bilayer normal (Grancelli et al., 2002).

III. 3. 3. 6. *Advantages and limitations*

NMR spectroscopy is a non-destructive and very sensitive method for studying the biological membrane. Indeed, ³¹P-NMR affords a technique for distinguishing the NMR signals arising from different lipids or from lipid molecules in different environment.

From the interpretation of the NMR spectra of phospholipids, several processes can be evaluated, such thermal phase transition, phase separation, and distribution of lipids molecules in the two monolayer of the bilayer (Michaelson et al., 1973;Yeagle et al., 1976). Furthermore, the effect of drugs in terms of headgroup orientation and motion can also be investigated, using chemical shift anisotropy, integrals as well as homo- and heteronuclear two-dimensional measurements (Martino et al., 2005).

Set against these advantages, a number of disadvantages need to be taken into account. First, this technique requires a large sample concentration (mM range), which makes it impossible to use with many investigational compounds usually available only in small quantities. Second, NMR spectroscopy is not appropriate for the study of complex mixtures (e.g. lipid extracted from cells), since considerable signal overlap occurs between individual phospholipid classes. Therefore, only one or two individual phospholipids can be analyzed (Schiller and Arnold, 2002).

Table 7. Overview of the main techniques used in this Thesis for the characterization of fluoroquinolones- lipids interactions

Technique	Physical Principle	Information deduced	Membrane model	Advantage	Limitation	References
Atomic Force Microscopy (AFM)	Measure the forces resulting from different interactions between a tip, which is attached to a cantilever and the atoms of the sample surface.	<ul style="list-style-type: none"> - Surface topography - Lipid domain structure - Molecular packing 	<ul style="list-style-type: none"> -Supported planar bilayer -LB film 	<ul style="list-style-type: none"> -Atomic resolution (nanometric) in air and under liquid. - <i>in situ</i> follow-up of membrane modification upon addition of drugs. 	<ul style="list-style-type: none"> - Contact between tip/ sample can cause damage of soft sample - Not appropriate for the thermotropic properties of lipids 	(Oliveira, 1992;Garcia-Manyes and Sanz, 2010;El Kirat et al., 2010;Giocondi et al., 2010).
Langmuir-Blodgett technology (LB)	Measure the surface pressure/area (π -A) of monomolecular layer upon compression	<ul style="list-style-type: none"> - Lipid molecular arrangement - Lipid phase transition - Lipid packing 	<ul style="list-style-type: none"> -LB film (monolayers) 	<ul style="list-style-type: none"> - Well-organized ultrathin films. - Can be used in AFM or ATR-FTIR 	<ul style="list-style-type: none"> - Lack of thermal stability - Some defects in LB films formation make them inappropriate for surface analysis 	(Oliveira, 1992;Girard-Egrot et al., 2005)
Fluorescence Spectroscopy	Measure the intensity of photons emitted by the molecule which is electronically excited. If the molecule is excited by polarized light, the fluorescence is polarized (anisotropy)	<ul style="list-style-type: none"> -Photochemical properties of drugs -Binding parameters of drugs to lipids (stoichiometry, affinity) -Conformational changes of lipids by using DPH, TMA-DPH probes (fluidity, thermotropic transition) - Membrane potential by using ANS probe 	<ul style="list-style-type: none"> -SUV -LUV 	<ul style="list-style-type: none"> - Simple and inexpensive technique. - Easy interpretation of spectra. - Good sensitivity (μM) 	<ul style="list-style-type: none"> -Require a fluorescent molecule with high quantum yield. - Perturbation of the signal by photobleaching, or light scattering 	(Lakowicz, 1999)

Technique	Physical Principle	Information deduced	Membrane model	Advantage	Limitation	References
Fourier Transform Infrared Spectroscopy (FTIR)	Measure the different IR radiation absorbed by a sample positioned in the path of an IR beam, as well as the intensities of these absorptions.	<ul style="list-style-type: none"> - Acyl chain conformation of lipids. - Acyl chain packing (molecular orientation, hydrocarbon chain tilt measurement). - Thermotropic transition profile of lipids. 	<ul style="list-style-type: none"> -Supported planar bilayer -LB film -SUV 	<ul style="list-style-type: none"> - Simultaneously study of the structure of lipids and drugs. - No external probe required. - Simple preparation of the samples. 	<ul style="list-style-type: none"> - Limited to the molecules that are sufficiently transparent and active in the IR region. - Overlap of absorption bands for lipid molecules. - Complex interpretation and identification of a single band. - Liquid water has broad absorption bands, overlapping a considerable part of the IR spectral range. 	<p>(Rothschild and Clark, 1979).</p> <p>(Fringeli and Gunthard, 1981).</p> <p>(Goormaghtigh et al., 1999).</p>
Nuclear Magnetic Resonance spectroscopy (NMR)	Measure the absorption of radio frequency electromagnetic waves by a nucleus that possesses a spin vector, under an external magnetic field.	<ul style="list-style-type: none"> - Membrane polymorphism and phase transitions of lipids (^{31}P NMR). - Drug metabolism, drug solubility and drug binding to biological compounds (^1H, ^{13}C, ^{19}F). - Drug effect on the orientation of phospholipids head groups (^{31}P NMR). 	-MLV	<ul style="list-style-type: none"> - Non-destructive method. - Atomic resolution. 	<ul style="list-style-type: none"> - Large sample concentration (mM) required. - Not appropriate for lipids mixtures due to signal overlaps. 	<p>(Smith Ian and Ekiel Ireana, 1984)</p> <p>(Wittebort et al., 1982)</p> <p>(Schiller and Arnold, 2002).</p> <p>(Watts and Spooner, 1991)</p>



AIMS OF THE THESIS



Aims of the Thesis

Probing fluoroquinolones/lipid interactions at the molecular level represents an important challenge in both membrane biophysics and pharmaceutical research. As presented in the Introduction, the broad antibacterial spectrum of fluoroquinolones implies their ability to enter prokaryotic organisms through lipids membrane and via porins in both prokaryotic and eukaryotic organisms. Conversely, intracellular accumulation of these drugs (e.g CIP *vs.* MXF in J774 macrophages cells) can be affected by efflux transporters. In both situations, the transport of fluoroquinolones could be examined in terms of their interactions with lipids membranes. In this respect, several biophysical studies, reviewed in the Introduction, have provided information about the spectroscopic properties of CIP and its effects on neutral model lipids membranes (e.g. changes in membrane potential and fluidity). In parallel, data have been reported the spectroscopic properties of MXF (e.g. degree of partition, partition coefficients) but without investigating its interaction with lipids.

Hence, a few specific informations are available from these studies about the effect of CIP and MXF on lipid domains and binding quantification or on the effect of the drugs on head group and acyl chains of phospholipids when interacting with lipids.

The main aim of my Thesis is therefore to characterize the effect of two fluoroquinolones, CIP and MXF, on the physicochemical properties of the major phospholipids of both the eukaryotic and prokaryotic membranes.

As model lipids membrane are a convenient material to study drug-lipids interactions, three of such models have been used: monolayer, supported bilayer and liposomes (SUV, LUV and MLV). To mimic the eukaryotic plasma membrane, zwitterionic phospholipids have been used (DOPC and DPPC), whereas, a negatively charged phospholipid (DPPG) has been used to mimic the prokaryotic plasma membrane.

Various biophysical methods have been used for their characterization, and our specific objectives are:

- ✓ To characterize the topographic images of supported bilayer of a mixture of (DOPC: DPPC) and to study the effect of drugs on domain formation using Atomic force microscopy.

- ✓ To study the effect of drugs on lipid packing by measuring the surface pressure-area using Langmuir monolayer.
- ✓ To determine acyl chain conformation and acyl chain orientation of DPPC in the absence and the presence of the two fluoroquinolones using Attenuated Total Reflection Fourier Transform Infrared spectroscopy.
- ✓ To determine the binding parameters (affinity) of the drugs to liposomes of interest by steady state anisotropy measurements.
- ✓ To investigate the effect of drugs on the orientation and/or mobility of phospholipids head groups (DPPC vs. DPPG) using Nuclear magnetic resonance spectroscopy.
- ✓ To follow lipid state transition of liposomes (DPPC vs. DPPG) in the absence and presence of the drugs using Attenuated Total Reflection Fourier Transform Infrared spectroscopy.
- ✓ To determine the molecular structure of lipids-fluoroquinolones complexes by computer-aided molecular modeling calculations.

These studies might bring more information on fluoroquinolones-lipids interactions.



RESULTS



CHAPTER 1

Investigation of the interaction of two fluoroquinolones (Ciprofloxacin and Moxifloxacin) with model lipids membranes

Chapter 1

Fluoroquinolones antibiotics exert a bactericidal activity against a large variety of intracellular organisms (e.g. *Listeria monocytogenes*, *Staphylococcus aureus*), due to their ability to accumulate inside eukaryotic cells. However, the intracellular accumulation of various fluoroquinolones in J774 murine macrophages cells shows significant differences with the following decreasing order: moxifloxacin>garenoxacin>levofloxacin>ciprofloxacin (Seral et al., 2005). The level of their intracellular accumulation actually results from differences in absolute influx rates for MXF, which is three to four fold faster than CIP, and the fractional efflux rates for MXF is seven fold faster than CIP in J774 cells (Michot et al., 2005). It seems that MXF crosses biomembranes in both directions much faster than CIP.

To test whether these differences in influx and efflux could be related to differential interactions with membranes, we investigated the physicochemical properties of lipid membranes by exposing different models (monolayer, supported bilayer, and SUV) made of the most abundant zwitterionic phospholipids of eukaryotes membranes to increasing antibiotic concentrations.

The quantification of the fluoroquinolones (CIP, MXF) was performed by fluorescence spectroscopy. Their release from lipid monolayer to aqueous phase and their effect on the lipids domains erosion were monitored by Langmuir-Blodgett technique and atomic force microscopy, respectively. Finally, their ability to change conformation and orientation of acyl chain of DPPC was investigated by Attenuated Total Reflection Fourier Transform Infrared spectroscopy.

The results show that both fluoroquinolones induced a shift towards lower area per molecule of (DOPC:DPPC:Drug) monolayer and erosion of the DPPC domains in the DOPC fluid phase. These effects were more pronounced with MXF, which exhibit a higher ability than CIP to decrease the number of all-trans conformation and erosion of micrometric domains. By contrast, CIP induced more disorder and modified the orientation of the acyl chains.

Our data show differences between CIP and MXF in terms of interactions with the lipids at the molecular level that could be related to differences in transport and cellular accumulation of these drugs.

Characterization of the Interactions between Fluoroquinolone Antibiotics and Lipids: a Multitechnique Approach

Hayet Bensikaddour,* Nathalie Fa,* Ingrid Burton,[†] Magali Deleu,[‡] Laurence Lins,[§] André Schanck,[¶] Robert Brasseur,[¶] Yves F. Dufrene,[†] Erik Goormaghtigh,^{||} and Marie-Paule Mingeot-Leclercq*

*Université Catholique de Louvain, Faculty of Medicine, Unité de Pharmacologie Cellulaire et Moléculaire, Brussels, Belgium;

[†]Université Catholique de Louvain, Faculty of Agronomy, Unité de Chimie des Interfaces, Louvain-la-Neuve, Belgium; [‡]Faculté Universitaire des Sciences Agronomiques de Gembloux, Unité de Chimie Biologique Industrielle, and [§]Centre de Biophysique Moléculaire Numérique, Faculté Universitaire des Sciences Agronomiques de Gembloux, Gembloux, Belgium; [¶]Université Catholique de Louvain, Louvain-la-Neuve, Faculty of Sciences, Unité de Chimie Structurale et des Mécanismes Réactionnels, Belgium; and ^{||}Université Libre de Bruxelles, Faculty of Sciences, Unité de Structure et Fonction des Membranes Biologiques, Brussels, Belgium

ABSTRACT Probing drug/lipid interactions at the molecular level represents an important challenge in pharmaceutical research and membrane biophysics. Previous studies showed differences in accumulation and intracellular activity between two fluoroquinolones, ciprofloxacin and moxifloxacin, that may actually result from their differential susceptibility to efflux by the ciprofloxacin transporter. In view of the critical role of lipids for the drug cellular uptake and differences observed for the two closely related fluoroquinolones, we investigated the interactions of these two antibiotics with lipids, using an array of complementary techniques. Moxifloxacin induced, to a greater extent than ciprofloxacin, an erosion of the DPPC domains in the DOPC fluid phase (atomic force microscopy) and a shift of the surface pressure-area isotherms of DOPC/DPPC/fluoroquinolone monolayer toward lower area per molecule (Langmuir studies). These effects are related to a lower propensity of moxifloxacin to be released from lipid to aqueous phase (determined by phase transfer studies and conformational analysis) and a marked decrease of all-*trans* conformation of acyl-lipid chains of DPPC (determined by ATR-FTIR) without increase of lipid disorder and change in the tilt between the normal and the germanium surface (also determined by ATR-FTIR). All together, differences of ciprofloxacin as compared to moxifloxacin in their interactions with lipids could explain differences in their cellular accumulation and susceptibility to efflux transporters.

INTRODUCTION

Since their discovery in the early 1960s, the quinolone group of antibacterials has generated considerable clinical and scientific interest including the development of the second-generation quinolones like ciprofloxacin. These wide spectrum drugs are characterized by the introduction of fluor into position C-6 on the molecule. Progressive modifications in their chemical structure have resulted in improved breadth and potency of in vitro activity and pharmacokinetics (1). The most significant developments have been enhancement of the therapeutic potential of fluoroquinolones thanks to liposomal encapsulation (2–4) and improved anti-Gram-positive activity of the newer compounds like moxifloxacin (5).

Due to their ability to accumulate inside phagocytes (1,6–8), fluoroquinolones are also useful for eliminating facultative intracellular pathogens that resist phagocytic death. We

recently showed that fluoroquinolones accumulate in macrophages and show activity against a large array of intracellular organisms including *Listeria monocytogenes* and *Staphylococcus aureus* (9). Quite significant differences among closely related derivatives have been observed with the following ranking in cellular accumulation and intracellular activity: ciprofloxacin < levofloxacin < garenoxacin < moxifloxacin (9). So far, to our knowledge, this has not received satisfactory explanation.

Characterization of fluoroquinolones uptake by eukaryotic cells suggested that both passive diffusion and active transport systems are involved. The transbilayer diffusion of fluoroquinolones has been demonstrated (10) and our group reported that ciprofloxacin, but not moxifloxacin, is subject to constitutive efflux in J774 macrophages through the activity of an MRP-related transporter (11).

Drug/lipid interactions can modulate not only translocation of the drug through the natural membranes but also its interaction with efflux proteins (12,13). In this respect, it is well known that 1), substrates have to be transported from the lipid bilayer to the transporter protein before a capture mechanism of the drug by the inner leaflet of the cytoplasmic membrane (14); and 2), the activity of transporter is critically dependent on the surrounding lipid bilayer environment (15,16), which may be modified by drugs.

In view of the critical role of lipids for the drug cellular uptake and differences observed for two closely related

Submitted June 15, 2007, and accepted for publication October 3, 2007.

Hayet Bensikaddour and Nathalie Fa contributed equally to the work.

Address reprint requests to Marie-Paule Mingeot-Leclercq, Tel.: 32-2-764-7374; E-mail: mingeot@facm.ucl.ac.be.

Nathalie Fa's present address is Campden & Chorleywood Food Research Association Group, Chipping Campden, Gloucestershire, GL55 6LD, UK.

This is an Open Access article distributed under the terms of the Creative Commons-Attribution Noncommercial License (<http://creativecommons.org/licenses/by-nc/2.0/>), which permits unrestricted noncommercial use, distribution, and reproduction in any medium, provided the original work is properly cited.

Editor: Petra Schwille.

© 2008 by the Biophysical Society
0006-3495/08/04/3035/12 \$2.00

doi: 10.1529/biophysj.107.114843

compounds, ciprofloxacin and moxifloxacin (Fig. 1), we investigated the interactions of these two fluoroquinolones with lipids, using an array of complementary techniques. For both ciprofloxacin and moxifloxacin, atomic force microscopy (AFM) reveals an erosion of dipalmitoylphosphatidylcholine (DPPC) domains within dioleoylphosphatidylcholine (DOPC) fluid phase while Langmuir studies show a condensing effect. Further molecular studies show that fluoroquinolones can 1), exchange from lipids to aqueous phases (phase transfer and molecular modeling studies); 2), decrease the all-*trans* conformation of lipid acyl chain (attenuated total reflection Fourier transform Infra-Red (ATR-FTIR)); and 3), increase the lipid disorder (ATR-FTIR). When the effects of the two fluoroquinolones are compared, it clearly appears that moxifloxacin has a higher condensing effect related to a lower propensity to be released in the aqueous phase from lipid monolayer and to a higher ability to decrease the all-*trans* conformation of lipid acyl chain without marked effect in lipid-chain orientation. All together, differences of ciprofloxacin as compared to moxifloxacin in their interactions with lipids can be related to differences in their cellular accumulation and therefore activity against intracellular bacteria.

MATERIAL AND METHODS

Materials

Dioleoylphosphatidylcholine (DOPC) and dipalmitoylphosphatidylcholine (DPPC) were purchased from Sigma (St. Louis, MO). Ciprofloxacin; microbiological standard, potency 85.5%, MW = 331.34 g/mol and moxifloxacin; microbiological standard, potency 91%, MW = 401.4 g/mol were obtained from Bayer Healthcare AG (Leverkusen, Germany). All other reagents were from E. Merck (Darmstadt, Germany).

Fluoroquinolone assays

Ciprofloxacin assay

Ciprofloxacin content was determined by a fluorimetric method (λ_{ex} , 275 nm; λ_{em} , 450 nm, using a model No. LS-30 Fluorescence Spectrophotometer; Perkin-Elmer, Beaconsfield, UK) as described previously (11). Under these conditions, our assay had a lower detection limit of ~ 5 ng/ml, a linearity ($r^2 \geq 0.99$) up to 200 ng/ml, and an intraassay reproducibility of 97%.

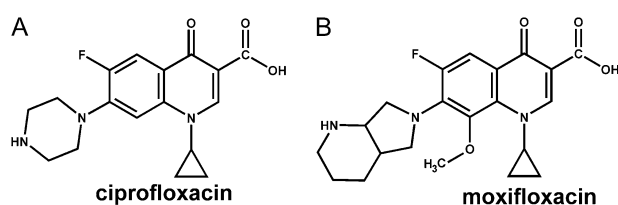


FIGURE 1 (A) Structural formula of ciprofloxacin (3-quinolinecarboxylic acid, 1-cyclopropyl-6-fluoro-1,4-dihydro-4-oxo-7-(1-piperazinyl)-(9CI)) and (B) moxifloxacin (3-quinolinecarboxylic acid, 1-cyclopropyl-6-fluoro-1,4-dihydro-8-methoxy-7-((4aS,7aS)-octahydro-6H-pyrrolo(3,4-b)pyridin-6-yl)-4-oxo-(9CI)).

Biophysical Journal 94(8) 3035–3046

Moxifloxacin assay

Fluorescent assay based on the same technique as that used for ciprofloxacin but using $\lambda_{\text{ex}} = 298$ nm and $\lambda_{\text{em}} = 504$ nm; lower limit of detection, 5 ng/ml; linearity up to 450 ng/ml ($r^2 \geq 0.99$); intraassay reproducibility, 98%.

Preparation of liposomes (MLVs, SUVs)

Lipid vesicles were prepared as described previously (17). Briefly, appropriate lipids were mixed in $\text{CHCl}_3/\text{CH}_3\text{OH}$ 2:1 (v/v), evaporated under nitrogen flow, and desiccated under vacuum for at least 4 h. The dried films were then resuspended at room temperature from the walls of the glass balloon by vigorous vortexing in aqueous buffer. Lipid in suspension flushed with nitrogen were kept in a water bath for 1 h at 37°C for pure DOPC or 45°C for liposomes containing DPPC. This procedure yields multilamellar vesicles (MLVs). The small unilamellar vesicles (SUVs) consisting of DOPC/DPPC (1:1 mol) were prepared from MLVs. The preparation, cooled down by an ice bath, was sonicated to clarity five times for 2 min each using a Fisher Bioblock Scientific 750 W sonicator (Avantec, Illkirch, France) set at 35% of the maximal power, and a 13-mm probe. The SUVs preparation was then filtered on 0.2 μm Acrodisc filters (Ann Arbor, MI) to eliminate titanium particles. The concentration of lipids, the nature of the buffer, and the lipid/drug ratio was adjusted for each type of experiment.

AFM imaging

Mica sheets were heated 1 h before fusion at 60°C and cleaved to obtain a flat and uniform surface. The SUV suspension of DOPC/DPPC (1:1) (10 mg lipids/ml; buffer 10:100:3 mM, pH 7.4), was put into contact with the mica surface for 45 min at 60°C and the sample was slowly cooled back to room temperature to prevent thermal shock. The excess of SUVs was then eliminated by four-times rinsing with a Tris/NaCl 10:100 mM buffer, pH 7.4. The sample was installed on the microscope without dewetting. The liquid meniscus was completed with the same buffer or solution containing 0.2 mM fluoroquinolones. All AFM measurements were carried out at room temperature in contact mode using an optical detection system equipped with a liquid cell (Nanoscope IV; Digital Instruments, Santa Barbara, CA). Topographic images were taken in the constant-deflection mode using oxide-sharpened microfabricated Si_3N_4 cantilevers (Park Scientific Instruments, Mountain View, CA) with typical curvature radii of 20 nm and spring constant of 0.01 N/m. Scan rate ranging from 4 to 6 Hz were tested. The applied force was maintained as low as possible (< 1 nN) during the imaging. All images were flattened.

Partition of fluoroquinolones—phase transfer assay between aqueous and lipid phases

For the phase transfer assays, 1 ml of the water phase (Tris pH7.4, 10mM), containing the fluoroquinolone (1 μM), was mixed by vortexing for 30 s, to 1 ml of organic phase (CHCl_3), with or without lipids (Egg yolk phosphatidylcholine (PC)) from a lipid/drug ratio of from 0.1:1 up to 50:1. Both phases were decanted overnight at 4°C. The fluoroquinolone recovered from the water, interfacial, and organic phases were quantified by fluorimetry (model No. LS30 fluorimeter; Perkin-Elmer).

Interaction between fluoroquinolones and a model membrane by molecular modeling: the IMPALA procedure

The ciprofloxacin or moxifloxacin molecule was inserted into an implicit simplified bilayer using the IMPALA method described previously (18). This method simulates the insertion of any molecule into a bilayer by adding energy restraint functions to the usual energy description of molecules. The lipid bilayer was defined by $C_{(z)}$, which represents an empirical function

describing membrane properties. This function is constant in the membrane plane (x and y axes), but varies along the bilayer thickness (z axis) and, more specifically, at the lipid/water interface corresponding to the transition between lipid acyl chains (no water = hydrophobic core) and the hydrophilic aqueous environment,

$$C_{(z)} = 1 - \frac{1}{1 + e^{\alpha(z-z_0)}},$$

where α is a constant equal to 1.99; z_0 corresponds to the middle of polar heads; and z is the position in the membrane.

Two restraints were imposed to simulate the lipid membrane: the bilayer hydrophobicity (E_{pho}); and the lipid perturbation (E_{lip}).

The hydrophobicity of the membrane is simulated by E_{pho} ,

$$E_{\text{pho}} = - \sum_{i=1}^N S_{(i)} E_{\text{tr}(i)} C_{(z_i)},$$

where N is the total number of atoms; $S_{(i)}$ the accessible surface to solvent of the i atom; $E_{\text{tr}(i)}$ its transfer energy per unit of accessible surface area; and $C_{(z_i)}$ the z_i position of atom i .

The perturbation of the bilayer by insertion of the molecule was simulated by the lipid perturbation restraint (E_{lip}),

$$E_{\text{lip}} = a_{\text{lip}} \sum_{i=1}^N S_{(i)} (1 - C_{(z_i)}),$$

where a_{lip} is an empirical factor fixed at $0.018 \text{ kcal mol}^{-1} \text{ \AA}^{-2}$.

The environment energy (E_{env}) applied on the drug that inserts into the membrane becomes equal to

$$E_{\text{env}} = E_{\text{pho}} + E_{\text{lip}}.$$

Restraint plots

Diagrams showing the restraint values versus the angle between the helix axis and the bilayer normal or versus the penetration of the mass center are obtained as follows: for each degree (angle) or for each $1/10 \text{ \AA}$ (penetration), the lowest restraint value obtained during the Monte Carlo simulation is taken. All the points are then joined to generate a profile of the simulation.

Calculations are performed on an Intel Pentium 4, CPU 3.80 GHz, 4.00 GB of RAM. The calculation software has been developed at the CBMN (Gembloux, Belgium). Molecular graphs were drawn using WinMGM 1.0 (Ab Initio Technology, Obernai, France) and SigmaPlot 5.0 (SPSS, Chicago, IL) was used for data analysis.

Surface-pressure isotherms of lipid monolayer—Langmuir trough experiments

An automatically controlled Langmuir trough (KSV Minitrough, KSV Instruments, Helsinki, Finland), equipped with a platinum Wilhelmy plate was used to obtain the surface pressure-area (Π - A) isotherms of monolayers at the air/water interface. The temperature was maintained at $25 \pm 0.1^\circ\text{C}$ by an external water bath circulation. The volume of the trough was 80 ml. The cleanliness of the surface was ensured by closing the barriers, followed by aspiration of the subphase surface, before each experiment. Each experiment was started when the fluctuation of the surface pressure was $<0.1 \text{ mN/m}$ during the compression cycle. Lipid mixture (DOPC/DPPC (1:1)) and DOPC/DPPC mixture with ciprofloxacin or moxifloxacin at different molar proportions (1:1:0.1, 1:1:0.4, 1:1:1, and 1:1:2) were spread from a 1 mM (1:1:0.1, 1:1:0.4, and 1:1:1 molar ratios) or 2 mM (1:1:2) $\text{CHCl}_3/\text{CH}_3\text{OH}$ (2:1, v/v) solution on a Tris 10 mM subphase adjusted at pH 7.4. Thirty minutes were allowed for solvent evaporation from the interface. The air/

water interface was then compressed with two Delrin barriers at a rate of $5.8 \text{ \AA}^2 \text{ molecule}^{-1} \text{ min}^{-1}$. The reproducibility of the area values remained $\sim 7\%$. The accuracy on surface pressure was within 0.1 mN/m .

Mean molecular area (A) of the components at the interface was calculated taking into account the percentage of fluoroquinolone remaining at the interface after 30 min. The following equation was used:

$$A = (A_{\text{trough}} \times 10^{16}/N) (MW \times 1000/C) \times V \times 10^3.$$

A_{trough} = Area of the trough (cm^2); N = Avogadro number (6.022×10^{23}); MW = Weighted average of the molecular weight of the components remaining at the interface; C = Weighted average of the concentration (mg/ml) of the components remaining at the interface; V = Sample volume spread at the interface.

Release of fluoroquinolones from lipid monolayer to aqueous phase—Langmuir experiments

The determination of the release of fluoroquinolones from lipid monolayer into the subphase (Tris buffer 10 mM, pH 7.4) was performed as described previously. In these experiments, mixed solutions of DOPC/DPPC/fluoroquinolone at different molar proportions (1:1:0.1, 1:1:0.4, 1:1:1, and 1:1:2) were spread from a $\text{CHCl}_3/\text{CH}_3\text{OH}$ (2:1, v/v) solution on the subphase until a surface pressure of $11.6 \pm 0.8 \text{ mN/m}$ was reached. Although this pressure is well below the estimated surface pressure of a biological membrane (31–34 mN/m (19,20)), it allows an accurate determination of the kinetics of the transfer of fluoroquinolones to the subphase. Immediately after spreading and every 5 min, two aliquots of $500 \mu\text{l}$ were taken from the subphase with a micropipette. Homogenization of the subphase was provided by a gentle constant stirring. Each experiment was replicated at least three times. The presence of lipids was detected by phospholipid assay and fluoroquinolones were assayed by fluorimetry.

Conformation and orientation of lipids in interaction with fluoroquinolones—ATR-FTIR spectroscopy

Attenuated total reflection Fourier transform infra-red (ATR-FTIR) is particularly well suited for the study of membranes and to characterize the effect of drug interacting with lipids on conformation and orientation of acyl chains of phospholipids (21). This technique is based on internal reflection of the infrared light within an internal reflection germanium plate, which creates an evanescent field at the surface of the plate where the lipid bilayer (and eventually the bound proteins or drugs) resides (22). After deposit of lipids on the germanium plate, while evaporating, capillary forces flatten the membranes which spontaneously form oriented multilayer arrangements (23). The internal reflection element was a $52 \times 20 \times 2 \text{ mm}$ trapezoidal germanium ATR plate (ACM, Villiers St. Frédéric, France) with an aperture angle of 45° yielding 25 internal reflections.

Infra-red spectra were obtained on a model No. IFS55 FTIR spectrophotometer (Bruker, Ettlingen, Germany) purged with N_2 (as described previously (24)). Spectra were recorded with 2 cm^{-1} spectral resolution with a broad-band MCT detector provided by Bruker between 4000 and 800 cm^{-1} ; 128 scan were averaged for one spectrum. A modified continuous flow ATR setup was equipped with a polarizer that can be oriented parallel or perpendicular to the incidence plane. Fifteen microliters of the sample containing DPPC with different lipid/antibiotic molar ratios (DPPC/drug ratio: 1:0, 1:0.2, 1:0.5, 1:1, and 1:2) were dried under a stream of nitrogen on one side of the germanium internal reflection element using an incident angle of 45° at 20°C . An elevator under computer control made it possible to move the

whole setup along a vertical axis (built for us by WOW Company, Nannine, Belgium). The software used for data processing was written under MatLab 6.5 (The MathWorks, Natick, MA). All spectra were corrected for water vapor contribution and CO₂ and finally apodized at a resolution of 4 cm⁻¹.

To analyze the conformation of lipids, nonpolarized spectra were recorded. The hydrocarbon chain in α -position of DPPC in the gel state is in all *trans* from the ester group down to the methyl group. This conformation allows a resonance to occur between the ester group and the CH₂ groups of the chain, giving rise to the so-called $\gamma_w(\text{CH}_2)$ progression between 1200 and 1350 cm⁻¹ (peaks at 1200, 1221, 1246, 1266, 1286, 1309, and 1330 cm⁻¹). The proportion of the α -chains in the all-*trans* conformation was evaluated from the area of the band at 1200 cm⁻¹ relative to the C-H stretching vibrations of the CH₂ and CH₃ at 3000–2800 cm⁻¹.

To get information about the orientation of lipids and chain ordering, dichroic spectra of DPPC and DPPC in interaction with ciprofloxacin or moxifloxacin were obtained by subtracting the spectrum measured with a perpendicular polarization of the incident light (A_{\perp}) from the spectrum of absorbance measured with a parallel polarization of the incident light (A_{\parallel}). The angle between the molecular axis and the membrane normal was calculated as reviewed in Goormaghtigh et al. (21) using the STDWAVE program developed in the laboratory of one of the authors.

RESULTS

AFM imaging of DOPC/DPPC bilayers incubated with ciprofloxacin and moxifloxacin

To gain insight into ciprofloxacin- and moxifloxacin-membrane interactions, supported lipid bilayers made of DOPC/DPPC were prepared by fusion of unilamellar vesicles on mica. Time-lapse AFM topographic images were recorded in solution, in the absence and in the presence of fluoroquinolones.

In the absence of drug, classical images previously published (13) were obtained. They displayed two discrete height levels reflecting phase separation between gel phase DPPC and liquid-crystalline phase DOPC. The DPPC gel domains were well defined and homogenous, with a size ranging from 0.15 to 1.5 μm . The height difference between DPPC domains and the fluid DOPC matrix was 1.10 ± 0.05 nm.

When bilayers were incubated with either ciprofloxacin (*top panels*) or moxifloxacin (*bottom panels*), we observed a decrease of the size of DPPC domain with time (Fig. 2). The height differences between gel phase DPPC and fluid phase DOPC remains constant during the incubation. We note that for all incubation times the bilayer surface was devoid of defects, i.e., holes in the upper monolayer or in the bilayer were never observed. To evaluate the kinetics of the erosion process, a plot of the average domain areas was represented as a function of time. Fig. 3 shows that within a few hours, the area of DPPC domains decreased from 114.1 to 75.6 μm^2 and 83.3 to 42.3 μm^2 for ciprofloxacin and moxifloxacin, respectively. Thus, ciprofloxacin induced a decrease of the surface occupied by the DPPC domain of 27%. This erosion process was more marked with moxifloxacin since it reached a value of 58%. The kinetic trend was also different for ciprofloxacin compared to moxifloxacin, as reflected by the linear and the exponential-like processes, respectively. This

suggests that, in contrast with ciprofloxacin, different regimes of erosion had to be distinguished with moxifloxacin. To assess whether such an alteration of DPPC domains could be due to mechanical perturbation by the scanning tip, we performed the same measurements on a control bilayer that was not incubated with drugs. We obtained an area decrease of 3% indicating that the time-dependent erosion of the DPPC gel domains is due to the action of the antibiotics rather than to a simple scanning effect.

Partition of ciprofloxacin and moxifloxacin measured by phase transfer

The differences in behavior of ciprofloxacin and moxifloxacin observed by AFM experiments might be related to their ability to partition between aqueous and hydrophobic environments. To this end, we followed the transfer of the ciprofloxacin and moxifloxacin from an aqueous to a lipidic phase, using egg yolk phosphatidylcholine dissolved in chloroform (Fig. 4). Mostly, egg yolk phosphatidylcholine is a mixture of C16 and C18 saturated alkyl chains at C-1, and C18 unsaturated alkyl chain at C-2. Its thickness and degree of hydration, as well as mean acyl-chain area, are well known (25,26). Egg yolk phosphatidylcholine is commonly used to mimic lipid membranes and shows close characteristics of synthetic lipids used in this study. For example, the thickness of egg yolk phosphatidylcholine bilayer was estimated to be 30 Å, a close value to the thickness of DPPC (29.3 Å) and DOPC (30 Å; deduced from the thickness of DSPC, which has the same carbon number in the alkyl chain as DOPC (26)). In the absence of lipid, more than 40% of ciprofloxacin was detected in the aqueous phase, while only 5% of moxifloxacin was found in these conditions. A huge amount of this latter was found at the interface. The addition of lipids to the organic phase, with a lipid/drug molar ratio up to 50:1 did not change significantly the drug phase transfer.

Transfer of fluoroquinolones from lipid monolayer to aqueous phase

To get more insight on the partition of fluoroquinolones between lipid and aqueous phases, we investigated the ability of fluoroquinolones to be released from a lipid monolayer to an aqueous phase, by using the Langmuir trough technique. The amount of fluoroquinolone found in the subphase increased with the initial quantity of fluoroquinolone in the monolayer (data not shown). For a DOPC/DPPC/fluoroquinolone ratio 1:1:2, a plateau value was reached within 10 min for ciprofloxacin and 15 min for moxifloxacin (Fig. 5). At this equilibrium state, the percentage of fluoroquinolone detected in the subphase was clearly higher for ciprofloxacin (~70%) as compared to moxifloxacin (at ~40%). In the experimental conditions used, no lipid was detected by phospholipid assay

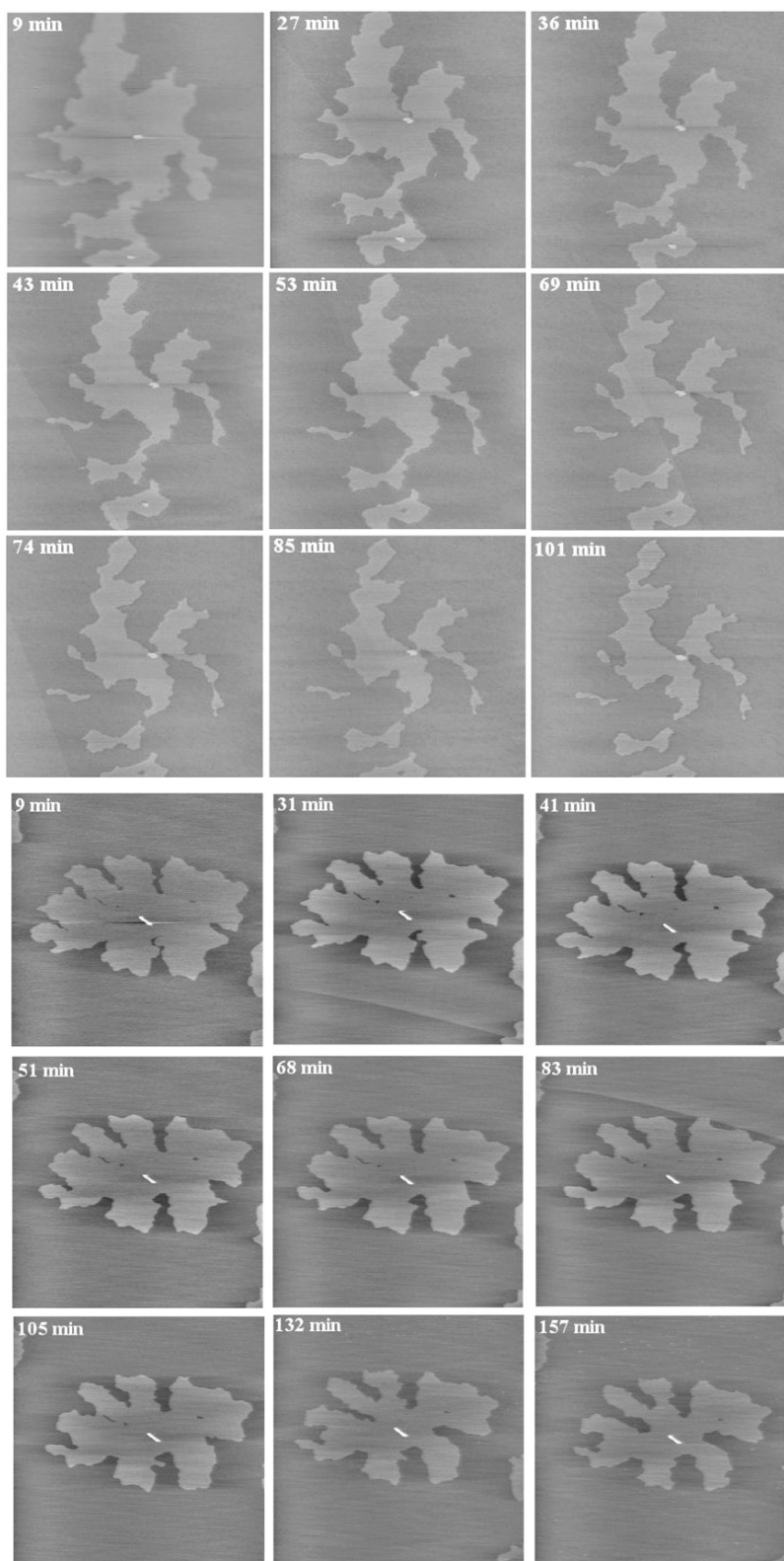


FIGURE 2 AFM height images ($20\ \mu\text{m} \times 20\ \mu\text{m}$ (top panels) or $15\ \mu\text{m} \times 15\ \mu\text{m}$ (bottom panels), z-scale: 5 nm) of a mixed DOPC/DOPC (1:1, mol/mol) bilayer recorded in Tris 10 mM, NaCl 100 mM buffer, pH 7.4 containing 1 mM of ciprofloxacin (top panels) or moxifloxacin (bottom panels) at increasing incubation time.

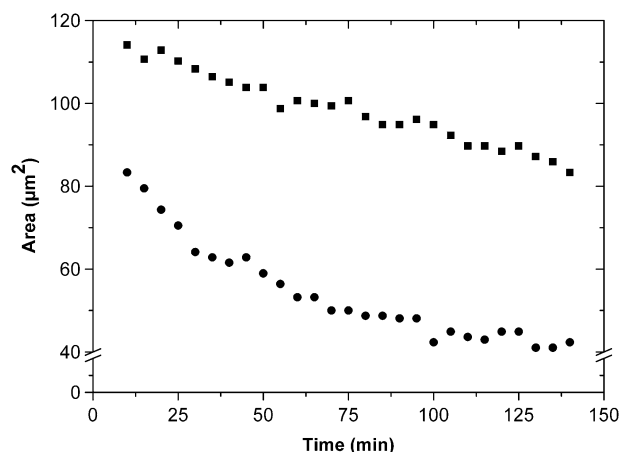


FIGURE 3 Evolution of the area of the DPPC domain (Fig. 2) with time for DOPC/DPPC bilayers incubated in Tris 10 mM, NaCl 100 mM buffer, pH 7.4, containing 1 mM of ciprofloxacin (solid squares) or moxifloxacin (solid circles).

in the buffer that supports the lipid-fluoroquinolone monolayer.

Conformational analysis of the interactions between fluoroquinolones and lipids

In an attempt to correlate our experimental data with molecular modeling, the interaction of ciprofloxacin and moxifloxacin with a model membrane was calculated using the IMPALA method. This procedure was used to study the membrane behavior of both molecules when crossing the bilayer from the hydrophilic environment to the hydrophobic.

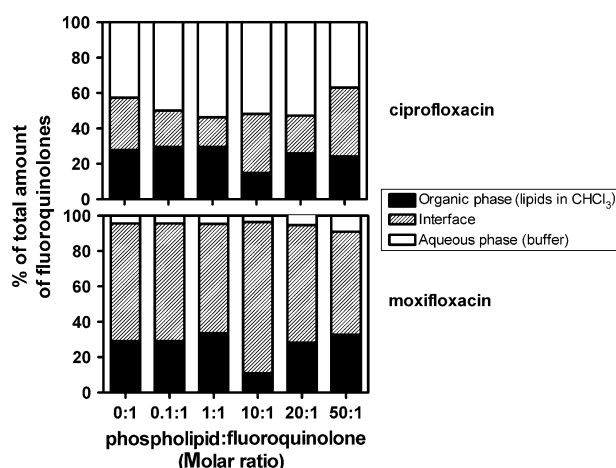


FIGURE 4 Phase transfer of ciprofloxacin (1 μ M, top panel) and moxifloxacin (1 μ M, bottom panel) in Tris buffer pH 7.4 against increasing amounts of PC (from 0.1:1 up to a lipid/drug ratio of 50:1) in chloroform. (Open bars) Drug in aqueous phase. (Hatched bars) Drug at interface (calculated from the difference between initial drug concentration and measured drug in aqueous and organic phase). (Solid bars) Drug in organic phase. Experiments were reproduced at least three times with similar results.

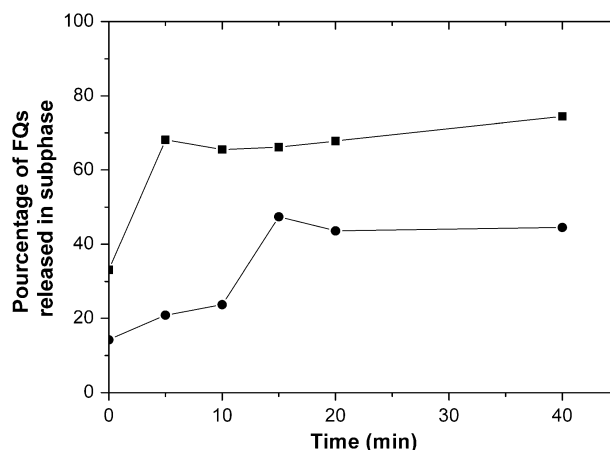


FIGURE 5 Kinetics of the release of fluoroquinolones from the mixed lipids/fluoroquinolones monolayer to the subphase (10 mM Tris pH 7.4, 25°C). Results are expressed as the percentage of fluoroquinolones initially present in the monolayer. Ciprofloxacin, \blacksquare ; and moxifloxacin, \bullet . Molar proportion of DPPC/DOPC/fluoroquinolones (1:1:2).

Fig. 6 A shows the most stable position of each molecule to the membrane. Both fluoroquinolones are clearly located at the hydrophilic-hydrophobic interface. The molecules were embedded into the membrane, with their mass center near the phospholipid headgroup/acyl-chain interface (~ 13 Å from the bilayer center), as shown on the plot of the mass center position versus the restraints (Fig. 6 B). It should be noted that differences were seen between ciprofloxacin and moxifloxacin. The interaction of moxifloxacin notably appeared more favorable than that of ciprofloxacin, since the restraint value of the most stable position was 1.5 kcal/mol lower for moxifloxacin as compared to ciprofloxacin.

Effect of fluoroquinolones on lipid monolayer—surface-pressure isotherms

To investigate the ability of fluoroquinolones to modify the surface pressure versus area isotherms of DOPC/DPPC (1:1) monolayers, we investigated the effect of increasing amounts of antibiotics on these isotherms curves.

For the sake of accuracy, we took into account the release of fluoroquinolones from the lipid to the aqueous phases in the determination of the quantity of drug remaining in the monolayer at the air-water interface, on the monolayers isotherms. We therefore recalculated the monolayer compression isotherms using the proportion of fluoroquinolones remaining in the monolayer after 30 min. Results are illustrated in Fig. 7.

The curve corresponding to pure DOPC/DPPC (1:1) is in perfect agreement with the one already reported (27). As already evoked by Montero et al. (28), pure ciprofloxacin or moxifloxacin does not form a film at the air-water interface.

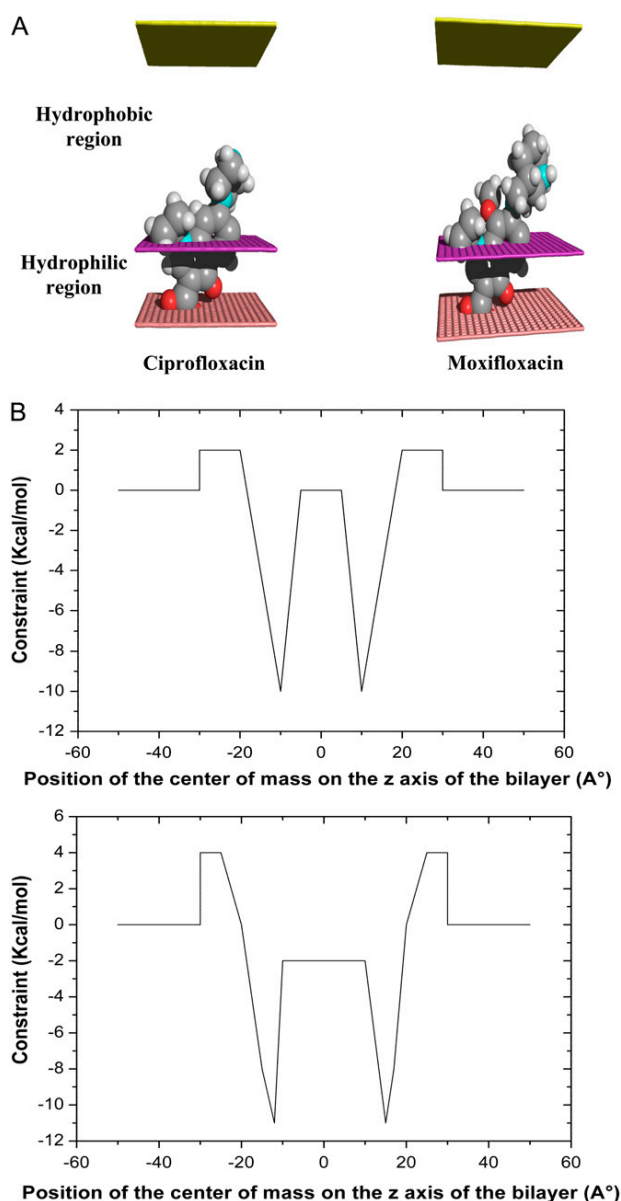


FIGURE 6 Molecular modeling of the interactions between ciprofloxacin and moxifloxacin with an implicit membrane. (A) Most favorable position of the ciprofloxacin (*left*) and moxifloxacin (*right*) in a lipid bilayer. (B) Restraints versus the position of the ciprofloxacin (*up*) and moxifloxacin (*down*) in the bilayer. Constraints are expressed in kcal/mol and the positions are expressed in Ångströms.

In presence of fluoroquinolones, the isotherms were shifted toward the small molecular areas. This effect is more pronounced with moxifloxacin (Fig. 7 B) than ciprofloxacin (Fig. 7 A).

In addition, fluoroquinolones also affected the collapse pressure: 46.0 mN/m for DOPC/DPPC; 45.9 mN/m, 44.8 mN/m, and 37.7 mN/m, for initial proportions of DOPC/DPPC/moxifloxacin of 1:1:0.4, 1:1:1, and 1:1:2, respec-

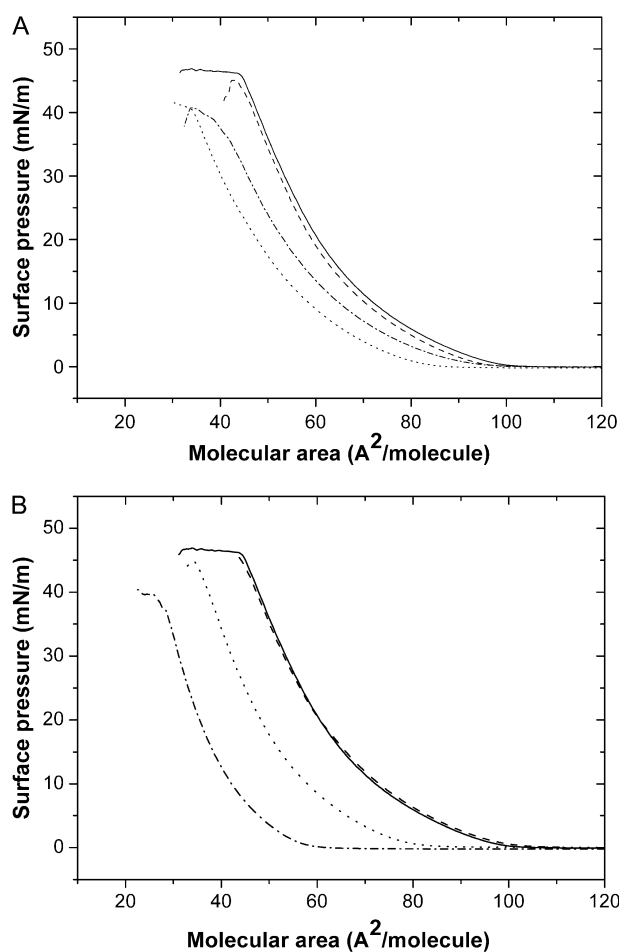


FIGURE 7 Surface pressure-molecular area isotherms of DOPC/DPPC in the presence of ciprofloxacin (A) and moxifloxacin (B), on a subphase of 10 mM Tris at pH 7.4 and 25°C. Mean molecular area were corrected to take into account the percentage of fluoroquinolone remaining at the interface. DOPC/DPPC/drug molar ratio were 1:1:0 (*continuous line*), 1:1:0.4 (*discontinuous line*), 1:1:1 (*dotted line*), and 1:1:2 (*dash-dotted line*).

tively; and 46.0 mN/m, 40.5 mN/m, and 37.8 mN/m, for initial proportions of DOPC/DPPC/ciprofloxacin of 1:1:0.4, 1:1:1, and 1:1:2, respectively. This disruption of the lipid monolayer stability at a high compression level is more pronounced at a high level of fluoroquinolone in the mixed monolayer.

Effect of fluoroquinolones on lipid conformation—ATR-FTIR

Because the lower area occupied by lipids in presence of fluoroquinolones might be partly due to a change in the orientation of lipid at the interface by straightening up their fatty acid chains, we used ATR-FTIR to investigate the effect of ciprofloxacin and moxifloxacin on conformation and orientation of acyl chain of lipids.

Nonpolarized ATR-FTIR spectra of supported layers of DPPC, drug (ciprofloxacin or moxifloxacin), and DPPC/drug at a molar ratio of 1:1 were recorded (Fig. 8, *top panel*). As the drug proportion increased, the drug spectrum appeared in the DPPC/drug mixture spectrum, notably at 1630 cm^{-1} . Interestingly, in DPPC/drug spectra, the DPPC $\nu(\text{C}=\text{O})$ band at 1736 cm^{-1} was modified in terms of frequency and shape, suggesting a modification of the interfacial lipid carbonyl groups. Analysis of the lipid C-H wagging ($\nu_w(\text{CH}_2)$) allowed us to get information on lipid chain conformation and proportion of the chains in the all-*trans* conformation (23). Here the wagging band at 1200 cm^{-1} was selected because it has little overlap with other lipid or drug absorption. As shown in Fig. 8, *bottom panel*, area evolution of DPPC peak at $1206\text{--}1193\text{ cm}^{-1}$ as function of increasing amounts of fluoroquinolones decreased by up to 60 and 72% for cipro-

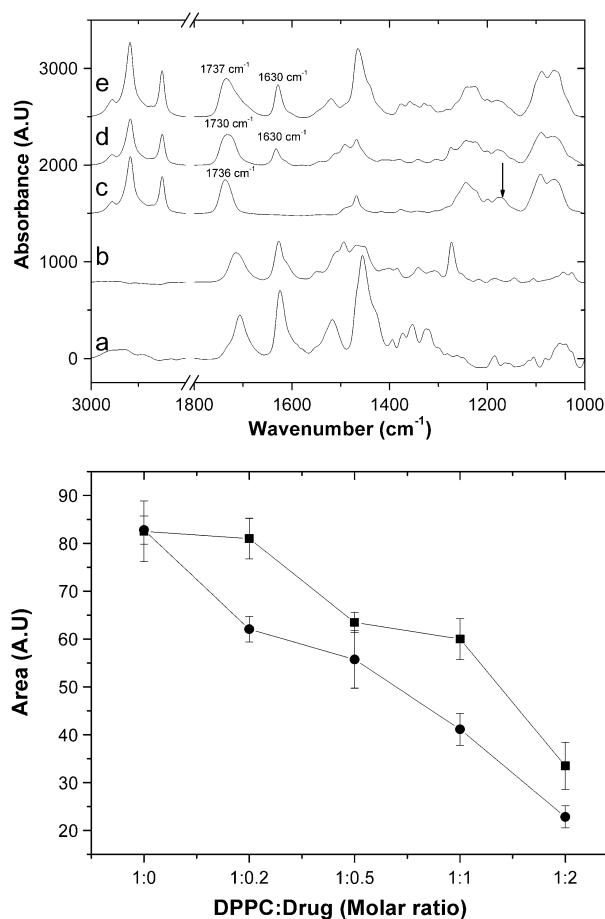


FIGURE 8 Fluoroquinolones effect on the conformation of DPPC monolayer as revealed by the infrared absorbance spectra. (*Top panel*) ATR-FTIR spectra of moxifloxacin (a), ciprofloxacin (b), DPPC (c), DPPC/ciprofloxacin (d), and DPPC/moxifloxacin (e). DPPC was used at 50 mg/ml and the molar ratio of lipid/drug was 1:1. (*Bottom panel*) Evolution of the peak area at 1200 cm^{-1} (wagging $\gamma_w(\text{CH}_2)$ band; integrated between 1206 and 1193 cm^{-1}) as a function of increasing lipid/drug ratio: 1:0, 1:0.2, 1:0.5, 1:1, and 1:2. Ciprofloxacin, ■; and moxifloxacin, ●.

floxacin and moxifloxacin, respectively. These data indicated a loss of all-*trans* conformation and the appearance of a kink somewhere between C-2 and C-6 of the chain.

Effect of fluoroquinolones on lipid orientation—ATR-FTIR

To get information on molecular orientation in the absence or in the presence of both fluoroquinolones, we took advantage from the fact that, in an ordered membrane deposited on the germanium crystal (oriented multilayers), all the molecules have the same orientation with respect to a normal to the germanium plate. Measuring the spectral intensity with two orientations of the incident-light electric field obtained with a polarizer allowed us to obtain information on several chemical groups of the lipid molecule. The dichroic spectrum of pure DPPC and DPPC/drug (molar ratio 1:1) mixture were obtained by subtracting the spectrum recorded with perpendicular-polarized light from that recorded with the parallel-polarized light using the lipid $\nu(\text{C}=\text{O})$ band at $1780\text{--}1700\text{ cm}^{-1}$ as a reference (Fig. 9) (29). Interestingly the dichroic spectra of DPPC/drug mixture displayed strong dichroism for bands assigned to the drug, notably at 1630 and 1465 cm^{-1} , suggesting a well-organized, well-defined orientation of the drug in the DPPC bilayer. The orientation of the lipid acyl chain can be estimated from the wagging band ($\nu_w(\text{CH}_2)$). The dipole of this transition is oriented parallel to the all-*trans* chain (23). In turn, positive deviations of the dichroism spectrum demonstrate that the chains are mainly perpendicular to the germanium surface, i.e., perpendicular to the membrane plane since AFM recording demonstrated that membranes orient themselves parallel to the germanium surface, even when natural membranes are used (30). In Fig. 9, *bottom panel*, we plotted the area evolution of the wagging peak integrated between 1206 and 1193 cm^{-1} as a function of the DPPC/drug molar ratio. Both fluoroquinolones induced a marked and similar decrease of the area when they were added at low concentration (1:0.2 molar ratio). When the amounts of fluoroquinolones were increased, the area decreased further in presence of ciprofloxacin but remained almost stable for moxifloxacin. This observation was similar for the four wagging peaks (indicated by arrows; Fig. 9, *top panel*) ($1275\text{--}1261\text{ cm}^{-1}$, $1253\text{--}1240\text{ cm}^{-1}$, $1229\text{--}1216\text{ cm}^{-1}$, and $1206\text{--}1193\text{ cm}^{-1}$).

To quantify the orientation of DPPC all-*trans* chains, we measured the dichroic ratio for wagging band at 1200 cm^{-1} . $R^{\text{ATR}}(A_{\parallel}/A_{\perp})$ was 6.8 with an isotropic dichroic ratio of 1.33 (calculated from $\nu(\text{C}=\text{O})$ band at $1755\text{--}1750\text{ cm}^{-1}$ (29)). On the basis of this determination, the angle between the acyl chains of DPPC and the normal at the germanium surface was found to be 21° . The same calculation was done in the presence of fluoroquinolones at a lipid/drug ratio of 1:1. The angle was 27° and 20° in the presence of ciprofloxacin and moxifloxacin, respectively. These data suggested that in contrast to ciprofloxacin, moxifloxacin had no effect on the

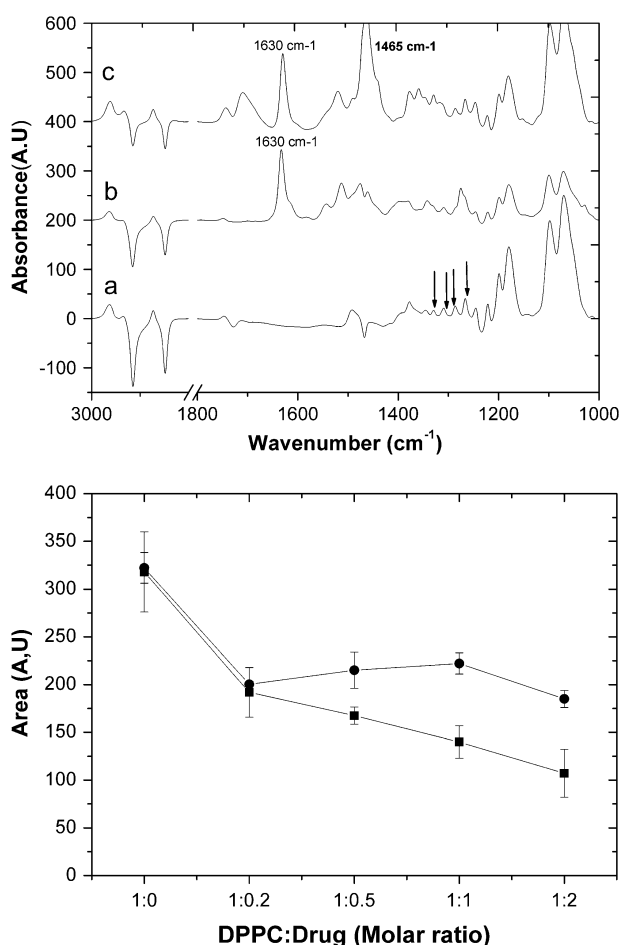


FIGURE 9 Fluoroquinolones effect on the orientation of DPPC monolayer as revealed by ATR-FTIR dichroic spectra. (Top panel) Polarized ATR-FTIR spectra of DPPC (a), DPPC/ciprofloxacin (b), and DPPC/moxifloxacin (c). DPPC was used at 50 mg/ml and the molar ratio of lipid/drug was 1:1. Wagging $\gamma_w(\text{CH}_2)$ bands are indicated by arrows. (Bottom panel) Area evolution of dichroic peak of 1200 cm^{-1} of DPPC in the presence of fluoroquinolones. Integration area of dichroic $\gamma_w(\text{CH}_2)$ band (integrated between 1206 and 1193 cm^{-1}) was plotted versus DPPC/drug molar ratio as indicated, in the presence of ciprofloxacin, ■; and moxifloxacin, ●.

orientation of the acyl chains and did not induce additional disorder.

DISCUSSION

Our previous studies showed differences in accumulation and intracellular activity between ciprofloxacin and moxifloxacin that may actually result from their differential susceptibility to efflux by the ciprofloxacin transporter (1). Moxifloxacin differs from ciprofloxacin by the presence of a C-8 methoxy group and a bulkier C-7 (octahydropyrrolo (3.4)-pyridinyl versus piperazinyl for ciprofloxacin) substituent (31). As previously shown (32), these changes resulted in an increase in hydrophobicity ($\log D \sim -0.28$ (33) for moxifloxacin and -0.79 (34) for ciprofloxacin). However, these structural

modifications between moxifloxacin and ciprofloxacin may not account for the differences in the pK values (from 6.25 to 6.09 (33,36), since these differences are below the experimental errors. Interestingly, these compounds were much weaker acids than aromatic carboxylic acids. The reduced acidity may be ascribed to the formation of an intramolecular hydrogen bond between the carboxyl and neighboring keto groups in the quinoline ring, resulting in stabilization of the protonated form of the carboxyl group.

The activity of efflux pumps in general, and those involved for ciprofloxacin or moxifloxacin cellular accumulation, in particular, is closely related to the interaction of the drug with lipids, regardless of the model proposed for their activity (i.e., flippase or hydrophobic vacuum cleaner). We therefore looked at the influence of the small changes in chemical structure between moxifloxacin and ciprofloxacin on their interaction with lipids. To address this crucial question, the interactions between model lipid membranes and the two fluoroquinolones were probed using a variety of techniques.

Nanoscale investigations by AFM revealed different behaviors for ciprofloxacin and moxifloxacin. AFM imaging showed a reduction of the size of the DPPC gel phase domains in presence of fluoroquinolones. The erosion process is greater for moxifloxacin compared to ciprofloxacin, and follows an exponential-like function-decrease for moxifloxacin and a linear-decrease for ciprofloxacin. Considering both molecules, the difference in their ability to erode the DPPC gel phase domains might be due to a better insertion of the moxifloxacin than the ciprofloxacin into the fluid matrix, and a more marked decrease of the line tension at the boundary of the DOPC/DPPC phases resulting from a fluidification of the DPPC.

This marked effect of moxifloxacin on lipids as compared to ciprofloxacin was confirmed by conformational analysis. In accordance with experimental data obtained for ciprofloxacin (37) or grepafloxacin (38), the fluoroquinolones are located at the lipid-water interface, near the first carbons of the acyl chains. Both molecules showed a minimum of energy when they are at the phospholipids headgroup/acyl-chains interface, and the interaction energy rose markedly when the molecule was forced into the hydrophobic domain. This energy increase was less marked for moxifloxacin as compared to ciprofloxacin, suggesting a higher affinity of moxifloxacin for lipid phase.

Taken together, our data suggest that ciprofloxacin and moxifloxacin interact in a very different way with lipids. The major challenge, however, is to understand the mechanism, at a molecular level, unraveling the interaction between lipids and fluoroquinolones and the path of these antibiotic molecules through lipid layers. Previous data reported by Montero et al. (28) showed a shift of the surface pressure-area isotherms of monolayer toward a lower area per molecule in the presence of ciprofloxacin. We extended these data to one major fluoroquinolone used in clinics, moxifloxacin. To go further in the mechanism involved, we monitored the amount

of fluoroquinolones in the subphase after the monolayer compression. In agreement with the hypothesis based on a dissolving effect in the subphase (39), we did find fluoroquinolones therein with a higher proportion of ciprofloxacin as compared to moxifloxacin. Taking into account the amount of fluoroquinolones present inside the monolayer, we corrected the surface-pressure-area isotherms of the monolayer and again observed a shift toward a lower area per molecule in the presence of fluoroquinolones. This effect was more marked with moxifloxacin as compared to ciprofloxacin. The dissolving effect in the aqueous phase is therefore probably essential, although not fully sufficient, to explain the condensing effect of fluoroquinolones.

Thus, we investigated a change in the lipid chain conformation and orientation using ATR-FTIR technique (21,40). Indeed, the drug-induced area condensation of lipids can derive from the acyl ordering attained when *trans-gauche* isomerization about the carbon-carbon bonds is reduced. The *trans* conformation is the most stable and has an estimated energy barrier of 3.5 kcal/mol to rotate past the eclipsed configuration to the *gauche* form. The all-*trans* conformation allows the chain to be maximally extended, whereas a *gauche* bond alters the direction of the chain inducing a kink in the chain. Our results clearly indicated that moxifloxacin has a higher ability than ciprofloxacin to markedly decrease the number of all-*trans* conformation. The related change in the packing of the acyl chains might allow moxifloxacin to be located in the pocket created by the presence of a kink in the acyl chain. In contrast, with ciprofloxacin, the appearance of a kink from the all-*trans* chain conformation would be less marked, suggesting a less important change in lipid packing. Interestingly, both condensing effects (lower area of mixed monolayer lipids/fluoroquinolones) have also been described when cholesterol was added to fluid-phase phosphatidylcholine (41–43).

The disorder in the lipid chains revealed by the decrease of all-*trans* conformations has also been analyzed in terms of orientation and tilt between the molecular axis (the membrane normal) and the transition dipole moments. In this analysis, the ciprofloxacin showed an additional cause of disorder, because it modifies the orientation of the acyl chain in relation to its higher ability to be released in an aqueous phase after monolayer compression.

Differences in the charge distribution of the molecule at the physiological pH could also explain changes for drug membrane location and bound hydration shell surrounding the headgroup of membrane lipids, which, in turn, could partly explain the more condensing effect of moxifloxacin as compared to ciprofloxacin. Moreover, the determinations were made in aqueous environment, whereas the condensing effect of moxifloxacin involved the presence of the drug with a lipidic phase.

All together, we showed that the condensing effect of fluoroquinolones on lipid layer resulted not only from a dissolving mechanism but also from an alteration of the in-

tramolecular acyl-chain order in relation to a reduction in *trans-gauche* isomerization about the carbon-carbon bonds, and change in the average molecular tilt of lipid acyl chain of DPPC. The two fluoroquinolones investigated showed difference in their effects. Ciprofloxacin had a lower ability to decrease the all-*trans* conformation of lipid chains than moxifloxacin but showed a higher capacity to affect the orientation of lipid chains and to disorder the membrane. These effects might explain its higher ability to be released from the lipid monolayer to aqueous phase and its lower effect on surface pressure-area isotherms of monolayers. In contrast, moxifloxacin has a lower capacity to induce membrane disorder and does not change the tilt between the molecular axis and the transition dipole moment. Moxifloxacin has also a higher tendency to decrease the number of all-*trans* conformations with increase of kink, creating a pocket in which moxifloxacin can be located. This can explain why the amount of moxifloxacin in the aqueous phase was lower than that found for ciprofloxacin and why the mean molecular area of lipids/fluoroquinolones monolayers after compression is significantly lower in the presence of moxifloxacin as compared to ciprofloxacin.

This model is entirely compatible with the physicochemical characteristics of the two fluoroquinolones. It suggested that small structural differences among fluoroquinolones (notably overall molecular hydrophobicity ($P_{app} = 0.089$ vs. 0.031 for ciprofloxacin and moxifloxacin, respectively (45)), bulkiness, and/or the internal dynamics of the C-7 substituent, could be important for drug lipid interactions and lipid packing. The diazabicyclonyl-ring at position 7 of moxifloxacin, by aligning the *sn-2* chain, probably contributes to the higher tendency of this antibiotic to induce a decrease of all-*trans* configuration as compared to ciprofloxacin. This is in line with data reported with *n*-alkyl-piperaziny-ciprofloxacin (39).

In conclusion, we provided a comprehensive picture of the interaction of the two major fluoroquinolones ciprofloxacin and moxifloxacin with lipids, and elucidate fundamental issues such as the relationship between lipid chain conformation and orientation with changes in membrane properties as determined by Langmuir studies and the ability of drugs to diffuse through membranes. All these parameters might be related to the activity of membranous proteins. Our work notably showed that an increase in drug lipophilicity and addition of a bulky moiety (moxifloxacin versus ciprofloxacin) produced marked changes in the packing of lipids. This was concomitant with a lower release of the more lipophilic drug from lipid monolayer and with a potential inefficient activity of efflux proteins which could be involved in a kind of futile cycle resulting in an increase in cellular accumulation (1). So far, progress in understanding the structure-function relationships of membranes and understanding of the lipid-drug interaction appears to be of crucial importance in understanding the mechanisms involved in cellular drug accumulation.

We thank Professor J. Poupaert for fruitful discussions, and Professors F. Van Bambeke and P. M. Tulkens for supporting the project.

R.B., E.G., L.L., M.D., and Y.D. are, respectively, Research Directors and Research Associates of the National Foundation for Scientific Research. H.B. is an assistant and doctoral fellow of the Université Catholique de Louvain. The support of the Région Wallonne, of the National Foundation for Scientific Research, of the Université Catholique de Louvain (Fonds Spéciaux de Recherche, Actions de Recherche Concertées), and of the Federal Office for Scientific, Technical and Cultural Affairs (Interuniversity Poles of Attraction Program), is gratefully acknowledged. We also thank Bayer Healthcare AG for providing us fluoroquinolone antibiotics.

REFERENCES

1. Michot, J. M., C. Seral, F. Van Bambeke, M. P. Mingeot-Leclercq, and P. Tulkens. 2005. Influence of efflux transporters on the accumulation and efflux of four quinolones (ciprofloxacin, levofloxacin, garenoxacin, and moxifloxacin) in J774 macrophages. *Antimicrob. Agents Chemother.* 49:2429–2437.
2. Bakker-Woudenberg, I. A., M. T. ten Kate, L. Guo, P. Working, and J. W. Mouton. 2001. Improved efficacy of ciprofloxacin administered in polyethylene glycol-coated liposomes for treatment of *Klebsiella pneumoniae* pneumonia in rats. *Antimicrob. Agents Chemother.* 45:1487–1492.
3. Bakker-Woudenberg, I. A., M. T. ten Kate, L. Guo, P. Working, and J. W. Mouton. 2002. Ciprofloxacin in polyethylene glycol-coated liposomes: efficacy in rat models of acute or chronic *Pseudomonas aeruginosa* infection. *Antimicrob. Agents Chemother.* 46:2575–2581.
4. Wong, J. P., H. Yang, K. L. Blasetti, G. Schnell, J. Conley, and L. N. Schofield. 2003. Liposome delivery of ciprofloxacin against intracellular *Francisella tularensis* infection. *J. Control. Release.* 92:265–273.
5. Rolston, K. V., D. Yadegarynia, D. P. Kontoyiannis, I. I. Raad, and D. H. Ho. 2006. The spectrum of Gram-positive bloodstream infections in patients with hematologic malignancies, and the in vitro activity of various quinolones against Gram-positive bacteria isolated from cancer patients. *Int. J. Infect. Dis.* 10:223–230.
6. Bounds, S. J., R. Nakkula, and J. D. Walters. 2000. Fluoroquinolone transport by human monocytes: characterization and comparison to other cells of myeloid lineage. *Antimicrob. Agents Chemother.* 44:2609–2614.
7. Hirota, M., T. Totsu, F. Adachi, K. Kamikawa, J. Watanabe, S. Kanegasaki, and K. Nakata. 2001. Comparison of antimycobacterial activity of grepafloxacin against *Mycobacterium avium* with that of levofloxacin: accumulation of grepafloxacin in human macrophages. *J. Infect. Chemother.* 7:16–21.
8. Hara, T., H. Takemura, K. Kanemitsu, H. Yamamoto, and J. Shimada. 2000. Comparative uptake of grepafloxacin and ciprofloxacin by a human monocytic cell line, THP-1. *J. Infect. Chemother.* 6:162–167.
9. Seral, C., M. Barcia-Macay, M. P. Mingeot-Leclercq, P. M. Tulkens, and F. Van Bambeke. 2005. Comparative activity of quinolones (ciprofloxacin, levofloxacin, moxifloxacin and garenoxacin) against extracellular and intracellular infection by *Listeria monocytogenes* and *Staphylococcus aureus* in J774 macrophages. *J. Antimicrob. Chemother.* 55:511–517.
10. Fresta, M., S. Guccione, A. R. Beccari, P. M. Fumeri, and G. Puglisi. 2002. Combining molecular modeling with experimental methodologies: mechanism of membrane permeation and accumulation of ofloxacin. *Bioorg. Med. Chem.* 10:3871–3889.
11. Michot, J. M., F. Van Bambeke, M. P. Mingeot-Leclercq, and P. M. Tulkens. 2004. Active efflux of ciprofloxacin from J774 macrophages through an MRP-like transporter. *Antimicrob. Agents Chemother.* 48:2673–2682.
12. Fernandez-Teruel, C., I. Gonzalez-Alvarez, V. G. Casabo, A. Ruiz-Garcia, and M. Bermejo. 2005. Kinetic modeling of the intestinal transport of sarafloxacin. Studies in situ in rat and in vitro in Caco-2 cells. *J. Drug Target.* 13:199–212.
13. Berquand, A., N. Fa, Y. F. Dufrene, and M. P. Mingeot-Leclercq. 2005. Interaction of the macrolide antibiotic azithromycin with lipid bilayers: effect on membrane organization, fluidity, and permeability. *Pharm. Res.* 22:465–475.
14. Siarheyeva, A., J. J. Lopez, and C. Glaubitz. 2006. Localization of multidrug transporter substrates within model membranes. *Biochemistry.* 45:6203–6211.
15. Hinrichs, J. W., K. Klappe, I. Hummel, and J. W. Kok. 2004. ATP-binding cassette transporters are enriched in non-caveolar detergent-insoluble glycosphingolipid-enriched membrane domains (DIGs) in human multidrug-resistant cancer cells. *J. Biol. Chem.* 279:5734–5738.
16. Hinrichs, J. W., K. Klappe, and J. W. Kok. 2005. Rafts as missing link between multidrug resistance and sphingolipid metabolism. *J. Membr. Biol.* 203:57–64.
17. Laurent, G., M. B. Carlier, B. Rollman, F. Van Hoof, and P. M. Tulkens. 1982. Mechanism of aminoglycoside-induced lysosomal phospholipidosis: in vitro and in vivo studies with gentamicin and amikacin. *Biochem. Pharmacol.* 31:3861–3870.
18. Ducarme, P., M. Rahman, and R. Brasseur. 1998. IMPALA: a simple restraint field to simulate the biological membrane in molecular structure studies. *Proteins.* 30:357–371.
19. Demel, R. A., W. S. Geurts van Kessel, R. F. Zwaal, B. Roelofsen, and L. L. van Deenen. 1975. Relation between various phospholipase actions on human red cell membranes and the interfacial phospholipid pressure in monolayers. *Biochim. Biophys. Acta.* 406:97–107.
20. Marsh, D. 1996. Lateral pressure in membranes. *Biochim. Biophys. Acta.* 1286:183–223.
21. Goormaghtigh, E., V. Raussens, and J. M. Ruyschaert. 1999. Attenuated total reflection infrared spectroscopy of proteins and lipids in biological membranes. *Biochim. Biophys. Acta.* 1422:105–185.
22. Tatulian, S. A. 2003. Attenuated total reflection Fourier transform infrared spectroscopy: a method of choice for studying membrane proteins and lipids. *Biochemistry.* 42:11898–11907.
23. Fringeli, U. P., and H. H. Gunthard. 1981. Infrared membrane spectroscopy. *Mol. Biol. Biochem. Biophys.* 31:270–332.
24. Fa, N., S. Ronkart, A. Schanck, M. Deleu, A. Gaigneaux, E. Goormaghtigh, and M. P. Mingeot-Leclercq. 2006. Effect of the antibiotic azithromycin on thermotropic behavior of DOPC or DPPC bilayers. *Chem. Phys. Lipids.* 144:108–116.
25. Komatsu, H., H. Saito, S. Okada, M. Tanaka, M. Egashira, and T. Handa. 2001. Effects of the acyl chain composition of phosphatidylcholines on the stability of freeze-dried small liposomes in the presence of maltose. *Chem. Phys. Lipids.* 113:29–39.
26. Hara, M., H. Yuan, Q. Yang, T. Hoshino, A. Yokoyama, and J. Miyake. 1999. Stabilization of liposomal membranes by thermozeaxanthins: carotenoid-glucoside esters. *Biochim. Biophys. Acta.* 1461:147–154.
27. Vie, V., N. Van Mau, E. Lesniewska, J. P. Goudonnet, F. Heitz, and C. Le Grimellec. 1998. Distribution of ganglioside G(M1) between two-component, two-phase phosphatidylcholine monolayers. *Langmuir.* 14:4574–4583.
28. Montero, M. T., J. Hernandez-Borrell, and K. M. W. Keough. 1998. Fluoroquinolone-biomembrane interactions: monolayer and calorimetric studies. *Langmuir.* 14:2451–2454.
29. Bechinger, B., J. M. Ruyschaert, and E. Goormaghtigh. 1999. Membrane helix orientation from linear dichroism of infrared attenuated total reflection spectra. *Biophys. J.* 76:552–563.
30. Ivanov, D., N. Dubreuil, V. Raussens, J. M. Ruyschaert, and E. Goormaghtigh. 2004. Evaluation of the ordering of membranes in multilayer stacks built on an ATR-FTIR germanium crystal with atomic force microscopy: the case of the H⁺, K⁺-ATPase-containing gastric tubulovesicle membranes. *Biophys. J.* 87:1307–1315.
31. Dalhoff, A., U. Petersen, and R. Endermann. 1996. In vitro activity of BAY 12–8039, a new 8-methoxyquinolone. *Chemotherapy.* 42:410–425.
32. Klopman, G., O. T. Macina, M. E. Levinson, and H. S. Rosenkranz. 1987. Computer automated structure evaluation of quinolone antibacterial agents. *Antimicrob. Agents Chemother.* 31:1831–1840.

33. Langlois, M. H., M. Montagut, J. P. Dubost, J. Grellet, and M. C. Saux. 2005. Protonation equilibrium and lipophilicity of moxifloxacin. *J. Pharm. Biomed. Anal.* 37:389–393.
34. Sun, J., S. Sakai, Y. Tauchi, Y. Deguchi, J. Chen, R. Zhang, and K. Morimoto. 2002. Determination of lipophilicity of two quinolone antibacterials, ciprofloxacin and grepafloxacin, in the protonation equilibrium. *Eur. J. Pharm. Biopharm.* 54:51–58.
35. Neves, P., A. Leite, M. Rangel, B. de Castro, and P. Gameiro. 2007. Influence of structural factors on the enhanced activity of moxifloxacin: a fluorescence and EPR spectroscopic study. *Anal. Bioanal. Chem.* 387:1543–1552.
36. Furet, Y. X., J. Deshusses, and J. C. Pechere. 1992. Transport of pefloxacin across the bacterial cytoplasmic membrane in quinolone-susceptible *Staphylococcus aureus*. *Antimicrob. Agents Chemother.* 36:2506–2511.
37. Hernandez-Borrell, J., and M. T. Montero. 2003. Does ciprofloxacin interact with neutral bilayers? An aspect related to its antimicrobial activity. *Int. J. Pharm.* 252:149–157.
38. Rodrigues, C., P. Gameiro, S. Reis, J. L. F. Lima, and B. de Castro. 2002. Interaction of grepafloxacin with large unilamellar liposomes: partition and fluorescence studies reveal the importance of charge interactions. *Langmuir.* 18:10231–10236.
39. Vazquez, J. L., M. T. Montero, S. Merino, O. Domenech, M. Berlanga, M. Vinas, and J. Hernandez-Borrell. 2001. Location and nature of the surface membrane binding site of ciprofloxacin: a fluorescence study. *Langmuir.* 17:1009–1014.
40. Pare, C., M. Laffleur, F. Liu, R. N. Lewis, and R. N. McElhaney. 2001. Differential scanning calorimetry and ^2H nuclear magnetic resonance and Fourier transform infrared spectroscopy studies of the effects of transmembrane α -helical peptides on the organization of phosphatidylcholine bilayers. *Biochim. Biophys. Acta.* 1511:60–73.
41. Smaby, J. M., M. Momen, V. S. Kulkarni, and R. E. Brown. 1996. Cholesterol-induced interfacial area condensations of galactosylceramides and sphingomyelins with identical acyl chains. *Biochemistry.* 35:5696–5704.
42. Smaby, J. M., M. M. Momen, H. L. Brockman, and R. E. Brown. 1997. Phosphatidylcholine acyl unsaturation modulates the decrease in interfacial elasticity induced by cholesterol. *Biophys. J.* 73:1492–1505.
43. Bin, X., S. L. Horswell, and J. Lipkowski. 2005. Electrochemical and PM-IRRAS studies of the effect of cholesterol on the structure of a DMPC bilayer supported at an Au₁₁₁ electrode surface, part 1: properties of the acyl chains. *Biophys. J.* 89:592–604.
44. Sun, J., S. Sakai, Y. Tauchi, Y. Deguchi, G. Cheng, J. Chen, and K. Morimoto. 2003. Protonation equilibrium and lipophilicity of olamifloxacin (HSR-903), a newly synthesized fluoroquinolone antibacterial. *Eur. J. Pharm. Biopharm.* 56:223–229.
45. Piddock, L. J., and Y. F. Jin. 1999. Antimicrobial activity and accumulation of moxifloxacin in quinolone-susceptible bacteria. *J. Antimicrob. Chemother.* 43:Suppl B:39–42.

CHAPTER 2

Investigation of the interaction of Ciprofloxacin with eukaryotic and prokaryotic model lipids membrane

Chapter 2

As reviewed in the introduction, fluoroquinolones should cross the plasma membrane of eukaryotic cells as well as the outer membrane of Gram-negative or plasma membrane of Gram-positive bacteria to reach their bacterial targets (topoisomerase IV and DNA gyrase). We previously showed that CIP induced disorder and modified the orientation of the acyl chains of zwitterionic lipids, which are related to its propensity to be expelled from a monolayer upon compression (Bensikaddour et al., 2008a).

To check whether CIP interacts differently with eukaryotic and prokaryotic lipids model membrane, two selected phospholipids were used: a zwitterionic lipid (DPPC) that exhibit eukaryotic-like membrane, and a negatively charged lipid (DPPG), that exhibit prokaryotic-like membrane.

The binding parameters of CIP with lipids (DPPC and DPPG), were performed by steady state fluorescence anisotropy and quasi-elastic light scattering measurements. Additionally, the effects of CIP on the mobility of phosphate head groups and on the thermotropic behavior of lipids were investigated by ^{31}P Nuclear Magnetic Resonance and Total Reflection Fourier Transform Infrared spectroscopy, respectively.

The results indicate that CIP bound to selected lipids with a stoichiometry of (1:1; M:M), and the binding affinity was dependent on the presence of negative charged lipids. In fact, CIP decreased more the mobility of phospholipids head groups and induced a marked broaden effect on the thermotropic curve of DPPG than of DPPC.

This work supports the view that electrostatic interaction plays a major role in the CIP-lipids interaction and the existence of a primary step in a binding of CIP to the phospholipids bilayer surface.



Interactions of ciprofloxacin with DPPC and DPPG: Fluorescence anisotropy, ATR-FTIR and ^{31}P NMR spectroscopies and conformational analysis

Hayet Bensikaddour^a, Karim Snoussi^b, Laurence Lins^c, Françoise Van Bambeke^a, Paul M. Tulkens^a, Robert Brasseur^c, Erik Goormaghtigh^d, Marie-Paule Mingeot-Leclercq^{a,*}

^a Université Catholique de Louvain, Faculty of Medicine, Unité de Pharmacologie Cellulaire et Moléculaire, UCL 73.70, Avenue E. Mounier 73, B-1200 Bruxelles, Belgium

^b Université Catholique de Louvain, Faculty of Sciences, Unité de Chimie Structurale et des Mécanismes Réactionnels, Place L. Pasteur, 1, B-1348 Louvain-la-Neuve, Belgium

^c Faculté Universitaire des Sciences Agronomiques de Gembloux, Centre de Biophysique Moléculaire Numérique, Passage des Déportés, 2, B-5030 Gembloux, Belgium

^d Université Libre de Bruxelles, Faculty of Sciences, Unité de Structure et Fonction des Membranes Biologiques, CP206/02, Boulevard du Triomphe, B-1050 Bruxelles, Belgium

ARTICLE INFO

Article history:

Received 5 March 2008

Received in revised form 11 August 2008

Accepted 12 August 2008

Available online 6 September 2008

Keywords:

Ciprofloxacin

DPPC

DPPG

Steady-state fluorescence anisotropy

Melting temperature

ATR-FTIR

^{31}P NMR

Conformational analysis

ABSTRACT

The interactions between a drug and lipids may be critical for the pharmacological activity. We previously showed that the ability of a fluoroquinolone antibiotic, ciprofloxacin, to induce disorder and modify the orientation of the acyl chains is related to its propensity to be expelled from a monolayer upon compression [1]. Here, we compared the binding of ciprofloxacin on DPPC and DPPG liposomes (or mixtures of phospholipids [DOPC:DPPC], and [DOPC:DPPG]) using quasi-elastic light scattering and steady-state fluorescence anisotropy. We also investigated ciprofloxacin effects on the transition temperature (T_m) of lipids and on the mobility of phosphate head groups using Attenuated Total Reflection Fourier Transform Infrared-Red Spectroscopy (ATR-FTIR) and ^{31}P Nuclear Magnetic Resonance (NMR) respectively. In the presence of ciprofloxacin we observed a dose-dependent increase of the size of the DPPG liposomes whereas no effect was evidenced for DPPC liposomes. The binding constants K_{app} were in the order of 10^5 M^{-1} and the affinity appeared dependent on the negative charge of liposomes: DPPG>DOPC:DPPG (1:1; M:M)>DPPC>DOPC:DPPC (1:1; M:M). As compared to the control samples, the chemical shift anisotropy ($\Delta\sigma$) values determined by ^{31}P NMR showed an increase of 5 and 9 ppm for DPPC:CIP (1:1; M:M) and DPPG:CIP (1:1; M:M) respectively. ATR-FTIR experiments showed that ciprofloxacin had no effect on the T_m of DPPC but increased the order of the acyl chains both below and above this temperature. In contrast, with DPPG, ciprofloxacin induced a marked broadening effect on the transition with a decrease of the acyl chain order below its T_m and an increase above this temperature. Altogether with the results from the conformational analysis, these data demonstrated that the interactions of ciprofloxacin with lipids depend markedly on the nature of their phosphate head groups and that ciprofloxacin interacts preferentially with anionic lipid compounds, like phosphatidylglycerol, present at a high content in these membranes.

© 2008 Elsevier B.V. All rights reserved.

1. Introduction

The introduction of fluoroquinolones, such as ciprofloxacin, more than 20 years ago offered clinicians a range of antimicrobial agents that have a broad spectrum of activity [2] together with an activity against several intracellular bacteria [3]. The central structural unit of ciprofloxacin (Fig. 1) is a quinolone ring with a fluorine atom at the 6-position, a piperazine moiety at the 7-position, a cyclopropyl ring at position 1 and a carboxyl group at position 3. The primary mechanism of action of these compounds involves inhibition of the intracellular DNA gyrase and topoisomerase IV [4]. Before they can exert their antibacterial effect, fluoroquinolones must enter bacterial cells. While

the outer membrane protein F (OmpF) plays an important role in the uptake of fluoroquinolones for Gram-negative bacteria together with a direct uptake by a lipid mediated pathway [5], the passage through the phospholipid bilayer is the major process involved for inner membrane of Gram-negative bacteria and membrane of Gram-positive organisms [6]. For their intracellular activity, fluoroquinolones have also to penetrate into cells and to accumulate within. Diffusion and efflux processes modulate this cellular accumulation [7–9].

With respect to the interactions of ciprofloxacin with lipids, it has been established that ciprofloxacin had a small but definite and measurable interaction with neutral and charged membranes at the headgroup region [10]. The binding appeared as the result of (i) hydrophobic forces between the lipid bilayer and ciprofloxacin [11–13] and (ii) an ionic interaction between negatively charged phosphate groups of the phospholipid and the positively charged piperazine ring at the C-7 position of the quinolone [12–14].

* Corresponding author. Tel.: +32 2 764 73 74; fax: +32 2 764 73 73.
E-mail address: mingeot@facm.ucl.ac.be (M.-P. Mingeot-Leclercq).

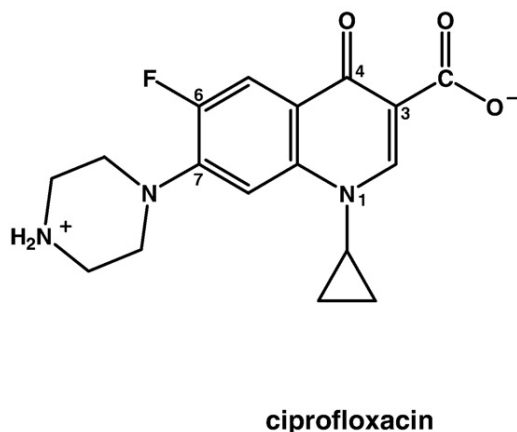


Fig. 1. Structural formula of ciprofloxacin (1-cyclopropyl-6-fluoro-1,4-dihydro-4-oxo-7-(1-piperazinyl)-3-quinolinecarboxylic acid).

To gain further information at the molecular level on the interaction between ciprofloxacin and lipids, we previously showed [1] in the presence of this antibiotic (i) the erosion of DPPC domains in the DOPC fluid phase as demonstrated by AFM, (ii) the shift of the surface pressure area–isotherms of DOPC:DPPC:ciprofloxacin monolayer towards the lower area per molecule as evidenced by Langmuir studies, and (iii) the decrease of the all-*trans* conformation of acyl lipid chains of DPPC together with a change of their orientation measured using ATR-FTIR.

Unfortunately, only few data [6,15] are available to compare the interaction of fluoroquinolones with both zwitterionic (DPPC) and negatively charged (DPPG) lipids in terms of their binding parameters together with the effect of the drugs on the dynamics of these lipids. Moreover, consequences of this interaction on temperature-dependent parameters such as the disorder of the hydrophobic tails of the lipids representing the major components of mammalian and bacterial membranes are still largely unexplored. Such information is however critical since the lipid composition of both bacterial and eukaryotic membranes markedly differs [16]. The bacterial plasmatic membrane mainly consists of a high amount of anionic lipids like phosphatidylglycerol whereas the membrane of eukaryotic cells appear uncharged and consisting almost exclusively of zwitterionic lipids, like phosphatidylcholine [17].

In this work, using DPPC, a zwitterionic lipid, and DPPG, an anionic lipid, mimicking the bulk lipid of eukaryotic membranes and the major component of bacterial membranes respectively, we therefore turned our efforts (i) to determine the binding parameters of ciprofloxacin to lipids using steady-state fluorescence anisotropy, (ii) to characterize the effect of the drug on the structure and dynamics of multilamellar vesicles using ^{31}P NMR and (iii) to follow, the influence of ciprofloxacin on the acyl chain order as a function of temperature, using ATR-FTIR. Results were related to the location of ciprofloxacin at the hydrophilic/hydrophobic interface, to the mean surface occupied by each DPPC and DPPG molecules in the presence and in the absence of ciprofloxacin, and to the energy of interaction between ciprofloxacin and DPPC or DPPG, as determined by molecular modeling.

2. Materials and methods

2.1. Materials

Dipalmitoylphosphatidyl glycerol (DPPG), dipalmitoylphosphatidylcholine (DPPC) and dioleoylphosphatidylcholine (DOPC) were purchased from Avanti Polar Lipids (Alabaster, AL, USA) and stored at $-20\text{ }^{\circ}\text{C}$. Ciprofloxacin (1-cyclopropyl-6-fluoro-1,4-dihydro-4-oxo-7-(1-piperazinyl)-3-quinoline carboxylic acid) was supplied as hydro-

chloride salt ($M_w=367.85\text{ g/mol}$; microbiological standard potency, 85.5%) by Bayer Healthcare AG (Leverkusen, Germany). Stock solutions were prepared in 10 mM Tris (pH 7.4).

2.2. Methods

2.2.1. Preparation of liposomes (MLVs, LUVs)

The large unilamellar vesicles (LUVs) consisting of DPPG, DOPC: DPPG (1:1; M:M), DOPC:DPPC (1:1; M:M), or DPPC were prepared as follows. Lipids were mixed in chloroform:methanol (2:1; V:V), evaporated under nitrogen flow and desiccated under vacuum overnight to remove any residual solvent. The dried films were then resuspended at $40\text{ }^{\circ}\text{C}$ from the walls of the glass tube by vigorous vortexing either in Tris:NaCl buffer 10:100 mM (pH 7.4) for binding experiments, or 10 mM Tris (pH 7.4) for binding stoichiometry, ATR-FTIR and ^{31}P NMR studies. Multilamellar vesicles (MLVs) were obtained by five heat-cooled cycles. Large unilamellar vesicles (LUVs) were then prepared by extrusion (ten times) of the MLV suspension through 100 nm of diameter polycarbonate filters (Nucleopore Costar Corporation, Badhoevedorp, Netherlands), using a thermostated ($40\text{ }^{\circ}\text{C}$) extruder (Lipex Biomembranes, Vancouver, Canada). The actual phospholipid content of each preparation was determined by phosphorus assay [18] and the concentration of liposomes was adjusted for each experiment.

2.2.2. Quasi-elastic light scattering measurements

The apparent average diameter of the LUVs and MLVs and the zeta potential of LUVs were determined using a Zetasizer (Zen 3600, Malvern Instruments, U.K.) with the following specifications: 60 s sampling time; 0.8872 cP medium viscosity; 1.33 refractive index; 90° scattering angle; $25\text{ }^{\circ}\text{C}$ temperature. Data were analyzed using the multimodal number distribution software included in the instrument for size determinations. The zeta potential values were calculated using Helmholtz–Smoluchowski's equation. All the measurements were performed using liposomes at a concentration of 0.5 mg/ml.

2.2.3. Steady-state fluorescence anisotropy

Fluorescence anisotropy is a powerful technique for investigating macromolecular dynamics, in which the sample is excited by linearly polarized light. The anisotropy was evaluated by observing the fluorescence at polarizations parallel (I_{\parallel}) and perpendicular (I_{\perp}) to the excitation according to:

$$r = (I_{\parallel} - I_{\perp}) / (I_{\parallel} + 2I_{\perp}). \quad (1)$$

The anisotropy titrations of LUV liposomes by ciprofloxacin were performed with a fluorescence spectrophotometer (Perkin Elmer LS-55, Beaconsfield, U.K.) in the T-format at $25\text{ }^{\circ}\text{C}$, by adding increasing concentrations of liposomes to a fixed amount of antibiotic ($5\text{ }\mu\text{M}$). Anisotropy measurements were performed every 20 s during 4 min. The emitted light was monitored through 390 nm interference filters. Excitation and emission bandwidths were both 9 nm. The excitation and emission wavelengths were set at 280 nm and 430 nm, respectively. The Scatchard equation was rewritten (Eq. 2) to directly fit the anisotropy r , as described previously [19]

$$r = r_0 - \frac{(r_0 - r_t)(1 + (L_t + nN_t)K_{app})^2 - \sqrt{(1 + (L_t + nN_t)K_{app})^2 - 4L_t nN_t K_{app}^2}}{2K_{app}} \quad (2)$$

where, r_0 and r correspond to the anisotropy of the ciprofloxacin in the absence and in the presence of a given concentration of the LUV liposomes. L_t and N_t designate the concentration of ciprofloxacin fixed at $5\text{ }\mu\text{M}$ and the concentration of lipids in LUV liposomes added, respectively. r_t is the anisotropy at the plateau value. K_{app} and n correspond to the apparent binding constant and the number of

binding sites, respectively. All fitting procedures were carried out with Origin™ 7.5 software.

2.2.4. ³¹P nuclear magnetic resonance (NMR)

The effect of ciprofloxacin on the mobility of phosphate headgroups of DPPC and DPPG prepared as MLV was investigated by static ³¹P NMR experiments. For a nonspherical charge distribution about the phosphorous nucleus, the shielding constant largely results from a local diamagnetic shielding contribution and a local paramagnetic shielding contribution. Because the charge distribution in a phosphorus molecule will be far from spherically symmetrical, the major contribution to the ³¹P chemical shift comes from the paramagnetic term. Asymmetry in the charge distribution implies that the ³¹P chemical shifts (or shielding constants) vary as a function of the orientation of the molecule relative to the external magnetic field. This gives rise to a chemical shift anisotropy ($\Delta\sigma$) which can be defined by three principal components σ_{11} , σ_{22} and σ_{33} of the shielding tensor and which is a frequently used parameter to characterize the ³¹P NMR spectra. For molecules which are axially symmetrical, with σ_{11} along the principal axis of symmetry, $\sigma_{11} = \sigma_{\parallel}$ (parallel component), and $\sigma_{22} = \sigma_{33} = \sigma_{\perp}$ (perpendicular component). The ³¹P chemical shift anisotropy is sensitive to both headgroup geometry and local dynamics. Rapid motion with limited amplitude along the molecular axis of the phospholipid normal to the membrane produces a supplementary averaging of the anisotropy tensor. The effective tensor still has axial symmetry but the chemical shift anisotropy is reduced. When ¹H decoupling is applied, ³¹P spectra are obtained that result solely from the chemical shift anisotropy. The chemical shift anisotropy can be measured by taking the difference of chemical shift between the low field shoulder (σ_{\parallel}) and the high-field peak (σ_{\perp}): $\Delta\sigma = \sigma_{\parallel} - \sigma_{\perp}$ [20].

Control samples of 450 μ l were prepared from MLV suspension (50 mg/ml) in 5 mm outer diameter tubes, by adding 50 μ l of D₂O for locking on the deuterium signal. To investigate the effect of the ciprofloxacin on the mobility of lipid (DPPC and DPPG) headgroups, a defined concentration of drug was added to MLV liposomes to reach a molar ratio of one.

Broadband proton-decoupled ³¹P NMR spectra were acquired by 1D NMR methods on a Bruker AVANCE 500 spectrometer at 202.5 MHz (11.7 Tesla) equipped with a Bruker 5 mm BBI (broad band inverse) probe. Typical Fourier transform spectral parameters were: 45° (6 μ s) flip angle, 50 kHz spectral width, 8K data points, 0.6 s repetition time. Sixty thousands transients were accumulated. An exponential multiplication corresponding to 70 Hz line broadening was applied to the free induction decay prior to Fourier transformation. All chemical shift values were quoted in parts per million (ppm) and were referenced to the isotropic chemical shift of H₃PO₄ (0 ppm). All spectra were recorded at a constant temperature of 45 °C.

2.2.5. Infrared spectroscopy

Attenuated Total Reflection Fourier Transform Infra-Red (ATR-FTIR) is particularly well suited for the study of membranes and to characterize the effect of drugs on melting temperature [21]. This technique is based on internal reflection of the infrared light within an internal reflection germanium plate, which creates an evanescent field at the surface of the plate where the lipid bilayer (and eventually the bound proteins or drugs) resides [22].

The internal reflection element was a 52×20×2 mm trapezoidal germanium ATR plate (ACM, Villiers St Frédéric, France) with an aperture angle of 45° yielding 25 internal reflections. 10 μ l of the sample containing DPPC or DPPG liposomes (50 mg/ml in Tris buffer 10 mM, pH 7.4) was dried under a stream of nitrogen on one side of the germanium internal reflection element at 20 °C. Under these conditions a well ordered multilayer stack is formed [23] and the stack is stable under a buffer flow [24]. The ciprofloxacin was added to the lipids at a ratio 1:1 as suggested by the stoichiometry binding experiments.

The germanium crystal was then placed in an ATR holder for liquid samples with an in- and out-let (Harrick, Ossining, NY, USA). The liquid cell was placed at 45 incidence on a Specac vertical ATR setup. The temperature was controlled with temperature-regulated water flowing in a cavity of the steal cell. The temperature was raised degree by degree.

An elevator under computer control made it possible to move the whole setup along a vertical axis (built for us by WOW Company SA, Nannine, Belgium). This allowed the crystal to be separated in different lanes. Here, one such lane contained the membrane film, the other was used for the background.

IR Spectra were obtained on a Bruker IFS55 FTIR spectrometer (Ettlingen, Germany) purged with N₂ as described previously [25]. Briefly, typically interferograms were recorded with 2 cm⁻¹ spectral resolution with broadband MCT detector between 4000–800 cm⁻¹, 128 scans were averaged for one spectrum.

The spectra were corrected from the water vapor and CO₂ contributions. They were then apodized in the Fourier domain in order to yield a final resolution of 4 cm⁻¹. Peak positions were determined according to a classical peak picking method. All the software used for data processing was written under MatLab 6.5 (Mathworks Inc., Natick, MA).

2.2.6. Assembly of ciprofloxacin with phospholipids by molecular modeling using the Hypermatrix procedure

The Hypermatrix method described elsewhere [26] was successfully used to study the interaction between different molecules and lipids [27–29]. In the Hypermatrix procedure, the lipid/water interface was taken into account by varying linearly the dielectric constant ϵ between 3 and 30.

The initial position and orientation of ciprofloxacin and of phospholipids (DPPC and DPPG) were those defined when using the TAMMO procedure [26]. To obtain a multimolecular assembly of ciprofloxacin and DPPC or DPPG with a 1:1 molar ratio, we first carried out the matching between one molecule of ciprofloxacin and one molecule of lipid. For that, the position of the ciprofloxacin was set constant while the lipid molecule was translated towards the ciprofloxacin molecule along the x axis by steps of 0.05 nm. The lipid rotated by steps of 30 around its z' axis and around the x axis. l was the number of positions tested along the x axis, m was the number of rotations around ciprofloxacin and n was the number of rotations around the lipid itself. For each set of l , m and n values, the energy of interaction between the ciprofloxacin and the lipid was calculated as the sum of van der Waals, electrostatic and hydrophobic terms [30]. Then, the lipid molecule was moved by 0.01 nm step along the z' axis perpendicular to the interface and the angle between the z' axis was bent by +1° with respect to the z axis. The most stable ciprofloxacin:lipid complex was used in the next step for the calculation of the multimolecular assembly. Following the same procedure, one ciprofloxacin:lipid complex was set constant and another 1:1 complex was moved towards it with the same combination of rotations and translations than that described above. The energy values together with the coordinates of all assemblies were stored in a matrix and classified according to a decreasing order. The position of the second complex corresponded to the most stable assembly in the matrix. The position of the next 1:1 complex was then defined as the next most energetically favorable orientation stored in the matrix, taking into account the steric and energy constraints due to the presence of the other molecules. The process ended when the central 1:1 complex was completely surrounded.

An assembly of lipids alone was made following the same process, with the central molecule being the lipid of interest. The mean area occupied by one lipid or one ciprofloxacin molecule in the multimolecular complex or in the lipid assembly was estimated by projection on the x - y plane using a grid of 1 Å².

Pex2dstats files [31] were generated during the simulations and allowed an easy and detailed analysis of each complex. All calculations were performed on an Intel® Pentium® 4, CPU 3.80 GHz, 4.00 Go of RAM.

3. Results

3.1. Size and zeta potential of LUV liposomes

In order to characterize the homogeneity of the LUV liposomes together with their surface charge, we investigated the size and zeta potential of the liposomes used (DPPG, DOPC:DPPG, DOPC:DPPC and DPPC). The results showed minor differences in the apparent mean diameters of liposomes which were centered on 100 nm (DPPG [124 nm], DOPC:DPPG [104 nm], DOPC:DPPC [92 nm], and DPPC [101 nm]). As expected for negatively charged (DPPG) liposomes, the zeta potential was more negative (−66 mV) than for DOPC:DPPG (−34 mV), DOPC:DPPC (−6 mV) or DPPC (−5 mV) vesicles.

3.2. Binding of ciprofloxacin to LUV liposomes

As a first step, to investigate the effect of ciprofloxacin on the lipid membrane models, we checked the effect of increasing amounts of ciprofloxacin on the size of the liposomes, by quasi-elastic light scattering (Table 1). The fluoroquinolone had no effect on the average diameter of DPPC LUVs whatever the molar ratio investigated (Lipid: drug ratios from 1:0.2 to 1:1). In contrast, for DPPG LUVs, the average diameter increased with the increase of the ciprofloxacin concentration, reaching a value of 256 nm for a lipid:drug ratio of 1. The average diameter was of 155 nm and 195 nm for a molar ratio of 1:0.2 and 1:0.5, respectively.

As a second step, we determined the binding constant, K_{app} , by adding increasing liposome concentrations to 5 μM ciprofloxacin in 10 mM Tris, 100 mM NaCl (pH 7.4) and following the steady-state fluorescence anisotropy. Fitting the experimental values according to Scatchard equation (Fig. 2), K_{app} values were close to 10^5 M^{-1} (Table 2). By comparing the affinity of ciprofloxacin to DPPG liposomes and DOPC:DPPG (1:1; M:M), it appeared that a decrease in the concentration of negatively charged lipids (DPPG) in the liposome mixture, led to a 2.5 fold K_{app} value decrease. The critical effect of DPPG on the interaction of ciprofloxacin was confirmed by comparing the K_{app} values of DPPC versus those of DPPG (3.5 times lower) or those of DOPC:DPPC versus those of DOPC:DPPG (3 times lower). Taken together, our data showed that the ciprofloxacin bound to lipid vesicles with the following preference: DPPG > DOPC:DPPG (1:1; M:M) > DPPC > DOPC:DPPC (1:1; M:M). To get further data on the binding between ciprofloxacin and lipids and to evaluate the stoichiometry of this binding, we reproduced these experiments in conditions in which NaCl was omitted. Saturation points for fitted binding curve approximately occur for lipids concentrations equimolar to respective ligand concentrations suggesting a stoichiometry of (1:1) (Fig. 2-inset). This was observed whichever the nature of the lipids investigated (DPPG or DPPC).

3.3. Effect of ciprofloxacin on the size and the mobility of phosphate heads of DPPC and DPPG MLVs

From quasi-elastic light scattering studies and binding parameters, the association of ciprofloxacin to lipids appears as strongly dependent on the presence of the negatively charged phospholipid, DPPG. To further explore this interaction, we measured by ^{31}P NMR

Table 1

Size of large unilamellar vesicles in the presence of increasing amounts of ciprofloxacin as determined by quasi-elastic light scattering

Lipid:drug molar ratio	Average size (nm)	
	DPPC	DPPG
1:0	101 ± 1	124 ± 1
1:0.2	100 ± 1	155 ± 2
1:0.5	98 ± 1	195 ± 2
1:1	105 ± 1	256 ± 5

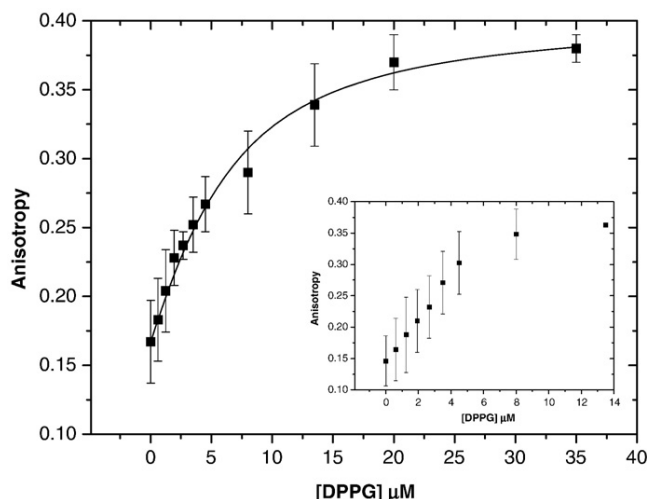


Fig. 2. Binding of ciprofloxacin to DPPG vesicles. Binding of ciprofloxacin to lipid vesicles was followed by steady-state anisotropy in the presence of increasing amounts of DPPG. The antibiotic concentration was 5 μM in Tris:NaCl buffer 10:100 mM (pH 7.4). The continuous line corresponds to the fit of the experimental points with Eq. (2) in order to determine the binding constant. The stoichiometry of the interaction between ciprofloxacin and lipids (inset) was performed in Tris buffer 10 mM (pH 7.4).

spectroscopy the effective chemical shift anisotropy ($\Delta\sigma$) of the MLV liposomes of DPPC and DPPG in the presence and in the absence of ciprofloxacin at 45 °C. As shown in Fig. 3, typical spectra obtained with multilamellar vesicles for both DPPC (top panel) and DPPG (bottom panel) were characteristic of a bilayer organization with a high-field maximum and a low field shoulder. In addition, the spectrum of ^{31}P NMR for DPPG revealed two peaks respectively at −10 ppm and 0 ppm. The latter was probably due to the presence of a liposome population (10%) of 150 nm of size as revealed by Nanosizer measurements. Moreover, we observed a marked difference between the chemical shift anisotropy ($\Delta\sigma$) value of DPPC as compared to that of DPPG, 41.5 and 25.5 ppm respectively. This can be related to the mean diameter of the major population of the MLVs which were 2100 nm for DPPC (100%) and 1375 nm for DPPG (90%) vesicles.

In the presence of ciprofloxacin, the $\Delta\sigma$ value was higher than that of the control, for both types of liposomes. We obtained an increase of the chemical shift anisotropy ($\Delta\sigma$) values of 5 and 9 ppm for DPPC and DPPG, respectively. The presence of a population of larger size, estimated around 5000 nm for DPPG vesicles and >10 μm for DPPC vesicles could also be related to the difference observed in terms of chemical shift anisotropy.

3.4. Effect of ciprofloxacin on the melting temperature of the lipids

As a sequel of the binding experiments, our further objective was to determine the effect of the interaction between ciprofloxacin on DPPC or DPPG on the melting behavior of the lipids.

To this end, we used ATR-FTIR spectroscopy. This method allowed us the detection of the transition of the lipid hydrocarbon chains from *trans* to *gauche* conformation which corresponds to the transition of the lipid bilayer from gel (L_{β}) to liquid-crystalline phase (L_{α}). It is known that the absorbance of the peaks corresponding to the

Table 2

Binding parameters obtained from steady-state anisotropy experiments

LUV liposomes composition	K_{app} (10^5 M^{-1})
DPPG	8.6 ± 0.5
DPPC	2.5 ± 0.1
DOPC:DPPG (1:1; M:M)	3.2 ± 0.9
DOPC:DPPC (1:1; M:M)	1.1 ± 0.2

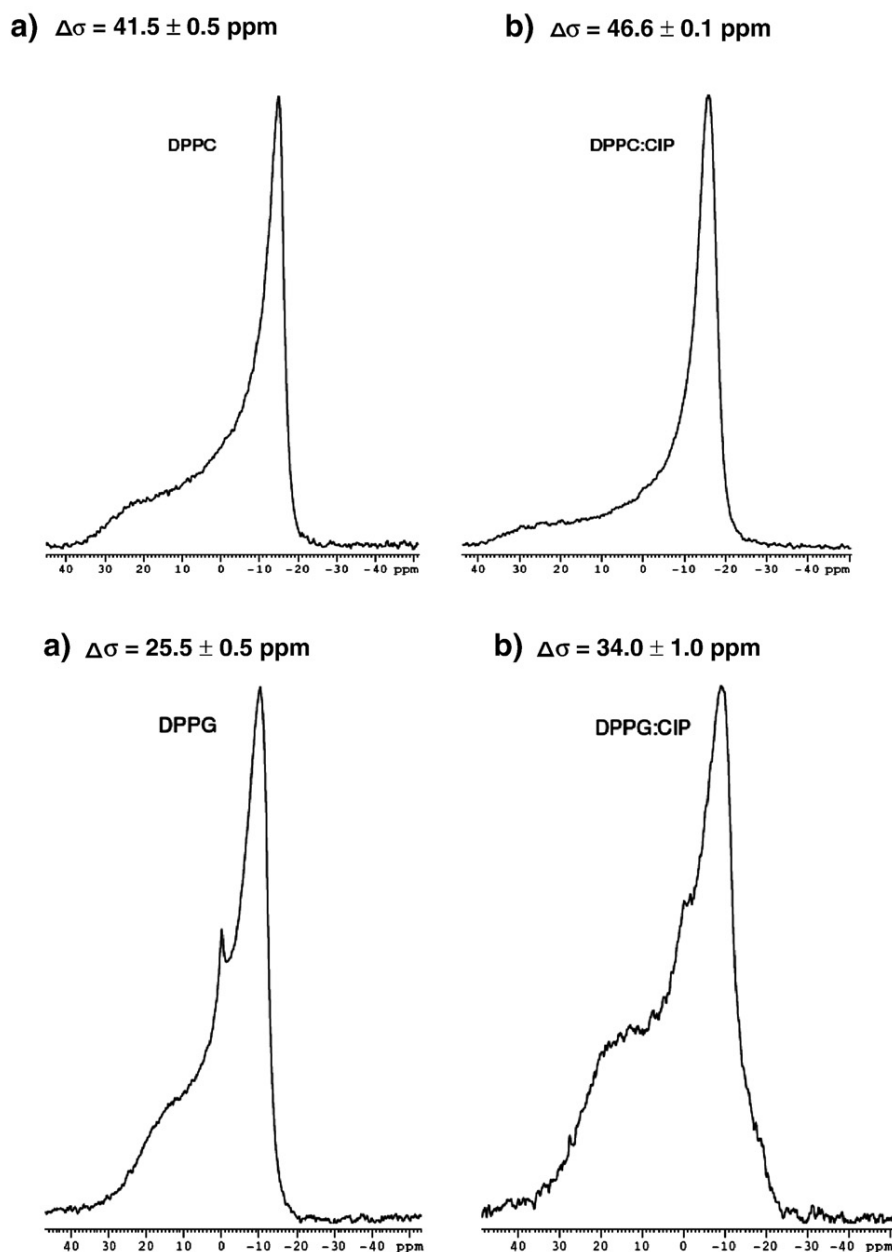


Fig. 3. Effect of ciprofloxacin on ^{31}P NMR spectra of multilamellar vesicles of DPPC (upper panel) and DPPG (lower panel). Liposomes (50 mg/ml) were prepared at pH 7.4 in 10 mM Tris buffer. The experiments were performed at 45 °C. The chemical shift anisotropy ($\Delta\sigma$) values are indicated at the top of the spectra in the absence (a) and in the presence (b) of ciprofloxacin added at a molar ratio of one.

asymmetric $\nu_{\text{as}}(\text{CH}_2)$ (2920 cm^{-1}), and symmetric $\nu_{\text{s}}\text{CH}_2$ (2850 cm^{-1}) stretching bands are sensitive to the intramolecular vibrational coupling and thus to the lateral packing of the hydrocarbon chains.

In order to determine accurately the peak maxima, a Gaussian line was fitted on the upper half of the position of the maximum for the asymmetric CH_2 stretching vibration ($\nu_{\text{as}}(\text{CH}_2)$) of DPPC (Fig. 4a) and DPPG (Fig. 4b) vesicles and the result was plotted as a function of temperature. Pure DPPC and DPPG vesicles (in Tris 10 mM, pH 7.4 buffer) exhibited a clear phase transition between the gel phase (L_{β}) and a liquid-crystalline phase (L_{α}). As expected, the DPPG melting temperature is slightly lower than for DPPC (42 °C) and is near (40 °C).

The melting curve obtained for DPPC in the presence of ciprofloxacin (Fig. 4a), showed a minor effect of the drug before and after the main transition temperatures of DPPC since the frequencies of the two dominant bands observed at 2917 cm^{-1} ($\nu_{\text{as}}(\text{CH}_2)$) and 2849 cm^{-1}

($\nu_{\text{s}}(\text{CH}_2)$; not shown) were slightly below those observed for pure DPPC. The melting temperature remained unchanged (42 °C).

In contrast, addition of ciprofloxacin to anionic lipid DPPG vesicles induced a significant change in the melting curve (Fig. 4b). Indeed, a net positive shift of $\nu_{\text{as}}(\text{CH}_2)$ stretching bands was observed at the pre-transition temperature (between 20 and 37.5 °C). At a temperature between 38 and 40 °C, the two bands centered at 2918 cm^{-1} ($\nu_{\text{as}}(\text{CH}_2)$) and 2850 cm^{-1} ($\nu_{\text{s}}(\text{CH}_2)$; not shown) were significantly changed. With further increase in temperature (>40 °C), the peak positions of stretching band remained significantly below those of the pure DPPG. These data suggest that the ciprofloxacin increased the membrane fluidity in the gel phase, as shown by the increase of the frequency of $\nu_{\text{as}}(\text{CH}_2)$ asymmetric vibration below T_{m} and decreased the membrane fluidity, notably in the liquid-crystalline phase (L_{α}), as shown by the decrease the frequency of $\nu_{\text{as}}(\text{CH}_2)$ asymmetric vibration above T_{m} .

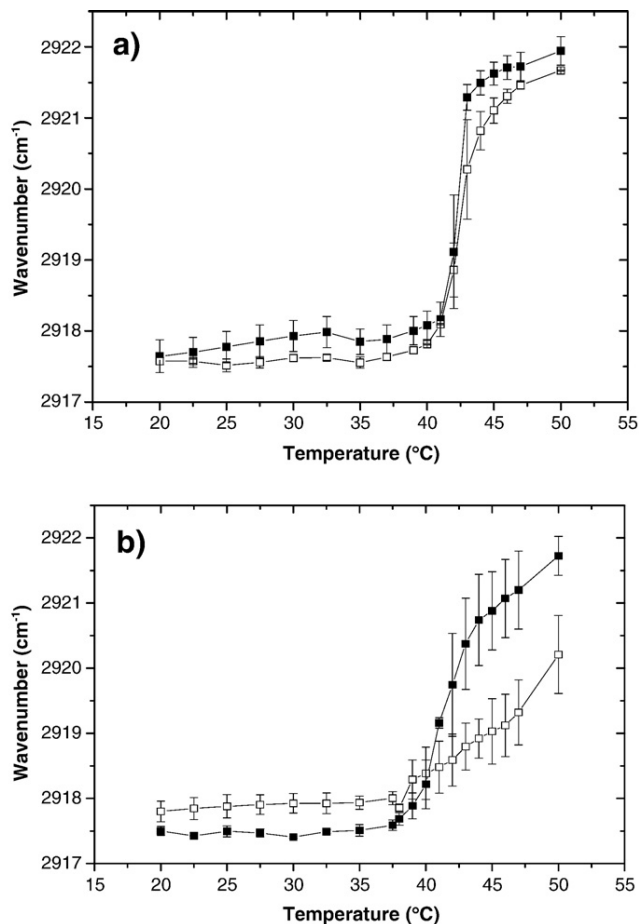


Fig. 4. Evolution of the maximum frequency of the $\nu_{as}(\text{CH}_2)$ as a function of temperature for DPPC (a) or DPPG (b) in the absence (closed square ■) or in the presence (open square □) of ciprofloxacin. The concentration of phospholipids was 50 mg/ml. The lipid: ciprofloxacin molar ratio was 1:1.

3.5. Molecular simulation of the interaction between ciprofloxacin and DPPC or DPPG

The interaction between ciprofloxacin and DPPC or DPPG at a (1:1) molar ratio was calculated using the Hypermatrix procedure [26] as described in the Materials and methods section. As shown in Fig. 5, ciprofloxacin is inserted at the level of the phospholipid headgroup/acyl chain interface for both lipids, as already suggested [1]. The calculation of the interaction energy between DPPC or DPPG and ciprofloxacin (Table 3) indicates that the association is more stable with DPPG, the energy going from -44.4 kcal/mol for DPPC: ciprofloxacin to -53.4 kcal/mol for DPPG: ciprofloxacin. Furthermore, the presence of ciprofloxacin in DPPG significantly increases the lipid interfacial area, the DPPG value going from 66 \AA^2 in a monolayer to 76 \AA^2 in the calculated multimolecular assembly. The increase is less important for DPPC, going from 63 \AA^2 for the lipid alone to 66 \AA^2 in the assembly (Table 3).

4. Discussion

While numerous studies have shown a critical role of the porin hydrophilic pathway for penetration of fluoroquinolones through the outer membrane of Gram-negative bacteria, the present work may shed new light on their passage through the inner membrane of these organisms (and through the membrane of Gram-positive bacteria) as well as through the pericellular membrane of eukaryotic cells. In the

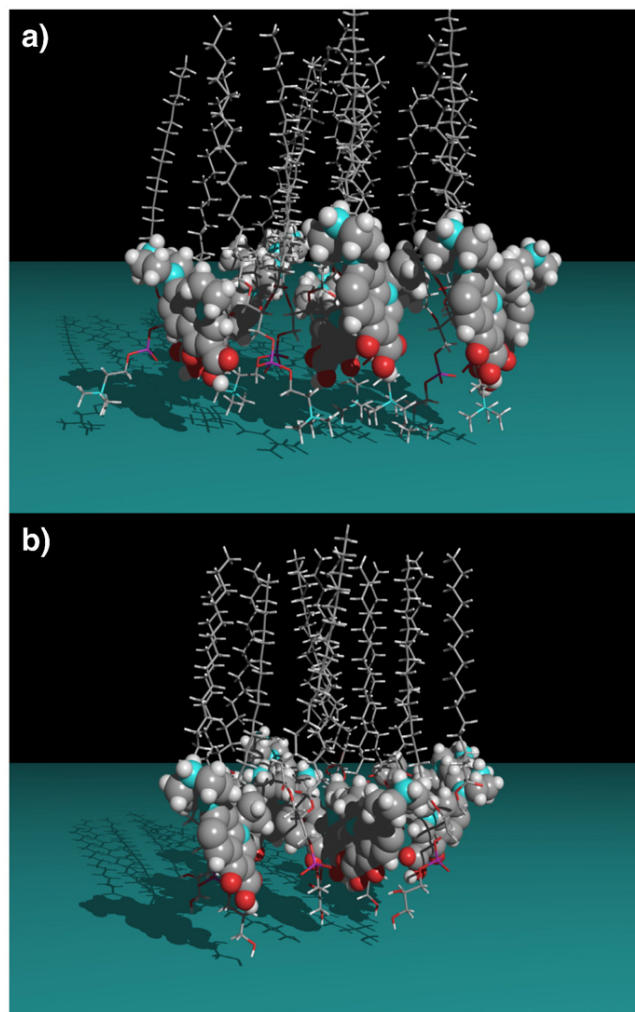


Fig. 5. Assembly of ciprofloxacin with DPPC (a) or DPPG (b) in a 1:1 molar ratio. Ciprofloxacin is represented in Corey-Pauling-Koltum (CPK) mode, whereas the phospholipids are in skeleton mode.

absence of demonstrated inward transporter, a direct interaction of fluoroquinolones with lipids allowing their diffusion through the so-called hydrophobic pathway and/or self-promoted pathway must indeed be considered critical for both the antibacterial activity and the tissue distribution and cell accumulation properties of fluoroquinolones.

In order to gain further insight in the interactions of fluoroquinolones with lipids, especially those found in bacterial membranes like the negatively charged phospholipid phosphatidylglycerol, as compared to the bulk lipids of eukaryotic membranes, phosphatidylcholine, we therefore determined (i) the binding parameters of ciprofloxacin in interaction with these lipids using steady-state fluorescence anisotropy, (ii) the effect of ciprofloxacin on the mobility

Table 3

Energy of interaction energy between lipid molecule and ciprofloxacin (CIP) and molecular area of the lipid molecule at the interface

	Energy of interaction (kcal/mol)	Area (\AA^2)
DPPC/DPPC	-30.5	63
DPPC/CIP	-44.4	66
DPPG/DPPG	-30.8	66
DPPG/CIP	-53.4	76

of phosphate headgroups using ^{31}P NMR spectroscopy and (iii) the effect of ciprofloxacin on the acyl chain order as a function of temperature using ATR-FTIR.

Steady-state anisotropy experiments showed that ciprofloxacin binds to the lipid vesicles tested with a stoichiometry of 1 and a moderate affinity (10^5 M^{-1}). This result is in agreement with the fair hydrophobicity of ciprofloxacin and derivatives at neutral pH [6]. A partial selectivity (DPPG>DOPC:DPPG (1:1)>DPPC>DOPC:DPPC (1:1)) was however evidenced. So, the greatest affinity observed with the negatively charged liposomes of DPPG or DOPC:DPPG reflected the potential role of electrostatic interactions between negatively charged phospholipid heads together with the H-bonding [12,32–34]. This is in agreement with the results from quasi-elastic light scattering which showed an effect of ciprofloxacin on the size of DPPG liposomes whereas no effect was observed with DPPC. This is also in accordance with the values of the energy of interaction as calculated by molecular modeling. These calculations are based on a semi-empirical force field [30] that can be compared to experimental values in terms of relative value (allowing a “ranking” of the different molecules in terms of preferential interaction) but not in terms of absolute value. The experimental interaction energy does not exactly correspond to calculated values of binding energy since (i) the calculated values depend on the energy force field and (ii) solvation, ionic strength, e.g. that contribute to the experimental measurements, are not taken into account in the calculations. Interestingly, even though the difference in the corresponding binding energy might be less than 1 kcal/mol, it might result from a compensating compromise between the enthalpy and the entropy of association as is often the case for biological systems and regulations. The preferential role of DPPG as compared to DPPC for the interaction between ciprofloxacin and lipids has been also showed with other fluoroquinolones like grepafloxacin [15] and ofloxacin [14] or with cyclic antimicrobial peptides [35,36]. However, in accordance with literature [11–13] and with calculations of the hydrophobic/hydrophilic environments of ciprofloxacin/lipid complex using the Molecular Hydrophobicity Potential (MHP), hydrophobic interactions could also play a critical role in the interaction between ciprofloxacin and lipids. Indeed, such computational analysis clearly revealed that most interactions are hydrophobic whatever the nature of the lipid selected (unpublished result). Because the main objective of the study is to shed light about the peculiar interactions between ciprofloxacin and DPPG, a lipid representative of bacterial membranes, on one hand and DPPC, a lipid mimicking the mammalian membranes, on the other hand, the relative contribution of electrostatic, hydrogen bonding, van der Waals interactions... has not been further investigated in this work.

The potential role played by the nature of the phosphate headgroup lead us to follow by ^{31}P NMR, the chemical shift anisotropy ($\Delta\sigma$) which depends on the local motions of the phosphodiester moiety and its orientation. Below their L_α -liquid-crystalline phase transition temperature, DPPG and DPPC in L_β -gel phase produce both an axially symmetric component and an asymmetric component required to fit their ^{31}P spectra. When the temperature is raised above the L_α -liquid-crystalline state phase transition value, the two static ^{31}P NMR components of the lipids collapse into a single axially symmetric contribution. This dynamically averaged ^{31}P NMR powder pattern results from axial rotation of the phosphodiester moiety about the bilayer normal, bond librations and overall lipid fluctuations and rotations [37]. Accordingly, the substantially smaller $\Delta\sigma$ of the L_α state compared to the L_β state is attributed to the considerable decrease in the correlation times of the ^{31}P headgroup motions by more than one to two orders of magnitude.

The $\Delta\sigma$ value obtained for DPPC is similar to that reported in the literature [38]. The lower value of the chemical shift anisotropy for DPPG as compared to DPPC could be due to the size of the main populations of DPPG liposomes (1375 nm) as compared to DPPC liposomes (2100 nm) together with the presence of a population

smaller liposomes of DPPG (centered on 150 nm). Unfortunately, values obtained by quasi-light scattering showed a large variability from one measurement to another which may be accounted for by the fact that this type of measurement is strongly influenced by the presence of small number of large vesicles [39].

Because rapid motions might exist for high curvature regions or isotropic phases, therefore giving rise to a motionally averaged isotropic chemical shift [40], the increase of $\Delta\sigma$ values in the presence of ciprofloxacin in interaction with DPPG, and in a lesser extent with DPPC, suggested the appearance of such structures. Our results also reflect the location of the fluoroquinolone at the polar heads and near the lipid–water interface [6,13]. The results that we obtained for the interaction of ciprofloxacin with DPPC differ from those of Grancelli et al. [13]. The latter reported a remarkable decrease of the second spectral moment in solid state ^{31}P NMR above T_m without modifications below T_m , suggesting an enhancement of the mobility of the headgroups of DPPC above T_m . At 45 °C, we observed an increase of $\Delta\sigma$ reflecting a decrease in the local mobility of the phosphate groups or a reorientation of the phosphate moiety in the presence of the drug, in accord with the binding of the drug to lipids. This discrepancy has not yet received satisfactory explanations. A possibility could be found in the preparation of the MLVs, and in the way the ciprofloxacin is added to interact with lipids. This appeared as critical since when the DPPG MLVs were prepared with the ciprofloxacin, we observed a precipitation of the sample, which could be interpreted as revealing a very strong electrostatic interaction between the negative charge of the phosphate groups and the electric dipole moment of ciprofloxacin. When ciprofloxacin was added into the DPPG MLVs, the mixture didn't flocculate, suggesting the probable existence of a metastable state between both partners. This phenomenon wasn't observed in the case of DPPC MLVs which are electrically neutral and possess an electric dipole moment implying a softer electrostatic interaction with ciprofloxacin.

At first glance, the ^{31}P chemical shift anisotropy variation upon addition of ciprofloxacin into the DPPC and DPPG samples indicates strongly that the drugs interact with the headgroups of the phospholipids. Nonetheless, ^{31}P magnetic relaxation dispersion measurements would be necessary to describe more precisely the microscopic details of the interactions and to know whether or not all the lipid layers of the vesicles are involved and contact the ciprofloxacin molecules.

To investigate further the effect of ciprofloxacin in interaction with lipids on the melting temperature of either DPPC or DPPG, ATR-FTIR experiments were performed. Lipids can exist in several lamellar phases depending on the temperature. For saturated phosphatidylcholines, such as DPPC, there are four recognized lamellar phases; namely, a liquid-crystalline phase (L_α), and phases with ordered hydrocarbon chain arrangements: ripple phase (P_β); gel phase (L_β); and subgel or crystal phase (L_c) [41]. The phase transition in lipid bilayers involves a cooperative structural change from a state in which the lipids are closely packed and their chains fully extended, to a state in which a large fraction of the molecules exhibits as many *gauche* rotations per molecule.

The frequencies of the CH_2 stretching vibrations reflect the order of the acyl chains. Highly ordered acyl chains with an all-*trans* conformation as observed in the gel phase lead to lower vibrational frequencies. With increasing fractions of *gauche* isomers and decreasing van der Waals attractions in the liquid-crystalline phase the absorption maxima of the stretching bands will be shifted to higher frequency [42]. The results indicated that ciprofloxacin did not affect dramatically the DPPC melting curve. However, we noted that ciprofloxacin increased the order of the acyl chains both below and above the transition temperature. This is in agreement with the ability of ciprofloxacin to alter the tilt angle of the acyl chain of DPPC as demonstrated previously by ATR-FTIR [1]. The slight effect of ciprofloxacin on the order of the acyl chains of DPPC is in agreement

with the fact that neither iodobenzene nor iododecanoic acid, both known as hydrophobic quenchers, were able to quench the fluorescence of ciprofloxacin in the presence of DPPC liposomes [34]. In contrast, the effect of ciprofloxacin on DPPG is major. It was reasonable to suggest that ciprofloxacin decreased the ordering of the acyl chain of DPPG below the transition together with its ability to increase the order above this temperature. These observations were similar to those reported for cholesterol [43], a lipid well-known for broadening the gel to fluid transition temperature [44]. Moreover, our observations to compare the effect of ciprofloxacin on the frequencies of the CH₂ stretching vibrations of DPPC and DPPG are consistent with the higher quenching of ciprofloxacin by iodide, in DPPC:DPPG as compared to DPPC vesicles [45]. Surprisingly, however, no effect in steady-state polarization of TMA-DPH as a function of temperature was observed when ciprofloxacin was added to DPPC:DPPG as compared to the effect on DPPC [45]. Further investigations have to be done in this respect to explain this intriguing observation.

Globally speaking the major effect of ciprofloxacin on DPPG as compared to the one on DPPC confirmed the importance of the nature of the polar heads of phospholipids. The role played by the electrostatic interactions between ciprofloxacin and lipids has however to be confirmed using other negatively charged lipids than DPPG, like phosphatidylserine, cardiolipin, sulfatides, gangliosides [46]. The ability of ciprofloxacin to interact with lipids through hydrogen bonding and van der Waals interactions must also be investigated. This would explain the mode of insertion of ciprofloxacin within the lipids.

The binding parameters as determined by steady-state fluorescence anisotropy were correlated with the mobility of phosphate heads as determined by ³¹P NMR and the acyl chain order as monitored by ATR-FTIR. Moreover, the increase of the area of DPPG at the lipid–water interface as evidenced by conformational analysis can be related to the local perturbations of the lipid bilayer observed by ³¹P NMR which in turn may upset physiological properties of membranes.

All our results support the existence of a primary step in a binding of ciprofloxacin to the phospholipid bilayer surface and a possible accumulation in enriched domains formed by negatively charged lipids. This could allow the establishment of a concentration gradient that would promote the diffusion of the drug through the bilayer.

This work thus provides new molecular insights in the interaction between a fluoroquinolone antibiotic, as a drug model, and lipids mimicking those found in bacterial and eukaryotic membranes. Finally, these results suggest that biophysical studies combined with conformational analyses might be a powerful additional tool for the characterization of the interactions between antibiotics and lipids.

Acknowledgements

H.B. is a doctoral assistantship recipient of the Catholic University of Louvain (UCL), E.G and R.B. are Research Directors, F.V B. is Senior Research Associate and L.L. is Research Associate of the National Foundation for the Scientific Research (F.N.R.S.). The support of the *Région wallonne*, of the F.N.R.S., of the *Université catholique de Louvain (Fonds Spéciaux de Recherche, Actions de Recherche Concertées)*, of the Federal Office for Scientific, Technical and Cultural Affairs (Inter-university Poles of Attraction Programme) is gratefully acknowledged. We also thank Bayer Healthcare AG for providing us with ciprofloxacin.

References

- [1] H. Bensikaddour, N. Fa, I. Burton, M. Deleu, L. Lins, A. Schanck, R. Brasseur, Y. Dufrene, E. Goormaghtigh, M.P. Mingeot-Leclercq, Characterization of the interactions between fluoroquinolone antibiotics and lipids: a multitechnique approach, *Biophys. J.* 94 (2008) 3035–3046.

- [2] F. Van Bambeke, J.M. Michot, J. Van Eldere, P.M. Tulkens, Quinolones in 2005: an update, *Clin. Microbiol. Infect.* 11 (2005) 256–280.
- [3] C. Seral, M. Barcia-Macay, M.P. Mingeot-Leclercq, P.M. Tulkens, F. Van Bambeke, Comparative activity of quinolones (ciprofloxacin, levofloxacin, moxifloxacin and garenoxacin) against extracellular and intracellular infection by *Listeria monocytogenes* and *Staphylococcus aureus* in J774 macrophages, *J. Antimicrob. Chemother.* 55 (2005) 511–517.
- [4] P.G. Higgins, A.C. Fluit, F.J. Schmitz, Fluoroquinolones: structure and target sites, *Curr. Drug Targets* 4 (2003) 181–190.
- [5] P. Neves, E. Berkane, P. Gameiro, M. Winterhalter, B. de Castro, Interaction between quinolones antibiotics and bacterial outer membrane porin OmpF, *Biophys. Chem.* 113 (2005) 123–128.
- [6] J.L. Vazquez, S. Merino, O. Domenech, M. Berlanga, M. Vinas, M.T. Montero, J. Hernandez-Borrell, Determination of the partition coefficients of a homologous series of ciprofloxacin: influence of the N-4 piperazinyl alkylation on the antimicrobial activity, *Int. J. Pharm.* 220 (2001) 53–62.
- [7] J.M. Michot, F. Van Bambeke, M.P. Mingeot-Leclercq, P.M. Tulkens, Active efflux of ciprofloxacin from J774 macrophages through an MRP-like transporter, *Antimicrob. Agents Chemother.* 48 (2004) 2673–2682.
- [8] J.M. Michot, C. Seral, F. Van Bambeke, M.P. Mingeot-Leclercq, P.M. Tulkens, Influence of efflux transporters on the accumulation and efflux of four quinolones (ciprofloxacin, levofloxacin, garenoxacin, and moxifloxacin) in J774 macrophages, *Antimicrob. Agents Chemother.* 49 (2005) 2429–2437.
- [9] J.M. Michot, M.F. Heremans, N.E. Caceres, M.P. Mingeot-Leclercq, P.M. Tulkens, F. Van Bambeke, Cellular accumulation and activity of quinolones in ciprofloxacin-resistant J774 macrophages, *Antimicrob. Agents Chemother.* 50 (2006) 1689–1695.
- [10] J. Bedard, L.E. Bryan, Interaction of the fluoroquinolone antimicrobial agents ciprofloxacin and enoxacin with liposomes, *Antimicrob. Agents Chemother.* 33 (1989) 1379–1382.
- [11] H. Nikaido, D.G. Thanassi, Penetration of lipophilic agents with multiple protonation sites into bacterial cells: tetracyclines and fluoroquinolones as examples, *Antimicrob. Agents Chemother.* 37 (1993) 1393–1399.
- [12] M.T. Montero, M. Pijoan, S. Merino-Montero, T. Vinuesa, J. Hernandez-Borrell, Interfacial membrane effects of fluoroquinolones as revealed by a combination of fluorescence binding experiments and atomic force microscopy observations, *Langmuir* 22 (2006) 7574–7578.
- [13] A. Grancelli, A. Morros, M.E. Cabanas, O. Domenech, S. Merino, J.L. Vazquez, T. Montero, M. Vinas, J. Hernandez-Borrell, Interaction of 6-fluoroquinolones with dipalmitoylphosphatidylcholine monolayers and liposomes, *Langmuir* 18 (2002) 9177–9182.
- [14] M. Fresta, S. Guccione, A.R. Beccari, P.M. Furneri, G. Puglisi, Combining molecular modeling with experimental methodologies: mechanism of membrane permeation and accumulation of ofloxacin, *Bioorg. Med. Chem.* 10 (2002) 3871–3889.
- [15] C. Rodrigues, P. Gameiro, S. Reis, J.L.F.C. Lima, B. de Castro, Interaction of grepafloxacin with large unilamellar liposomes: partition and fluorescence studies reveal importance of charge interactions, *Langmuir* 18 (2002) 10231–10236.
- [16] K. Lohner, E.J. Prenner, Differential scanning calorimetry and X-ray diffraction studies of the specificity of the interaction of antimicrobial peptides with membrane-mimetic systems, *Biochim. Biophys. Acta* 1462 (1999) 141–156.
- [17] R.F. Epand, P.B. Savage, R.M. Epand, Bacterial lipid composition and the antimicrobial efficacy of cationic steroid compounds (Ceragenins), *Biochim. Biophys. Acta* 1768 (2007) 2500–2509.
- [18] G.R. Bartlett, Colorimetric assay methods for free and phosphorylated glyceric acids, *J. Biol. Chem.* 234 (1959) 469–471.
- [19] C. Vuilleumier, E. Bombarda, N. Morellet, D. Gerard, B.P. Roques, Y. Mely, Nucleic acid sequence discrimination by the HIV-1 nucleocapsid protein NCp7: a fluorescence study, *Biochemistry* 38 (1999) 16816–16825.
- [20] J. Seelig, ³¹P nuclear magnetic resonance and the head group structure of phospholipids in membranes, *Biochim. Biophys. Acta* 515 (1978) 105–140.
- [21] E. Goormaghtigh, V. Raussens, J.M. Ruyschaert, Attenuated total reflection infrared spectroscopy of proteins and lipids in biological membranes, *Biochim. Biophys. Acta* 1422 (1999) 105–185.
- [22] S.A. Tatulian, Attenuated total reflection Fourier transform infrared spectroscopy: a method of choice for studying membrane proteins and lipids, *Biochemistry* 42 (2003) 11898–11907.
- [23] D. Ivanov, N. Dubreuil, V. Raussens, J.M. Ruyschaert, E. Goormaghtigh, Evaluation of the ordering of membranes in multilayer stacks built on an ATR-FTIR germanium crystal with atomic force microscopy: the case of the H⁽⁺⁾/K⁽⁺⁾-ATPase-containing gastric tubulovesicle membranes, *Biophys. J.* 87 (2004) 1307–1315.
- [24] F. Scheirlinckx, V. Raussens, J.M. Ruyschaert, E. Goormaghtigh, Conformational changes in gastric H⁽⁺⁾/K⁽⁺⁾-ATPase monitored by difference Fourier-transform infrared spectroscopy and hydrogen/deuterium exchange, *Biochem. J.* 382 (2004) 121–129.
- [25] N. Fa, S. Ronkart, A. Schanck, M. Deleu, A. Gaigneaux, E. Goormaghtigh, M.P. Mingeot-Leclercq, Effect of the antibiotic azithromycin on thermotropic behavior of DOPC or DPPC bilayers, *Chem. Phys. Lipids* 144 (2006) 108–116.
- [26] R. Brasseur, TAMMO: theoretical analysis of membrane molecular organisation, in: R. Brasseur (Ed.), *Molecular Description of Biological Membrane Components by Computer-aided Conformational Analysis*, CRC Press, Boca Raton, 1990, pp. 203–219.
- [27] L. Lins, P. Ducarme, E. Breukink, R. Brasseur, Computational study of nisin interaction with model membrane, *Biochim. Biophys. Acta* 1420 (1999) 111–120.
- [28] N. Fa, L. Lins, P.J. Courtney, Y. Dufrene, P. Vandersmissen, R. Brasseur, D. Tyteca, M.P.

- Mingeot-Leclercq, Decrease of elastic moduli of DOPC bilayers induced by a macrolide antibiotic, azithromycin, *Biochim. Biophys. Acta* 1768 (2007) 1830–1838.
- [29] M.P. Mingeot-Leclercq, L. Lins, M. Bensliman, A. Thomas, F. Van Bambeke, J. Peuvot, A. Schanck, R. Brasseur, Piracetam inhibits the lipid-destabilising effect of the amyloid peptide Abeta C-terminal fragment, *Biochim. Biophys. Acta* 1609 (2003) 28–38.
- [30] L. Lins, R. Brasseur, The hydrophobic effect in protein folding, *FASEB J.* 9 (1995) 535–540.
- [31] A. Thomas, N. Benhabiles, R. Meurisse, R. Ngwabije, R. Brasseur, Pex, analytical tools for PDB files. II. H-Pex: noncanonical H-bonds in alpha-helices, *Proteins* 43 (2001) 37–44.
- [32] Y.X. Furet, J. Deshusses, J.C. Pechere, Transport of pefloxacin across the bacterial cytoplasmic membrane in quinolone-susceptible *Staphylococcus aureus*, *Antimicrob. Agents Chemother.* 36 (1992) 2506–2511.
- [33] K. Takacs-Novak, B. Noszal, I. Hermech, G. Kereszturi, B. Podanyi, G. Szasz, Protonation equilibria of quinolone antibacterials, *J. Pharm. Sci.* 79 (1990) 1023–1028.
- [34] J. Hernandez-Borrell, M.T. Montero, Does ciprofloxacin interact with neutral bilayers? An aspect related to its antimicrobial activity, *Int. J. Pharm.* 252 (2003) 149–157.
- [35] P.M. Abuja, A. Zenz, M. Trabi, D.J. Craik, K. Lohner, The cyclic antimicrobial peptide RTD-1 induces stabilized lipid-peptide domains more efficiently than its open-chain analogue, *FEBS Lett.* 566 (2004) 301–306.
- [36] F. Bringezu, S. Wen, S. Dante, T. Hauss, M. Majerowicz, A. Waring, The insertion of the antimicrobial peptide dicynthaurin monomer in model membranes: thermodynamics and structural characterization, *Biochemistry* 46 (2007) 5678–5686.
- [37] E.J. Dufourc, C. Mayer, J. Stohrer, G. Althoff, G. Kothe, Dynamics of phosphate head groups in biomembranes. Comprehensive analysis using phosphorus-31 nuclear magnetic resonance lineshape and relaxation time measurements, *Biophys. J.* 61 (1992) 42–57.
- [38] R. El Jastimi, K. Edwards, M. Lafleur, Characterization of permeability and morphological perturbations induced by nisin on phosphatidylcholine membranes, *Biophys. J.* 77 (1999) 842–852.
- [39] M.P. Mingeot-Leclercq, A. Schanck, M.F. Ronveaux-Dupal, M. Deleers, R. Brasseur, J. M. Ruyschaert, G. Laurent, P.M. Tulkens, Ultrastructural, physico-chemical and conformational study of the interactions of gentamicin and bis(beta-diethylaminoethyl) hexestrol with negatively-charged phospholipid layers, *Biochem. Pharmacol.* 38 (1989) 729–741.
- [40] G.P. Holland, S.K. McIntyre, T.M. Alam, Distinguishing individual lipid headgroup mobility and phase transitions in raft-forming lipid mixtures with 31P MAS NMR, *Biophys. J.* 90 (2006) 4248–4260.
- [41] H.W. Meyer, K. Semmler, W. Rettig, W. Pohle, A.S. Ulrich, S. Grage, C. Selle, P.J. Quinn, Hydration of DMPC and DPPC at 4 degrees C produces a novel subgel phase with convex-concave bilayer curvatures, *Chem. Phys. Lipids* 105 (2000) 149–166.
- [42] L.K. Tamm, S.A. Tatulian, Infrared spectroscopy of proteins and peptides in lipid bilayers, *Q. Rev. Biophys.* 30 (1997) 365–429.
- [43] J.A. Clarke, A.J. Heron, J.M. Seddon, R.V. Law, The diversity of the liquid ordered (Lo) phase of phosphatidylcholine/cholesterol membranes: a variable temperature multinuclear solid-state NMR and X-ray diffraction study, *Biophys. J.* 90 (2006) 2383–2393.
- [44] M.R. Vist, J.H. Davis, Phase equilibria of cholesterol/dipalmitoylphosphatidylcholine mixtures: 2H nuclear magnetic resonance and differential scanning calorimetry, *Biochemistry* 29 (1990) 451–464.
- [45] J. Vazquez, M.T. Montero, S. Merino, O. Domenech, M. Berlanga, M. Vinas, J. Hernandez-Borrell, Location and nature of the surface membrane binding site of ciprofloxacin: a fluorescence study, *Langmuir* 17 (2001) 1009–1014.
- [46] P.R. Beining, E. Huff, B. Prescott, T.S. Theodore, Characterization of the lipids of mesosomal vesicles and plasma membranes from *Staphylococcus aureus*, *J. Bacteriol.* 121 (1975) 137–143.

GENERAL DISCUSSION AND PERSPECTIVES

General Discussion

The biological functions of cell membranes are strongly coupled with their fundamental physicochemical properties. The membrane electrostatics, phase state, conformation, orientation and dynamics of the lipids components determine the overall membrane structure and control the binding, the transport and the correct insertion of drugs. Therefore, studying the physicochemical properties of lipid model membrane interacting with drug *in vitro* is an important task both for membrane biophysics and molecular pharmacology.

In the context of this Thesis, focused on two antibiotics that act against bacteria primarily by interacting with intra-bacterial targets (DNA gyrase and DNA topoisomerase), passage through membranes is an essential requisite. Moreover, fluoroquinolones also show a fast accumulation in eukaryotic cells and show activity against intracellular bacteria, which implies that these drugs must also be able to pass across the pericellular and intracellular membranes. For these reasons, both prokaryotic and eukaryotic membranes have been modeled in our studies.

Fluoroquinolones, however, are also subject to transmembrane transport via specialized proteins that play a critical role in their influx as well as in their efflux. Thus, in Gram-negative bacteria, passage through the outer membrane is critically dependent of porins through which the drug must pass to reach the inter-membrane space, before crossing the inner membrane (Bryan and Bedard, 1991; Ceccarelli, 2009). Efflux is observed not only in both Gram-negative and Gram-positive bacteria, but also in eukaryotic cells (Alvarez et al., 2008; Brillault et al., 2009; Michot et al., 2004; Michot et al., 2005). Efflux plays a critical role in reducing the intra-bacterial as well as the intracellular drug concentration, and contributes to decrease the activity of fluoroquinolones. The bacterial and cellular content in fluoroquinolones upon exposure to those drugs is actually governed by and is the result of a balance between mutually opposite mechanisms (Figure 27).

Interestingly enough, MXF is, generally speaking, considerably less susceptible than CIP to efflux both in prokaryotic and eukaryotic cells (Luzzaro, 2008; Michot et al., 2005), which explains its activity against bacteria that are resistant to CIP through the expression of efflux transporters (e.g., NorA in *S.aureus*) and its larger accumulation compared to CIP in many eukaryotic cells.

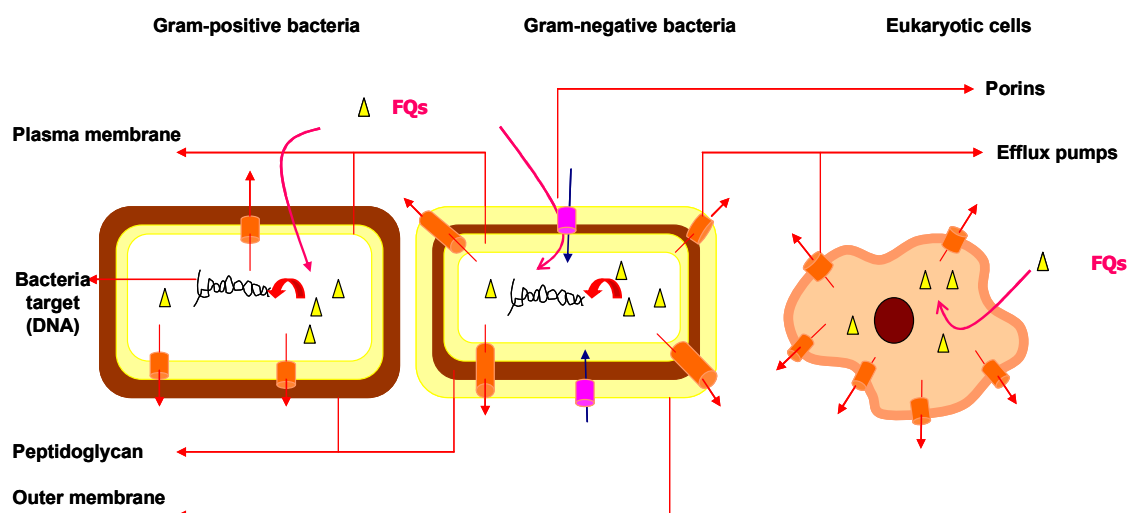


Figure 27. Overview of the transport pathway of fluoroquinolones through bacterial and eukaryotic membranes.

Fluoroquinolones can pass through porins channel (magenta tubes) in Gram-negative bacteria. In all cases (Gram-positive, Gram-negative bacteria and eukaryotic cells), they can reach intracellular compartment by crossing the naked plasma membrane, but can also be expelled back to the extracellular milieu via efflux pumps proteins (orange tubes).

Studies performed in our laboratory have shown that this apparent lack of susceptibility to efflux by an eukaryotic transporter (Mrp4) is associated with a considerably faster passage of MXF in and out of the cells (Marquez et al., 2009). Our work was initiated to try providing a rational explanation to this intriguing phenomenon.

For this purpose, a multidisciplinary approach aimed at characterizing and comparing the interaction of CIP and MXF with membrane models has been used.

Fluorescence spectroscopy, a well established method for providing broad information on membrane properties, by using appropriate probes and examining their fluorescence characteristics (wavelength maximum, fluorescence intensity, polarization), was applied in conjunction with AFM, Langmuir, ATR-FTIR and NMR to provide complementary informations on the physicochemical properties of both fluoroquinolones and lipids.

By analogy with previous studies examining the interaction of the macrolide antibiotic azithromycin and lipids (e.g. fluidity, membrane organization, elasticity) (Fa et al., 2007; Tyteca et al., 2003), our aim was to explore the importance and the nature of head groups and acyl chain of phospholipids in the mechanism of interaction between

CIP and MXF with lipid models membrane. Understanding at molecular level how CIP and MXF interact with appropriate model lipid membranes could, indeed, bring answers on their transport pathway cross the plasma and/or bacterial membranes.

An overview of the interactions between CIP and MXF and lipid membranes mimicking the prokaryotic membranes (DPPG) and the eukaryotic membranes (DPPC) is presented in Figures 28 and 29.

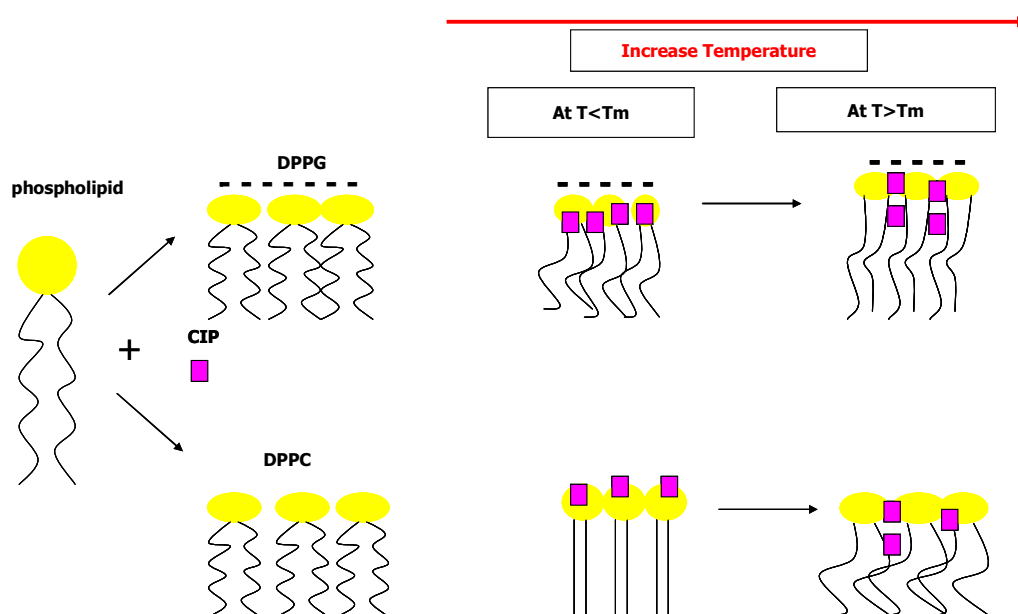


Figure 28. Proposed schematic model for phospholipids (DPPC, DPPG) destabilization upon interaction with CIP. The antibiotic is represented by magenta square. The first step of interaction is the binding of CIP to the headgroups of phospholipids, which is stronger with negatively charged (DPPG) than with zwitterionic phospholipids (DPPC). At pre-transition temperature, CIP decreases the order of acyl chain of DPPG and increases it at post-transition temperature. However, CIP has no effect on thermotropic state transition profile of DPPC.

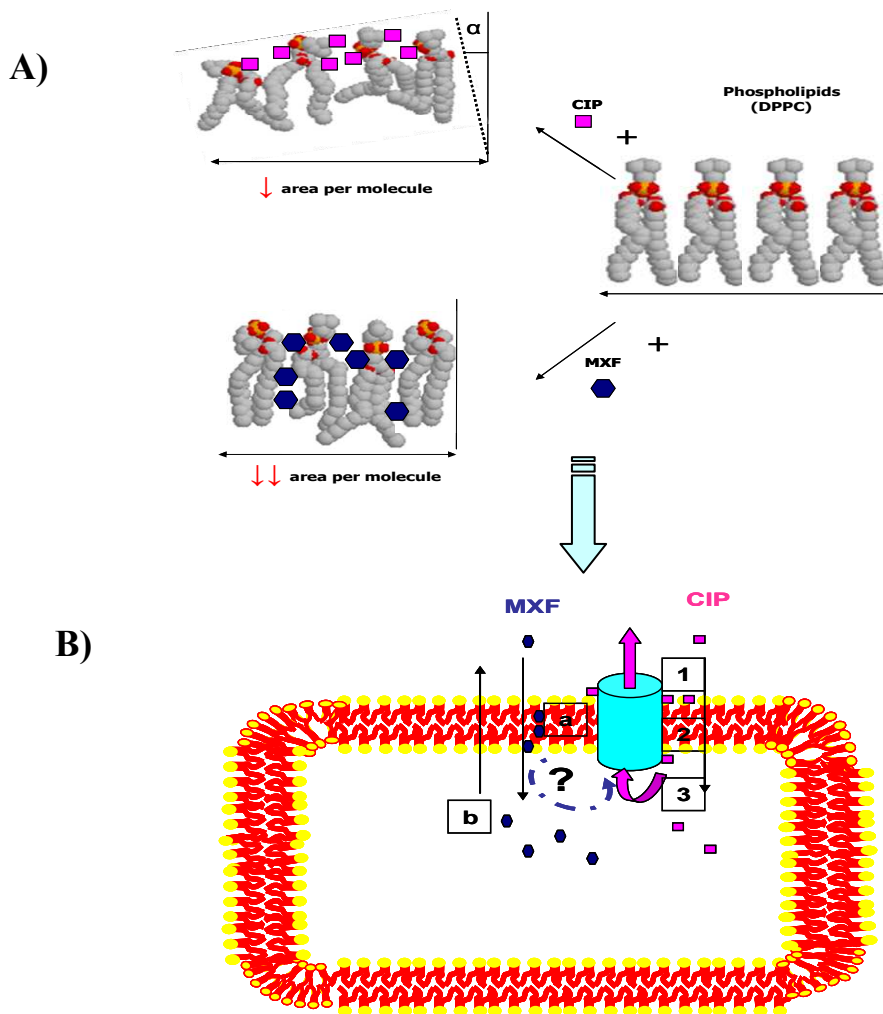


Figure 29. (A) Schematic representation of the effect of fluoroquinolones (CIP versus MXF) on the acyl-chain of zwitterionic phospholipids (DPPC). Although both of drugs induce a decrease of the area per molecule, CIP induces more disorder and modifies the orientation of acyl chain, whereas MXF has a higher packing effect. (B) Proposed model for passage of these drugs through eukaryotic plasma membrane. CIP adsorbs first on the head group of phospholipids (1) before reaching the hydrophobic domain, where it could have access to the transmembrane domain of the efflux pump protein (2), allowing its recognition and transport outside of the cell. However, CIP could also reach the inner face of the membrane and be taken up by efflux transporter from the cytosol (3). MXF interacts more directly with hydrophobic domain of the membrane lipids (deeper along the acyl chain (a)), and could also pass to the extracellular compartment via the phospholipids bilayer (b), which may explain why it could be less subject of efflux pump from the cytosol. Another hypothesis could be that MXF is effluxed from the bilayer and immediately uptake suggesting a very fast turnover of the drug between the extracellular milieu and the membrane.

With respect to models mimicking the prokaryotic membranes, the main finding is that CIP binds more tightly to negatively charged (DPPG) rather than to zwitterionic (DOPC or DPPC) phospholipids, which may represent a primary step in the access of fluoroquinolones to the bacterial cytoplasm. These data suggest that the stability of CIP-phospholipids interaction is strongly dependent upon the presence of a glycerol headgroup. This is in agreement with other studies (Grancelli et al., 2002; Vazquez et al., 2001c), which reported the ability of CIP to bind to the headgroups of lipids by electrostatic interactions. This interaction could however be influenced by the presence or the position of hydrophobic substituent (e.g. N-4-butylpiperazinyl ciprofloxacin, N-3-methylpiperazinyl ciprofloxacin *versus*. N-4-methylpiperazinyl ciprofloxacin) (Montero et al., 2006).

The role played by the nature of the phosphate heads in itself (Bensikaddour et al., 2008b) is consistent with previous studies (Maurer et al., 1998; Vazquez et al., 2001c).

Molecular modeling studies rationalize this conclusion by showing a difference in the energies of interaction ($\Delta\Delta G$) between the (DPPG:CIP) and the (DPPC:CIP) complexes of about -9Kcal/mol. This implies that CIP forms a more stable complex with DPPG than DPPC. To corroborate the theoretical values with the experimental binding affinity data, we calculated energy of interaction using Gibbs' equation 24:

$$\Delta G = -RT \ln K \quad [\text{Eq. 24}]$$

where R is the gas constant ($1.987 \text{ cal M}^{-1}\text{K}^{-1}$), T is the temperature in Kelvin and K is affinity constant at equilibrium. Our experimental data, however, suggest a much lower difference (-0.72 Kcal/mol) between (DPPG:CIP) and (DPPC:CIP) complexes. This may result from the effects of solvation and ionic strength, as these contribute to the experimental measurements, but are not taken into account in the theoretical calculations. Although, the difference in energy of interaction is less than 1 Kcal/mol, it might result from a compensating compromise between enthalpy and entropy of association.

Furthermore, it seems that the presence of double bond in acyl chain can affect the stability of interaction. Indeed, the addition of DOPC, an analogue of DPPC phospholipid with one double bond ($\text{C}_{18:1}$), to the vesicle formed with either DPPC or DPPG, decreases the energy of interaction. In comparison with the energy of (DPPG vesicles:CIP) complexes, a $\Delta\Delta G^{25^\circ}$ of (-1.21Kcal/mol) is observed for (DOPC:DPPC vesicles:CIP) complexes, and a $\Delta\Delta G^{25^\circ}$ of (-0.58Kcal/mol) for (DOPC:DPPG vesicles ;CIP) complexes. This could be related to the state order of phospholipids. As our

experiments were performed at room temperature, DOPC was in fluid state ($T_m \approx -20^\circ\text{C}$), which enhances the fluidity of the vesicles prepared with a (DOPC:DPPC) or a (DOPC:DPPG) mixture.

These data support the contribution of electrostatic interactions between CIP and the polar heads of phospholipids. Because, phosphatidylglycerol is present at a high content in bacterial membranes, we believe that the major effects of CIP on these membranes should be related to its interaction with anionic lipid compounds. However, we do not know at this stage, whether this conclusion may be generalized to other negatively charged lipids. Regarding other fluoroquinolones such as grepafloxacin, it has been shown that it has a partition coefficient in DMPG ten times higher than in DMPC liposomes (Rodrigues et al., 2002).

With respect to models mimicking the eukaryotic membranes, we show that MXF also interacts deeper than CIP, reaching the hydrophobic domain of the phospholipids (acyl chains). This is consistent with the observation that MXF induces (i) a larger erosion of the gel phase made of DPPC domains in the DOPC fluid phase phase than CIP, (ii) a higher shift of the surface pressure-area isotherms of DOPC: DPPC: FQs monolayer towards the lower area per molecule compared to CIP, which is also rationalized by the molecular modeling calculations.

Globally speaking, we can therefore conclude that while CIP binds to membranes and induces a disorder by modifying the orientation of the acyl chain, MXF causes less perturbations probably because it has a higher tendency to decrease the number of all-trans conformation as compared to CIP, without dramatic changes in the orientation of acyl chains as revealed by the analysis of polarized and non polarized ATR-FTIR spectra. This may explain, at least in part, the faster penetration of MXF in eukaryotic cells.

Moxifloxacin and ciprofloxacin locations in the lipid bilayers

According to our results, the differential behaviors between CIP and MXF could be due to differences in their lipophilicity ($\log D$), which experimental studies suggest to be around (-0.79) for CIP vs. (-0.28) for MXF at pH 7.4 (Sun et al., 2002). (*This difference is probably due to the potential hydrophobicity and shape of the piperazinyl and the octa hydro-1H-pyrolo (3,4) pyridinyl moities of CIP and MXF, respectively*).

Thus, MXF is located in a more hydrophobic environment of lipids, probably by creating a pocket at the interfacial domain and penetrating deeply into the membrane the lipid bilayer. In contrast, CIP seems to be located at surface level, near the head group-acyl chain interface, since this drug interacts with head group of lipids, and modifies the orientation of acyl chain.

These results are corroborated by epifluorescence and atomic force microscopy observations performed for CIP with monolayer of DPPC and supported planar bilayer of lipids extracted from *E. coli*. The results show that CIP is able to adsorb on the phospholipid surface (Hernandez-Borrell and Montero, 2003; Montero et al., 2006).

The localization of CIP and MXF was recently illustrated in the comparative study of their interaction with mixed micelles of phospholipids and OmpF protein. The OmpF porin is the most abundant channel in the outer cell wall of *E. coli* that allows the passage of fluoroquinolones through the outer membrane of this bacteria. The structure of this protein is a trimer and each monomer contains two tryptophan residues: Trp₂₁₄ at the lipid-protein interface and Trp₆₁ at the trimer interface (Figure 30).

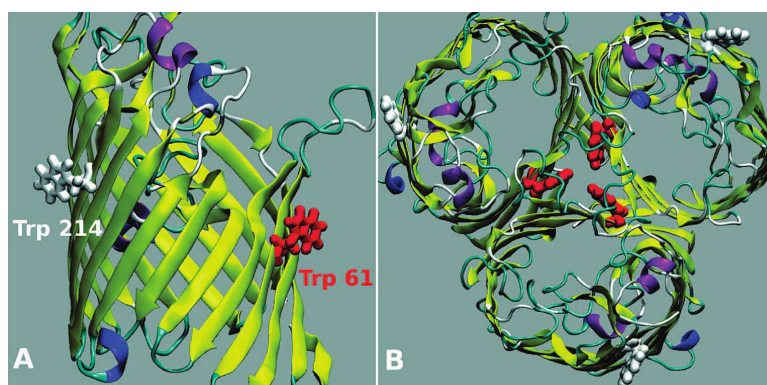


Figure 30. Views of OmpF organization: (A) a monomer shown from the side with the positions of the two Tryptophan residues (Trp₆₁ and Trp₂₁₄), shown in red and white, respectively and (B) the functional trimer shown from top (Mach et al., 2008).

By using fluorescence quenchers (iodide or acrylamide) of tryptophan residues (Trp₂₁₄ and Trp₆₁) of OmpF protein, which is mixed in micelles of zwitterionic (DMPC) or anionic (DPMG) phospholipid, and in the presence of the two fluoroquinolones, Neves and coworkers (Neves et al., 2009) showed that:

- i) CIP interacts with OmpF near Trp₂₁₄ located at the protein-lipid interface
- ii) MXF interacts with OmpF near Trp₆₁ located in an hydrophobic environment (in interior of the channel)

Moreover, there was a possible destabilization of the lipid packing in the presence of MXF, in order to change the conformation of protein associated with the translocation of the drug. The negatively charged lipids (DMPG) surrounding protein can also modulate the conformation and dynamic of OmpF.

These observations were confirmed by molecular dynamic simulations (Mach et al., 2008).

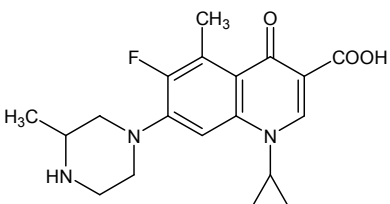
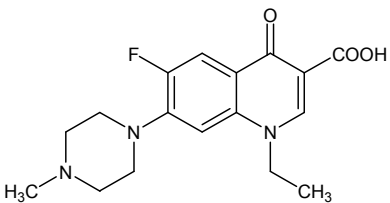
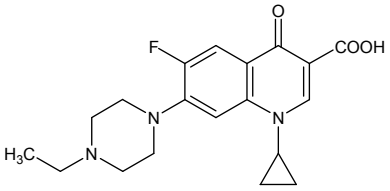
Perspectives

In the short term our work opens new perspectives to study the interactions between fluoroquinolones and lipids membranes.

First, our approaches could be applied to others fluoroquinolones, with systematic and stepwise changes in their lipophilicity and overall structures. Some of these molecules are shown in Table 8, with potential candidate for investigating the role of hydrophobicity in their interactions with lipids membrane. A typical exemple is grepafloxacin, a fluoroquinolone with two methyl groups, and having an effect on the lipid transition temperature as monitored by TMA-DPH anisotropy (Rodrigues et al., 2002).

Table 8. Chemical structure of some fluoroquinolones that exhibit an increase of their lipophilicity.

The reported log P (octanol: water partition coefficient) and log D (octanol/water partition coefficient at pH 7.4) were obtained from Reaxys software

Molecular structure	logD at pH 7.4	logP
<p style="text-align: center;">Grepafloxacin</p> 	-0.43	2.48
<p style="text-align: center;">Pefloxacin</p> 	+0.16	1.83
<p style="text-align: center;">Enrofloxacin</p> 	+0.58	2.29

functions of the transporters. Indeed, their activity seems to be dependent on the lipid environment. The overexpression of efflux pump proteins has been shown to be associated with a change in the lipid composition of the membrane affecting mainly sphingolipids (ceramides and glucosylceramides) (Gouaze et al., 2004;Gouaze et al., 2005;Lavie et al., 1996;Sietsma et al., 2001). In this respect, our preliminary studies on the identification and the quantification of lipids present in J774 cells wild type and those overexpressing Mrp4 protein (resistant to CIP) show that the latter exhibit a alteration in the sphingolipids composition, with an increased level of glucosylceramides, and a decreased content in ceramide and in sphingomyelin (Bensikaddour *et al.*, unpublished data). Further analysis focusing on the determination of the lipid composition of J774 cells overexpressing Mrp4 proteins *vs.* their wild type counterparts needs to be performed, for which mass spectrometry appears to be a promising method.

Finally, a study examining the correlation between the membrane lipid composition and the expression of efflux pump protein(s) could shed more light on the role played by lipids in drug transport.



REFERENCES



- Abankwa,D., A.A.Gorfe, and J.F.Hancock. 2008. Mechanisms of Ras membrane organization and signaling: Ras on a rocker. *Cell Cycle* 7:2667-2673.
- Akashi,K., H.Miyata, H.Itoh, and K.Kinosita. 1998a. Formation of giant liposomes promoted by divalent cations: Critical role of electrostatic repulsion. *Biophys. J.* 74:2973-2982.
- Akashi,K., H.Miyata, H.Itoh, and K.Kinosita. 1998b. Giant liposomes with multiple membrane-linking pores. *Biophys. J.* 74:A373.
- Allen,A., E.Bygate, D.Clark, A.Lewis, and V.Pay. 2000. The effect of food on the bioavailability of oral gemifloxacin in healthy volunteers. *Int. J. Antimicrob. Agents.* 16:45-50.
- Allen,T.M. and P.R.Cullis. 2004. Drug delivery systems: Entering the mainstream. *Science* 303:1818-1822.
- Alvarez,A.I., M.Perez, J.G.Prieto, A.J.Molina, R.Real, and G.Merino. 2008. Fluoroquinolone efflux mediated by ABC transporters. *J. Pharm. Sci.* 97:3483-3493.
- Andersen,J., N.Delihas, K.Ikenaka, P.J.Green, O.Pines, O.Ilercil, and M.Inouye. 1987. The isolation and characterization of RNA coded by the micF gene in Escherichia coli. *Nucleic Acids Res.* 15:2089-2101.
- Andes,D. and W.A.Craig. 2002a. Animal model pharmacokinetics and pharmacodynamics: a critical review. *Int. J. Antimicrob. Agents* 19:261-268.

- Andes,D. and W.A.Craig. 2002b. Pharmacodynamics of the new fluoroquinolone gatifloxacin in murine thigh and lung infection models. *Antimicrob. Agents Chemother.* 46:1665-1670.
- Anstead,G.M., K.J.Hwang, and J.A.Katzenellenbogen. 1993. Characterization of the spectroscopic properties of a tetrahydrochrysenone system containing a rigidified hydroxynitrostilbene chromophore: an inherently fluorescent ligand designed for the estrogen receptor. *Photochem. Photobiol.* 57:616-628.
- Arrondo,J.L., F.M.Goni, and J.M.Macarulla. 1984. Infrared spectroscopy of phosphatidylcholines in aqueous suspension. A study of the phosphate group vibrations. *Biochim. Biophys. Acta* 794:165-168.
- Asher,I.M. and I.W.Levin. 1977. Effects of temperature and molecular interactions on the vibrational infrared spectra of phospholipid vesicles. *Biochim. Biophys. Acta* 468:63-72.
- Bachoual,R., L.Dubreuil, C.J.Soussy, and J.Tankovic. 2000. Roles of gyrA mutations in resistance of clinical isolates and in vitro mutants of *Bacteroides fragilis* to the new fluoroquinolone trovafloxacin. *Antimicrob. Agents Chemother.* 44:1842-1845.
- Ball,P. 2000. Quinolone generations: natural history or natural selection? *Antimicrob. Agents Chemother.* 46:17-24.
- Ball,P. 2003. Adverse drug reactions: implications for the development of fluoroquinolones. *Antimicrob. Agents Chemother.* 51:21-27.

- Ball,P., R.Stahlmann, R.Kubin, S.Choudhri, and R.Owens. 2004. Safety profile of oral and intravenous moxifloxacin: Cumulative data from clinical trials and postmarketing studies. *Clinical Therapeutics* 26:940-950.
- Baumgart,T., A.T.Hammond, P.Sengupta, S.T.Hess, D.A.Holowka, B.A.Baird, and W.W.Webb. 2007. Large-scale fluid/fluid phase separation of proteins and lipids in giant plasma membrane vesicles. *Proc. Natl. Acad. Sci. U. S. A* 104:3165-3170.
- Bensikaddour,H., N.Fa, I.Burton, M.Deleu, L.Lins, A.Schanck, R.Brasseur, Y.F.Dufrene, E.Goormaghtigh, and M.P.Mingeot-Leclercq. 2008a. Characterization of the interactions between fluoroquinolone antibiotics and lipids: a multitechnique approach. *Biophys. J.* 94:3035-3046.
- Bensikaddour,H., K.Snoussi, L.Lins, F.Van Bambeke, P.M.Tulkens, R.Brasseur, E.Goormaghtigh, and M.P.Mingeot-Leclercq. 2008b. Interactions of ciprofloxacin with DPPC and DPPG: fluorescence anisotropy, ATR-FTIR and ³¹P NMR spectroscopies and conformational analysis. *Biochim. Biophys. Acta* 1778:2535-2543.
- Benz,R. and B.F.Gisin. 1978. Influence of membrane structure on ion transport through lipid bilayer membranes. *J. Membr. Biol.* 40:293-314.
- Benz,R., K.Janko, W.Boos, and P.Lauger. 1978. Formation of large, ion-permeable membrane channels by the matrix protein (porin) of Escherichia coli. *Biochim. Biophys. Acta* 511:305-319.
- Berquand,A., M.P.Mingeot-Leclercq, and Y.F.Dufrene. 2004. Real-time imaging of drug-membrane interactions by atomic force microscopy. *Biochim. Biophys. Acta* 1664:198-205.

- Beschiaschvili,G. and J.Seelig. 1992. Peptide Binding to Lipid Bilayers - Nonclassical Hydrophobic Effect and Membrane-Induced Pk Shifts. *Biochemistry* 31:10044-10053.
- Bilski,P., L.J.Martinez, E.B.Koker, and C.F.Chignell. 1996. Photosensitization by norfloxacin is a function of pH. *Photochem. Photobiol.* 64:496-500.
- Bilski,P., L.J.Martinez, E.B.Koker, and C.F.Chignell. 1998. Influence of solvent polarity and proticity on the photochemical properties of norfloxacin. *Photochem. Photobiol.* 68:20-24.
- Binnig,G., C.F.Quate, and C.Gerber. 1986. Atomic force microscope. *Phys. Rev. Lett.* 56:930-933.
- Brannigan,G., J.Henin, R.Law, R.Eckenhoff, and M.L.Klein. 2008. Embedded cholesterol in the nicotinic acetylcholine receptor. *Proceedings of the National Academy of Sciences of the United States of America* 105:14418-14423.
- Bright-Wilson,E.J., J.C.Decius, and P.C.Cross. 1955. Molecular Vibrations: The theory of Infrared and Raman Vibrational spectra. McGraw-Hill Book Company,INC.
- Brillault,J., W.V.De Castro, T.Harnois, A.Kitzis, J.C.Olivier, and W.Couet. 2009. P-Glycoprotein-Mediated Transport of Moxifloxacin in a Calu-3 Lung Epithelial Cell Model. *Antimicrob. Agents Chemother.* 53:1457-1462.
- Bryan,L.E. and J.Bedard. 1991. Impermeability to Quinolones in Gram-Positive and Gram-Negative Bacteria. *Eur J Clin Microbiol Infect Dis.* 10:232-239.
- Bryskier,A. and J.F.Chantot. 1995. Classification and structure-activity relationships of fluoroquinolones. *Drugs* 49 Suppl 2:16-28.

- Bush,S.F.L.H.L.I.W. 1980. *Chem Phys Lipids*. 27:101-111.
- Cameron,D.G. and H.H.Mantsch. 1978. The phase transition of 1,2-dipalmitoyl-sn-glycero-3-phosphocholine as seen by Fourier transform infrared difference spectroscopy. *Biochem. Biophys. Res. Commun.* 83:886-892.
- Cao,A., E.Hantzbrachet, B.Azize, E.Taillandier, and G.Perret. 1991. The Interaction of D-Propranolol and Dimyristoyl Phosphatidylcholine Large Unilamellar Vesicles Investigated by Quasi-Elastic Light-Scattering and Fourier-Transform Infrared-Spectroscopy. *Chem Phys Lipids*. 58:225-232.
- Casal,H.L., D.G.Cameron, I.C.P.Smith, and H.H.Mantsch. 1980. Acholeplasma-Laidlawii Membranes - Fourier-Transform Infrared Study of the Influence of Protein on Lipid Organization and Dynamics. *Biochemistry* 19:444-451.
- Casal,H.L. and H.H.Mantsch. 1984. Polymorphic phase behaviour of phospholipid membranes studied by infrared spectroscopy. *Biochim. Biophys. Acta* 779:381-401.
- Casal,H.L., H.H.Mantsch, and D.G.Cameron. 1984. A Vibrational Spectroscopic Study of the Ice-Melting-Induced Transition of 1,2-Dibehenoyl-Sn-Glycero-3-Phosphocholine. *Chem Phys Lipids*.35:77-86.
- Casal,H.L., A.Martin, and H.H.Mantsch. 1987. Infrared Spectroscopic Characterization of the Interaction of Lipid Bilayers with Phenol, Salicylic-Acid and Ortho-Acetylsalicylic Acid. *Chem Phys Lipids*. 43:47-53.
- Cavet,M.E., M.West, and N.L.Simmons. 1997. Fluoroquinolone (ciprofloxacin) secretion by human intestinal epithelial (Caco-2) cells. *Br. J. Pharmacol.* 121:1567-1578.

- Ceccarelli,M. 2009. Simulating transport properties through bacterial channels. *Frontiers in Bioscience-Landmark* 14:3222-3238.
- Chang,R. 2005. Physical chemistry for the biosciences. University Sciences Books. San Salites. California.
- Chapman,D., R.M.Williams, and B.D.Ladbrooke. 1967. *Chem Phys Lipids*. 1:445-475.
- Chien,S.C., A.T.Chow, J.Natarajan, R.R.Williams, F.A.Wong, M.C.Rogge, and R.K.Nayak. 1997a. Absence of age and gender effects on the pharmacokinetics of a single 500-milligram oral dose of levofloxacin in healthy subjects. *Antimicrob. Agents Chemother*. 41:1562-1565.
- Chien,S.C., M.C.Rogge, L.G.Gisclon, C.Curtin, F.Wong, J.Natarajan, R.R.Williams, C.L.Fowler, W.K.Cheung, and A.T.Chow. 1997b. Pharmacokinetic profile of levofloxacin following once-daily 500-milligram oral or intravenous doses. *Antimicrob. Agents Chemother*. 41:2256-2260.
- Chow,A.T., C.Fowler, R.R.Williams, N.Morgan, S.Kaminski, and J.Natarajan. 2001. Safety and pharmacokinetics of multiple 750-milligram doses of intravenous levofloxacin in healthy volunteers. *Antimicrob. Agents Chemother*. 45:2122-2125.
- Cohen,S.P., L.M.McMurry, D.C.Hooper, J.S.Wolfson, and S.B.Levy. 1989. Cross-resistance to fluoroquinolones in multiple-antibiotic-resistant (Mar) *Escherichia coli* selected by tetracycline or chloramphenicol: decreased drug accumulation associated with membrane changes in addition to OmpF reduction. *Antimicrob. Agents Chemother*. 33:1318-1325.
- Conover,W.W. 1984. Carbon-13 NMR. *J. Spectrosc*. 4:37-51.

- Cortijo,M. and D.Chapman. 1981. A Comparison of the Interactions of Cholesterol and Gramicidin A with Lipid Bilayers Using An Infrared Data Station. *Febs Letters* 131:245-248.
- Costello,M.J., P.Viitanen, N.Carrasco, D.L.Foster, and H.R.Kaback. 1984. Morphology of Proteoliposomes Reconstituted with Purified Lac Carrier Protein from Escherichia-Coli. *J. Biol. Chem.* 259:5579-5586.
- Cuquerella,M.C., F.Bosca, and M.A.Miranda. 2004. Photonucleophilic aromatic substitution of 6-fluoroquinolones in basic media: Triplet quenching by hydroxide anion. *J. Org. Chem.* 69:7256-7261.
- Dalhoff,A., U.Petersen, and R.Endermann. 1996. In vitro activity of BAY 12-8039, a new 8-methoxyquinolone. *Chemotherapy* 42:410-425.
- Davies,M.A., J.W.Brauner, H.F.Schuster, and R.Mendelsohn. 1990. A Quantitative Infrared Determination of Acyl Chain Conformation in Gramicidin Dipalmitoylphosphatidylcholine Mixtures. *Biochem. Biophys. Res. Comm.* 168:85-90.
- Davis,P.J., B.D.Fleming, K.P.Coolbear, and K.M.Keough. 1981. Gel to liquid-crystalline transition temperatures of water dispersions of two pairs of positional isomers of unsaturated mixed-acid phosphatidylcholines. *Biochemistry* 20:3633-3636.
- Davis,R., A.Markham, and J.A.Balfour. 1996. Ciprofloxacin. An updated review of its pharmacology, therapeutic efficacy and tolerability. *Drugs* 51:1019-1074.

- Deleu, M., M. Paquot, and T. Nylander. 2005. Fengycin interaction with lipid monolayers at the air-aqueous interface - implications for the effect of fengycin on biological membranes. *J. Colloid Interface Sci.* 283:358-365.
- Deslauriers, R., I. Ekiel, R. A. Byrd, H. C. Jarrell, and I. C. Smith. 1982. A ³¹P-NMR study of structural and functional aspects of phosphate and phosphonate distribution in *Tetrahymena*. *Biochim. Biophys. Acta* 720:329-337.
- Djurdjevic, P., L. Joksovic, R. Jelic, A. Djurdjevic, and M. J. Stankov. 2007. Solution equilibria between aluminum(III) ion and some fluoroquinolone family members. Spectroscopic and potentiometric study. *Chem. Pharm. Bull. (Tokyo)* 55:1689-1699.
- Dorobantu, L. S. and M. R. Gray. 2010. Application of atomic force microscopy in bacterial research. *Scanning* 32:74-96.
- Dudley, M. N., J. Ericson, and S. H. Zinner. 1987. Effect of dose on serum pharmacokinetics of intravenous ciprofloxacin with identification and characterization of extravascular compartments using noncompartmental and compartmental pharmacokinetic models. *Antimicrob. Agents Chemother.* 31:1782-1786.
- Dufourc, E. J. 2008. Sterols and membrane dynamics. *J. Chem. Biol.* 1:63-77.
- Dupont, P., D. Hocquet, K. Jeannot, P. Chavanet, and P. Plesiat. 2005. Bacteriostatic and bactericidal activities of eight fluoroquinolones against MexAB-OprM-overproducing clinical strains of *Pseudomonas aeruginosa*. *J. Antimicrob. Chemother.* 55:518-522.

- Edgar,R. and E.Bibi. 1997. MdfA, an Escherichia coli multidrug resistance protein with an extraordinarily broad spectrum of drug recognition. *J. Bacteriol.* 179:2274-2280.
- El Garch,F., A.Lismond, L.J.Piddock, P.Courvalin, P.M.Tulkens, and F.Van Bambeke. 2010. Fluoroquinolones induce the expression of patA and patB, which encode ABC efflux pumps in Streptococcus pneumoniae. *J. Antimicrob. Chemother.* 65:2076-2082.
- El Kirat,K., S.Morandat, and Y.F.Dufrene. 2010. Nanoscale analysis of supported lipid bilayers using atomic force microscopy. *Biochim. Biophys. Acta* 1798:750-765.
- Eliopoulos,G.M. 2004. Quinolone resistance mechanisms in pneumococci. *Clin. Infect. Dis.* 38 Suppl 4:S350-S356.
- Epand,R.F., P.B.Savage, and R.M.Epand. 2007. Bacterial lipid composition and the antimicrobial efficacy of cationic steroid compounds (Ceragenins). *Biochim. Biophys. Acta -Biomembranes* 1768:2500-2509.
- Fa,N., L.Lins, P.J.Courtoy, Y.Dufrene, P.Van Der Smissen, R.Brasseur, D.Tyteca, and M.P.Mingeot-Leclercq. 2007. Decrease of elastic moduli of DOPC bilayers induced by a macrolide antibiotic, azithromycin. *Biochim. Biophys. Acta - Biomembranes* 1768:1830-1838.
- Fahy,E., S.Subramaniam, H.A.Brown, C.K.Glass, A.H.Merrill, R.C.Murphy, C.R.H.Raetz, D.W.Russell, Y.Seyama, W.Shaw, T.Shimizu, F.Spener, G.van Meer, M.S.VanNieuwenhze, S.H.White, J.L.Witztum, and E.A.Dennis. 2005. A comprehensive classification system for lipids. *Eur. J. Lipid Sci. Technol.* 107:337-364.

- Ferrero,L., B.Cameron, and J.Crouzet. 1995. Analysis of gyrA and grlA mutations in stepwise-selected ciprofloxacin-resistant mutants of Staphylococcus aureus. *Antimicrob. Agents Chemother.* 39:1554-1558.
- Firsov,A.A., S.N.Vostrov, A.A.Shevchenko, Y.A.Portnoy, and S.H.Zinner. 1998. A new approach to in vitro comparisons of antibiotics in dynamic models: equivalent area under the curve/MIC breakpoints and equiefficient doses of trovafloxacin and ciprofloxacin against bacteria of similar susceptibilities. *Antimicrob. Agents Chemother.* 42:2841-2847.
- Fischman,A.J., J.W.Babich, N.M.Alpert, J.Vincent, R.J.Callahan, J.A.Correia, and R.H.Rubin. 1996a. Pharmacokinetics of F-18 trovafloxacin in normal and E-coli infected rabbits studied with PET. *J. Nucl. Med.* 37:1076.
- Fischman,A.J., J.W.Babich, A.A.Bonab, N.M.Alpert, J.Vincent, R.J.Callahan, J.A.Correia, and R.H.Rubin. 1998. Pharmacokinetics of [F-18]trovafloxacin in healthy human subjects studied with positron emission tomography. *Antimicrob. Agents Chemother.*42:2048-2054.
- Fischman,A.J., E.Livni, J.W.Babich, N.M.Alpert, A.Bonab, S.Chodosh, F.McGovern, P.Kamitsuka, Y.Y.Liu, R.Cleeland, B.L.Prosser, J.A.Correia, and R.H.Rubin. 1996b. Pharmacokinetics of [F-18]fleroxacin in patients with acute exacerbations of chronic bronchitis and complicated urinary tract infection studied by positron emission tomography. *Antimicrob. Agents. Chemother.* 40:659-664.
- Fournier,B., X.L.Zhao, T.Lu, K.Drlica, and D.C.Hooper. 2000. Selective targeting of topoisomerase IV and DNA gyrase in Staphylococcus aureus: Different patterns

- of quinolone-induced inhibition of DNA synthesis. *Antimicrob. Agents Chemother.* 44:2160-2165.
- Fringeli, U.P. and H.H. Gunthard. 1981. Infrared membrane spectroscopy. *Mol. Biol. Biochem. Biophys.* 31:270-332.
- Fukuda, H. and K. Hiramatsu. 1999. Primary targets of fluoroquinolones in *Streptococcus pneumoniae*. *Antimicrob. Agents Chemother.* 43:410-412.
- Futerman, A.H. and Y.A. Hannun. 2004. The complex life of simple sphingolipids. *Embo Reports* 5:777-782.
- Gadian, D.G. 1982. Nuclear magnetic resonance and its applications to living systems. University of Oxford.
- Garcia-Manyes, S., G. Oncins, and F. Sanz. 2005. Effect of temperature on the nanomechanics of lipid bilayers studied by force spectroscopy. *Biophys. J.* 89:4261-4274.
- Garcia-Manyes, S. and F. Sanz. 2010. Nanomechanics of lipid bilayers by force spectroscopy with AFM: a perspective. *Biochim. Biophys. Acta* 1798:741-749.
- Giocondi, M.C., V. Vie, E. Lesniewska, P.E. Milhiet, M. Zinke-Allmang, and C. Le Grimellec. 2001. Phase topology and growth of single domains in lipid bilayers. *Langmuir* 17:1653-1659.
- Giocondi, M.C., D. Yamamoto, E. Lesniewska, P.E. Milhiet, T. Ando, and C. Le Grimellec. 2010. Surface topography of membrane domains. *Biochim. Biophys. Acta* 1798:703-718.

- Girard-Egrot,A.P., S.Godoy, and L.J.Blum. 2005. Enzyme association with lipidic Langmuir-Blodgett films: interests and applications in nanobioscience. *Adv. Colloid Interface Sci.* 116:205-225.
- Goormaghtigh,E., V.Raussens, and J.M.Ruysschaert. 1999. Attenuated total reflection infrared spectroscopy of proteins and lipids in biological membranes. *Biochim. Biophys. Acta* 1422:105-185.
- Gorfe,A.A. and J.A.McCammon. 2008. Similar membrane affinity of mono- and di-S-acylated Ras membrane anchors: A new twist in the role of protein lipidation. *J. Am. Chem. Soc.* 130:12624.
- Gouaze,V., Y.Y.Liu, C.S.Prickett, J.Y.Yu, A.E.Giuliano, and M.C.Cabot. 2005. Glucosylceramide synthase blockade down-regulates P-glycoprotein and resensitizes multidrug-resistant breast cancer cells to anticancer drugs. *Cancer Res.* 65:3861-3867.
- Gouaze,V., J.Y.Yu, R.J.Bleicher, T.Y.Han, Y.Y.Liu, H.Wang, M.M.Gottesman, A.Bitterman, A.E.Giuliano, and M.C.Cabot. 2004. Overexpression of glucosylceramide synthase and P-glycoprotein in cancer cells selected for resistance to natural product chemotherapy. *Mol. Cancer Ther.* 3:633-639.
- Grancelli,A., A.Morros, M.E.Cabanas, O.Domenech, S.Merino, J.L.Vazquez, M.T.Montero, M.Vinas, and J.Hernandez-Borrell. 2002. Interaction of 6-fluoroquinolones with dipalmitoylphosphatidylcholine monolayers and liposomes. *Langmuir* 18:9177-9182.
- Haines,T.H. 2001. Do sterols reduce proton and sodium leaks through lipid bilayers? *Prog. Lipid. Res.* 40:299-324.

- Hanada,K., M.Nishijima, and Y.Akamatsu. 1990. A temperature-sensitive mammalian cell mutant with thermolabile serine palmitoyltransferase for the sphingolipid biosynthesis. *J. Biol. Chem.* 265:22137-22142.
- Harder,S., U.Fuhr, D.Beermann, and A.H.Staib. 1990. Ciprofloxacin Absorption in Different Regions of the Human Gastrointestinal-Tract - Investigations with the Hf-Capsule. *Br. J. Clin. Pharmacol.* 30:35-39.
- Henkart,P. and R.Blumenthal. 1975. Interaction of lymphocytes with lipid bilayer membranes: a model for lymphocyte-mediated lysis of target cells. *Proc. Natl. Acad. Sci. U. S. A* 72:2789-2793.
- Hernandez-Borrell,J. and M.T.Montero. 2003. Does ciprofloxacin interact with neutral bilayers? An aspect related to its antimicrobial activity. *Int. J. Pharm.* 252:149-157.
- HernandezBorrell,J. and M.T.Montero. 1997. Calculating microspecies concentration of zwitterion amphoteric compounds: Ciprofloxacin as example. *J. Chem. Educ.* 74:1311-1314.
- Hiasa,H. and M.E.Shea. 2000. DNA gyrase-mediated wrapping of the DNA strand is required for the replication fork arrest by the DNA gyrase-quinolone-DNA ternary complex. *J. Biol. Chem.* 275:34780-34786.
- Hori,S., Y.Ohshita, Y.Utsui, and K.Hiramatsu. 1993. Sequential acquisition of norfloxacin and ofloxacin resistance by methicillin-resistant and -susceptible *Staphylococcus aureus*. *Antimicrob. Agents Chemother.* 37:2278-2284.
- Huang, Z, Huang, H., Cai, R., Lin, Z., Korenaca, T., and Zeng, Y. E. 13, 77-80. 1997.

Ref Type: Report

- Huwiler,A., T.Kolter, J.Pfeilschifter, and K.Sandhoff. 2000. Physiology and pathophysiology of sphingolipid metabolism and signaling. *Biochim. Biophys. Acta-Molecular and Cell Biology of Lipids* 1485:63-99.
- Illinger,D., G.Duportail, Y.Mely, N.Poirel-Morales, D.Gerard, and J.G.Kuhry. 1995. A comparison of the fluorescence properties of TMA-DPH as a probe for plasma membrane and for endocytic membrane. *Biochim. Biophys. Acta* 1239:58-66.
- Jacoby,G.A. 2005. Mechanisms of resistance to quinolones. *Clin. Infect. Dis.* 41 Suppl 2:S120-S126.
- Jain,M.K. and R.C.Wagner. 1988. Introduction to biological membranes. Wiley, New York.
- Jass,J., T.Tjarnhage, and G.Puu. 2000. From liposomes to supported, planar bilayer structures on hydrophilic and hydrophobic surfaces: an atomic force microscopy study. *Biophys. J.* 79:3153-3163.
- Kato,J., Y.Nishimura, R.Imamura, H.Niki, S.Hiraga, and H.Suzuki. 1990. New Topoisomerase Essential for Chromosome Segregation in Escherichia-Coli. *Cell* 63:393-404.
- Keough,K.M. and P.J.Davis. 1979. Gel to liquid-crystalline phase transitions in water dispersions of saturated mixed-acid phosphatidylcholines. *Biochemistry* 18:1453-1459.
- Khodursky,A.B. and N.R.Cozzarelli. 1998. The mechanism of inhibition of topoisomerase IV by quinolone antibacterials. *J. Biol. Chem.* 273:27668-27677.

- Kinosita, K., Jr., S. Kawato, and A. Ikegami. 1977. A theory of fluorescence polarization decay in membranes. *Biophys. J.* 20:289-305.
- Klopman, G., O.T. Macina, M.E. Levinson, and H.S. Rosenkranz. 1987. Computer automated structure evaluation of quinolone antibacterial agents. *Antimicrob. Agents Chemother.* 31:1831-1840.
- Knaub, S.R., M.J. Priston, M.D. Morton, J.D. Slechta, D.G. Vander Velde, and C.M. Riley. 1995. A ¹⁹F NMR study of lomefloxacin in human erythrocytes and its interaction with hemoglobin. *J. Pharm. Biomed. Anal.* 13:1225-1233.
- Kohler, S.J. and M.P. Klein. 1976. ³¹P nuclear magnetic resonance chemical shielding tensors of phosphorylethanolamine, lecithin, and related compounds: Applications to head-group motion in model membranes. *Biochemistry* 15:967-974.
- Lacy, M.K., W. Lu, X. Xu, P.R. Tessier, D.P. Nicolau, R. Quintiliani, and C.H. Nightingale. 1999. Pharmacodynamic comparisons of levofloxacin, ciprofloxacin, and ampicillin against *Streptococcus pneumoniae* in an in vitro model of infection. *Antimicrob. Agents Chemother.* 43:672-677.
- Lakowicz, J.R. 1999. Principles of Fluorescence Spectroscopy. Kluwer Academic/Plenum Publishers, New York..
- Langlois, M.H., M. Montagut, J.P. Dubost, J. Grellet, and M.C. Saux. 2005. Protonation equilibrium and lipophilicity of moxifloxacin. *J. Pharmaceut. Biomed.* 37:389-393.

Larijani,B. and E.J.Dufourc. 2006. Polyunsaturated phosphatidylinositol and diacylglycerol substantially modify the fluidity and polymorphism of biomembranes: a solid-state deuterium NMR study. *Lipids* 41:925-932.

Lavie,Y., H.T.Cao, S.L.Bursten, A.E.Giuliano, and M.C.Cabot. 1996. Accumulation of glucosylceramides in multidrug-resistant cancer cells. *J. Biol. Chem.* 271:19530-19536.

Lee, C. D and Chapman, D. Infrared spectroscopic studies of biomembranes and model membranes. Vol 6 N°3. 1986.

Ref Type: Report

Lee, Moses. Identifying an unknown compound by infrared spectroscopy. 1997.

Ref Type: Personal Communication

Levin,I.W.M.E.B.R. 1982. *J. Raman Spectrosc.* 13:231-234.

Li,X.Z. 2005. Quinolone resistance in bacteria: emphasis on plasmid-mediated mechanisms. *Int. J. Antimicrob. Agents* 25:453-463.

Lingwood,D. and K.Simons. 2010. Lipid rafts as a membrane-organizing principle. *Science* 327:46-50.

Linseisen,F.M., M.Hetzer, T.Brumm, and T.M.Bayerl. 1997. Differences in the physical properties of lipid monolayers and bilayers on a spherical solid support. *Biophys. J.* 72:1659-1667.

Lohner,K. and E.J.Prenner. 1999. Differential scanning calorimetry and X-ray diffraction studies of the specificity of the interaction of antimicrobial peptides with membrane-mimetic systems. *Biochim. Biophys. Acta* 1462:141-156.

- Lomovskaya,O. and K.Lewis. 1992. Emr, an Escherichia coli locus for multidrug resistance. *Proc. Natl. Acad. Sci. U. S. A* 89:8938-8942.
- Lubasch,A., I.Keller, K.Borner, P.Koeppel, and H.Lode. 2000. Comparative pharmacokinetics of ciprofloxacin, gatifloxacin, grepafloxacin, levofloxacin, trovafloxacin, and moxifloxacin after single oral administration in healthy volunteers. *Antimicrob. Agents Chemother.* 44:2600-2603.
- Luckey,M. 2008. Membrane Structural Biology with Biochemical and Biophysical Foundation. Cambridge University Press.
- Luzzaro,F. 2008. [Fluoroquinolones and Gram-negative bacteria: antimicrobial activity and mechanisms of resistance]. *Infez. Med.* 16 Suppl2:5-11.
- Ma,J.Y., J.K.Ma, and K.C.Weber. 1985. Fluorescence studies of the binding of amphiphilic amines with phospholipids. *J. Lipid Res.* 26:735-744.
- Mach,T., P.Neves, E.Spiga, H.Weingart, M.Winterhalter, P.Ruggerone, M.Ceccarelli, and P.Gameiro. 2008. Facilitated permeation of antibiotics across membrane channels- -interaction of the quinolone moxifloxacin with the OmpF channel. *J. Am. Chem. Soc.* 130:13301-13309.
- Mandell,L.A., R.G.Wunderink, A.Anzueto, J.G.Bartlett, G.D.Campbell, N.C.Dean, S.F.Dowell, T.M.File, Jr., D.M.Musher, M.S.Niederman, A.Torres, and C.G.Whitney. 2007. Infectious Diseases Society of America/American Thoracic Society consensus guidelines on the management of community-acquired pneumonia in adults. *Clin. Infect. Dis.* 44 Suppl 2:S27-S72.

- Marchbanks,C.R., J.R.McKiel, D.H.Gilbert, N.J.Robillard, B.Painter, S.H.Zinner, and M.N.Dudley. 1993. Dose ranging and fractionation of intravenous ciprofloxacin against *Pseudomonas aeruginosa* and *Staphylococcus aureus* in an in vitro model of infection. *Antimicrob. Agents Chemother.* 37:1756-1763.
- Marquez,B., N.E.Caceres, M.P.Mingeot-Leclercq, P.M.Tulkens, and F.Van Bambeke. 2009. Identification of the Efflux Transporter of the Fluoroquinolone Antibiotic Ciprofloxacin in Murine Macrophages: Studies with Ciprofloxacin-Resistant Cells. *Antimicrob. Agents Chemother.*53:2410-2416.
- Marrer,E., K.Schad, A.T.Satoh, M.G.Page, M.M.Johnson, and L.J.Piddock. 2006. Involvement of the putative ATP-dependent efflux proteins PatA and PatB in fluoroquinolone resistance of a multidrug-resistant mutant of *Streptococcus pneumoniae*. *Antimicrob. Agents Chemother.* 50:685-693.
- Martin,G.E. and A.S.Zektzer. 1988. Two dimensional NMR Methods of establishing molecular connectivity. VHC. Weinheim.
- Martin,Y., C.C.Williams, and H.K.Wickramasinghe. 1987. Atomic Force Microscope Force Mapping and Profiling on A Sub 100-A Scale. *J. Appl.Phys.* 61:4723-4729.
- Martinez-Martinez,L., A.Pascual, and G.A.Jacoby. 1998. Quinolone resistance from a transferable plasmid. *Lancet* 351:797-799.
- Martino,R., V.Gilard, F.Desmoulin, and M.Malet-Martino. 2005. Fluorine-19 or phosphorus-31 NMR spectroscopy: a suitable analytical technique for quantitative in vitro metabolic studies of fluorinated or phosphorylated drugs. *J. Pharm. Biomed. Anal.* 38:871-891.

- Maurer,N., K.F.Wong, M.J.Hope, and P.R.Cullis. 1998. Anomalous solubility behavior of the antibiotic ciprofloxacin encapsulated in liposomes: a H-1-NMR study. *Biochim. Biophys. Acta -Biomembranes* 1374:9-20.
- Mcnairn,E., N.Nibhriain, and C.J.Dorman. 1995. Overexpression of the Shigella-Flexneri Genes-Coding for Dna Topoisomerase-Iv Compensates for Loss of Dna Topoisomerase-I - Effect on Virulence Gene-Expression. *J. Mol. Microbiol.* 15:507-517.
- Merino,S., J.L.Vazquez, O.Domenech, M.Berlanga, M.Vinas, M.T.Montero, and J.Hernandez-Borrell. 2002. Fluoroquinolone - Biomembrane interaction at the DPPC/PG lipid - Bilayer interface. *Langmuir* 18:3288-3292.
- Mesaros,N., Y.Glupczynski, L.Avrain, N.E.Caceres, P.M.Tulkens, and F.Van Bambeke. 2007. A combined phenotypic and genotypic method for the detection of Mex efflux pumps in Pseudomonas aeruginosa. *J. Antimicrob. Chemother.* 59:378-386.
- Michaelson,D.M., A.F.Horwitz, and M.P.Klein. 1973. Transbilayer asymmetry and surface homogeneity of mixed phospholipids in cosonicated vesicles. *Biochemistry* 12:2637-2645.
- Michot,J.M., M.F.Heremans, N.E.Caceres, M.P.Mingeot-Leclercq, P.M.Tulkens, and F.Van Barnbeke. 2006. Cellular accumulation and activity of quinolones in ciprofloxacin-resistant J774 macrophages. *J. Antimicrob. Chemother.*50:1689-1695.
- Michot,J.M., C.Seral, F.Van Bambeke, M.P.Mingeot-Leclercq, and P.M.Tulkens. 2005. Influence of efflux transporters on the accumulation and efflux of four quinolones

- (ciprofloxacin, levofloxacin, garenoxacin, and moxifloxacin) in J774 macrophages. *J. Antimicrob. Chemother.* 49:2429-2437.
- Michot, J.M., F. Van Bambeke, M.P. Mingeot-Leclercq, and P.M. Tulkens. 2004. Active efflux of ciprofloxacin from J774 macrophages through an MRP-like transporter. *J. Antimicrob. Chemother.* 48:2673-2682.
- Mingeot-Leclercq, M.P., M. Deleu, R. Brasseur, and Y.F. Dufrene. 2008. Atomic force microscopy of supported lipid bilayers. *Nat. Protoc.* 3:1654-1659.
- Mingeot-Leclercq, M.P., L. Lins, M. Bensliman, F. Van Bambeke, S.P. Van Der, J. Peuvot, A. Schanck, and R. Brasseur. 2002. Membrane destabilization induced by beta-amyloid peptide 29-42: importance of the amino-terminus. *Chem. Phys. Lipids* 120:57-74.
- Montero, M.T., J. Freixas, and J. Hernandez-Borrell. 1997. Expression of the partition coefficients of a homologous series of 6-fluoroquinolones. *Int. J. Pharm.* 149:161-170.
- Montero, M.T., J. Hernandez-Borrell, and K.M.W. Keough. 1998. Fluoroquinolone-biomembrane interactions: Monolayer and calorimetric studies. *Langmuir* 14:2451-2454.
- Montero, M.T., M. Pijoan, S. Merino-Montero, T. Vinuesa, and J. Hernandez-Borrell. 2006. Interfacial membrane effects of fluoroquinolones as revealed by a combination of fluorescence binding experiments and atomic force microscopy observations. *Langmuir* 22:7574-7578.
- Mushayakarara, E.L.I.W. 1980. *J. Phys. Chem.* 86:2324-2327.

- Naber,K.G., K.Hollauer, D.Kirchbauer, and W.Witte. 2000. In vitro activity of gatifloxacin compared with gemifloxacin, moxifloxacin, trovafloxacin, ciprofloxacin and ofloxacin against uropathogens cultured from patients with complicated urinary tract infections. *Int. J. Antimicrob. Agents* 16:239-243.
- Nagai,K., T.A.Davies, B.E.Dewasse, M.R.Jacobs, and P.C.Appelbaum. 2001. Single- and multi-step resistance selection study of gemifloxacin compared with trovafloxacin, ciprofloxacin, gatifloxacin and moxifloxacin in *Streptococcus pneumoniae*. *J. Antimicrob. Chemother.* 48:365-374.
- Nelson,D.L. and M.M.Cox. 2000. Lehninger principals of biochemistry.
- Nelson,D.L. and M.M.Cox. 2005. Lehninger principals of biochemistry .
- Neves,P., I.Sousa, M.Winterhalter, and P.Gameiro. 2009. Fluorescence quenching as a tool to investigate quinolone antibiotic interactions with bacterial protein OmpF. *J. Membr. Biol.* 227:133-140.
- Neyfakh,A.A., C.M.Borsch, and G.W.Kaatz. 1993. Fluoroquinolone resistance protein NorA of *Staphylococcus aureus* is a multidrug efflux transporter. *Antimicrob. Agents Chemother.* 37:128-129.
- Nikaido,H. and D.G.Thanassi. 1993. Penetration of lipophilic agents with multiple protonation sites into bacterial cells: tetracyclines and fluoroquinolones as examples. *Antimicrob. Agents Chemother.* 37:1393-1399.
- Nix,D.E., W.A.Watson, M.E.Lener, R.W.Frost, G.Krol, H.Goldstein, J.Lettieri, and J.J.Schentag. 1989. Effects of aluminum and magnesium antacids and ranitidine on the absorption of ciprofloxacin. *Clin. Pharmacol. Ther.* 46:700-705.

- North,D.S., D.N.Fish, and J.J.Redington. 1998. Levofloxacin, a second-generation fluoroquinolone. *Pharmacotherapy* 18:915-935.
- Ofoefule,S.I. and M.Okonta. 1999. Adsorption studies of ciprofloxacin: evaluation of magnesium trisilicate, kaolin and starch as alternatives for the management of ciprofloxacin poisoning. *Boll. Chim. Farm.* 138:239-242.
- Ohki,R. and M.Murata. 1997. bmr3, a third multidrug transporter gene of *Bacillus subtilis*. *J. Bacteriol.* 179:1423-1427.
- Okano,T., H.Maegawa, K.Inui, and R.Hori. 1990. Interaction of ofloxacin with organic cation transport system in rat renal brush-border membranes. *J. Pharmacol. Exp. Ther.* 255:1033-1037.
- Okusu,H., D.Ma, and H.Nikaido. 1996. AcrAB efflux pump plays a major role in the antibiotic resistance phenotype of *Escherichia coli* multiple-antibiotic-resistance (Mar) mutants. *J. Bacteriol.* 178:306-308.
- Oliveira,O.N. 1992. Langmuir-Blodgett Films: Properties and Possible. *Brazilian. J.Phys.* 22:69.
- Pan,J., S.Tristram-Nagle, and J.F.Nagle. 2009. Effect of cholesterol on structural and mechanical properties of membranes depends on lipid chain saturation. *Phys. Rev. E. Stat. Nonlin. Soft. Matter Phys.* 80:021931.
- Pan,X.S., J.Ambler, S.Mehtar, and L.M.Fisher. 1996. Involvement of topoisomerase IV and DNA gyrase as ciprofloxacin targets in *Streptococcus pneumoniae*. *Antimicrob. Agents Chemother.* 40:2321-2326.

- Pan,X.S. and L.M.Fisher. 1996. Cloning and characterization of the parC and parE genes of *Streptococcus pneumoniae* encoding DNA topoisomerase IV: role in fluoroquinolone resistance. *J. Bacteriol.* 178:4060-4069.
- Pan,X.S. and L.M.Fisher. 1998. DNA gyrase and topoisomerase IV are dual targets of clinafloxacin action in *Streptococcus pneumoniae*. *Antimicrob. Agents Chemother.* 42:2810-2816.
- Pan,X.S., G.Yague, and L.M.Fisher. 2001. Quinolone resistance mutations in *Streptococcus pneumoniae* GyrA and ParC proteins: mechanistic insights into quinolone action from enzymatic analysis, intracellular levels, and phenotypes of wild-type and mutant proteins. *Antimicrob. Agents Chemother.* 45:3140-3147.
- Paniagua, Juan-Carlos. Pons Miquel. NMR Spectroscopy. 2005.
- Ref Type: Personal Communication
- Park,H.R., T.H.Kim, and K.M.Bark. 2002. Physicochemical properties of quinolone antibiotics in various environments. *Eur. J. Med. Chem.* 37:443-460.
- Park,H.R., H.C.Lee, T.H.Kim, J.K.Lee, K.Yang, and K.M.Bark. 2000. Spectroscopic properties of fluoroquinolone antibiotics and nanosecond solvation dynamics in aerosol-OT reverse micelles. *Photochem. Photobiol.* 71:281-293.
- Park,H.R., C.H.Oh, H.C.Lee, L.S.Ryong, K.Yang, and K.M.Bark. 2004. Spectroscopic properties of various quinolone antibiotics in aqueous-organic solvent mixtures. *Photochem. Photobiol.* 80:554-564.

- Park, Y.H., B.H.Jung, B.C.Chung, J.Park, and C.Mitoma. 1997. Metabolic disposition of the new fluoroquinolone antibacterial agent DW116 in rats. *Drug Metab Dispos.* 25:1101-1103.
- Perichon, B., P.Courvalin, and M.Galimand. 2007. Transferable resistance to aminoglycosides by methylation of G1405 in 16S rRNA and to hydrophilic fluoroquinolones by QepA-mediated efflux in *Escherichia coli*. *J.Antimicrob. Agents Chemother.* 51:2464-2469.
- Perichon, B., J.Tankovic, and P.Courvalin. 1997. Characterization of a mutation in the parE gene that confers fluoroquinolone resistance in *Streptococcus pneumoniae*. *J.Antimicrob. Agents Chemother.* 41:1166-1167.
- Pestova, E., J.J.Millichap, G.A.Noskin, and L.R.Peterson. 2000. Intracellular targets of moxifloxacin: a comparison with other fluoroquinolones. *J. Antimicrob. Agents Chemother.* 45:583-590.
- Philips, M. and D.Chapman. 1968. *Biochim. Biophys. Acta* 163-301.
- Polk, R.E., D.P.Healy, J.Sahai, L.Drwal, and E.Racht. 1989. Effect of ferrous sulfate and multivitamins with zinc on absorption of ciprofloxacin in normal volunteers. *J. Antimicrob. Agents Chemother.* 33:1841-1844.
- Poole, K. 2000a. Efflux-mediated resistance to fluoroquinolones in gram-negative bacteria. *J.Antimicrob. Agents Chemother.* 44:2233-2241.
- Poole, K. 2000b. Efflux-mediated resistance to fluoroquinolones in gram-positive bacteria and the mycobacteria. *J.Antimicrob. Agents Chemother.* 44:2595-2599.

- Poole,K. 2005. Efflux-mediated antimicrobial resistance. *J. Antimicrob. Chemother.* 56:20-51.
- Poole,K., K.Krebes, C.McNally, and S.Neshat. 1993. Multiple antibiotic resistance in *Pseudomonas aeruginosa*: evidence for involvement of an efflux operon. *J. Bacteriol.* 175:7363-7372.
- Putman,M., H.W.van Veen, and W.N.Konings. 2000. Molecular properties of bacterial multidrug transporters. *Microbiol. Mol. Biol. Rev.* 64:672-693.
- Rabbaa,L., S.Dautrey, N.ColasLinhart, C.Carbon, and R.Farinotti. 1997. Absorption of ofloxacin isomers in the rat small intestine. *Antimicrob Agents. Chemother.* 41:2274-2277.
- Reece,R.J. and A.Maxwell. 1991. Dna Gyrase - Structure and Function. *Crit Rev Biochem Mol Biol.* 26:335-375.
- Renooij,W., L.M.Van Golde, R.F.Zwaal, and L.L.Van Deenen. 1976. Topological asymmetry of phospholipid metabolism in rat erythrocyte membranes. Evidence for flip-flop of lecithin. *Eur. J. Biochem.* 61:53-58.
- Reviakine,I. and A.Brisson. 2000. Formation of supported phospholipid bilayers from unilamellar vesicles investigated by atomic force microscopy. *Langmuir* 16:1806-1815.
- Rinia,H.A. and B.de Kruijff. 2001. Imaging domains in model membranes with atomic force microscopy. *FEBS Lett.* 504:194-199.

- Robicsek,A., J.Strahilevitz, G.A.Jacoby, M.Macielag, D.Abbanat, C.H.Park, K.Bush, and D.C.Hooper. 2006. Fluoroquinolone-modifying enzyme: a new adaptation of a common aminoglycoside acetyltransferase. *Nat. Med.* 12:83-88.
- Robillard,N.J. and A.L.Scarpa. 1988. Genetic and physiological characterization of ciprofloxacin resistance in *Pseudomonas aeruginosa* PAO. *Antimicrob. Agents Chemother.* 32:535-539.
- Rodrigues,C., P.Gameiro, S.Reis, J.L.F.C.Lima, and B.de Castro. 2002. Interaction of grepafloxacin with large unilamellar liposomes: Partition and fluorescence studies reveal the importance of charge interactions. *Langmuir* 18:10231-10236.
- Rothschild,K.J. and N.A.Clark. 1979. Polarized infrared spectroscopy of oriented purple membrane. *Biophys. J.* 25:473-487.
- Rothschild,K.J., R.Sanches, T.L.Hsiao, and N.A.Clark. 1980. A Spectroscopic Study of Rhodopsin Alpha-Helix Orientation. *Biophysical Journal* 31:53-64.
- Sahu,S. and W.S.Lynn. 1977. Lipid composition of human alveolar macrophages. *Inflammation* 2:83-91.
- Saldanha,C., N.C.Santos, and J.Martins-Silva. 2002. Fluorescent probes DPH, TMA-DPH and C-17-HC induce erythrocyte exovesiculation. *J. Membr. Biol.* 190:75-82.
- Schiller,J. and K.Arnold. 2002. Application of high resolution ³¹P NMR spectroscopy to the characterization of the phospholipid composition of tissues and body fluids - a methodological review. *Med. Sci. Monit.* 8:MT205-MT222.
- Schmitz,F.J., A.C.Fluit, M.Luckefahr, B.Engler, B.Hofmann, J.Verhoef, H.P.Heinz, U.Hadding, and M.E.Jones. 1998. The effect of reserpine, an inhibitor of

- multidrug efflux pumps, on the in-vitro activities of ciprofloxacin, sparfloxacin and moxifloxacin against clinical isolates of *Staphylococcus aureus*. *J. Antimicrob. Chemother.* 42:807-810.
- Seelig,J. 1978. ³¹P nuclear magnetic resonance and the head group structure of phospholipids in membranes. *Biochim. Biophys. Acta* 515:105-140.
- Seelig,J. 1985. Magnetic-Resonance of Membranes and Micelles. *Abstracts of Papers of the American Chemical Society* 189:138-COLL.
- Seelig,J., F.Borle, and T.A.Cross. 1985. Magnetic-Ordering of Phospholipid-Membranes. *Biochim Biophys Acta.* 814:195-198.
- Seral,C., M.Barcia-Macay, M.P.Mingeot-Leclercq, P.M.Tulkens, and F.Van Bambeke. 2005. Comparative activity of quinolones (ciprofloxacin, levofloxacin, moxifloxacin and garenoxacin) against extracellular and intracellular infection by *Listeria monocytogenes* and *Staphylococcus aureus* in J774 macrophages. *J. Antimicrob. Chemother.* 55:511-517.
- Shen,L.L., L.A.Mitscher, P.N.Sharma, T.J.Odonnell, D.W.T.Chu, C.S.Cooper, T.Rosen, and A.G.Pernet. 1989. Mechanism of Inhibition of Dna Gyrase by Quinolone Antibacterials - A Cooperative Drug-Dna Binding Model. *Biochemistry* 28:3886-3894.
- Sietsma,H., R.J.Veldman, and J.W.Kok. 2001. The involvement of sphingolipids in multidrug resistance. *J. Membr. Biol.*181:153-162.
- Simons,K. and E.Ikonen. 1997. Functional rafts in cell membranes. *Nature* 387:569-572.

- Simons,K. and W.L.C.Vaz. 2004. Model systems, lipid rafts, and cell membranes. *Annu Rev Biophys Biomol Struct.* 33:269-295.
- Singer,S.J. and G.L.Nicolson. 1972. The fluid mosaic model of the structure of cell membranes. *Science* 175:720-731.
- Sinko,B., J.Kokosi, A.Avdeef, and K.Takacs-Novak. 2009. A PAMPA study of the permeability-enhancing effect of new ceramide analogues. *Chem. Biodivers.* 6:1867-1874.
- Smith Ian,C.P. and H.Ekiel Ireana. 1984. Phosphorus 31 NMR of phospholipids in membranes. In Phosphorus 31 NMR: Principals and Applications.
- Spratte,K. and H.Riegler. 1994. Steady-State Morphology and Composition of Mixed Monomolecular Films (Langmuir Monolayers) at the Air/Water Interface in the Vicinity of the 3-Phase Line - Model-Calculations and Experiments. *Langmuir* 10:3161-3173.
- Stass,H. and D.Kubitza. 1999. Pharmacokinetics and elimination of moxifloxacin after oral and intravenous administration in man. *J. Antimicrob. Chemother.* 43 Suppl B:83-90.
- Stass,H. and D.Kubitza. 2001a. Effects of iron supplements on the oral bioavailability of moxifloxacin, a novel 8-methoxyfluoroquinolone, in humans. *Clin. Pharmacokinet.* 40 Suppl 1:57-62.
- Stass,H. and D.Kubitza. 2001b. Profile of moxifloxacin drug interactions. *Clin. Infect. Dis.* 32 Suppl 1:S47-S50.

- Steiner,R.F. 1991. In Topics in Fluorescence Spectroscopy. *In* Fluorescence anisotropy: theory and applications. Plenum Press, New York..
- Steitz,R., E.E.Mitchell, and I.R.Peterson. 1991. Relationships Between Fatty-Acid Monolayer Structure on the Subphase and on Solid Substrates. *Thin Solid Films* 205:124-130.
- Sulavik,M.C., C.Houseweart, C.Cramer, N.Jiwani, N.Murgolo, J.Greene, B.DiDomenico, K.J.Shaw, G.H.Miller, R.Hare, and G.Shimer. 2001. Antibiotic susceptibility profiles of Escherichia coli strains lacking multidrug efflux pump genes. *Antimicrob. Agents Chemother.* 45:1126-1136.
- Sullivan,J.T., M.Woodruff, J.Lettieri, V.Agarwal, G.J.Krol, P.T.Leese, S.Watson, and A.H.Heller. 1999. Pharmacokinetics of a once-daily oral dose of moxifloxacin (Bay 12-8039), a new enantiomerically pure 8-methoxy quinolone. *Antimicrob. Agents Chemother.* 43:2793-2797.
- Sun,J., S.Sakai, Y.Tauchi, Y.Deguchi, J.M.Chen, R.H.Zhang, and K.Morimoto. 2002. Determination of lipophilicity of two quinolone antibacterials, ciprofloxacin and grepafloxacin, in the protonation equilibrium. *Eur J Pharmaceut Biopharmaceut.* 54:51-58.
- Takacs-Novak,K., B.Noszal, I.Hermecz, G.Kereszturi, B.Podanyi, and G.Szasz. 1990. Protonation equilibria of quinolone antibacterials. *J. Pharm. Sci.* 79:1023-1028.
- Tamai,I., J.Yamashita, Y.Kido, A.Ohnari, Y.Sai, Y.Shima, K.Naruhashi, S.Koizumi, and A.Tsuji. 2000. Limited distribution of new quinolone antibacterial agents into brain caused by multiple efflux transporters at the blood-brain barrier. *J Pharmacol Exp Ther.* 295:146-152.

- Tran,J.H. and G.A.Jacoby. 2002. Mechanism of plasmid-mediated quinolone resistance. *Proc. Natl. Acad. Sci. U. S. A* 99:5638-5642.
- Tran,J.H., G.A.Jacoby, and D.C.Hooper. 2005. Interaction of the plasmid-encoded quinolone resistance protein Qnr with Escherichia coli DNA gyrase. *Antimicrob. Agents Chemother.* 49:118-125.
- Tyteca,D., A.Schanck, Y.F.Dufrene, M.Deleu, P.J.Courtoy, P.M.Tulkens, and M.P.Mingeot-Leclercq. 2003. The macrolide antibiotic azithromycin interacts with lipids and affects membrane organization and fluidity: studies on Langmuir-Blodgett monolayers, liposomes and J774 macrophages. *J. Membr. Biol.* 192:203-215.
- Van Bambeke,F., J.M.Michot, J.Van Eldere, and P.M.Tulkens. 2005. Quinolones in 2005: an update (vol 11, pg 256, 2005). *Clin. Microbiol. Infec.* 11:513.
- Van Bambeke,F. and P.M.Tulkens. 2009. Safety Profile of the Respiratory Fluoroquinolone Moxifloxacin Comparison with Other Fluoroquinolones and Other Antibacterial Classes. *Drug Safety* 32:359-378.
- van Meer,G. 2005. Cellular lipidomics. *Embo Journal* 24:3159-3165.
- Vazquez,J.L., M.Berlanga, S.Merino, O.Domenech, M.Vinas, M.T.Montero, and J.Hernandez-Borrell. 2001a. Determination by fluorimetric titration of the ionization constants of ciprofloxacin in solution and in the presence of liposomes. *J. Photochem. Photobiol.* 73:14-19.
- Vazquez,J.L., S.Merino, O.Domenech, M.Berlanga, M.Vinas, M.T.Montero, and J.Hernandez-Borrell. 2001b. Determination of the partition coefficients of a

homologous series of ciprofloxacin: influence of the N-4 piperazinyl alkylation on the antimicrobial activity. *Int. J.Pharm.* 220:53-62.

Vazquez,J.L., M.T.Montero, S.Merino, O.Domenech, M.Berlanga, M.Vinas, and J.Hernandez-Borrell. 2001c. Location and nature of the surface membrane binding site of ciprofloxacin: A fluorescence study. *Langmuir* 17:1009-1014.

Verity,J.E., N.Chhabra, K.Sinnathamby, and C.M.Yip. 2009. Tracking molecular interactions in membranes by simultaneous ATR-FTIR-AFM. *Biophys. J.* 97:1225-1231.

Waibel,B. and U.Holzgrabe. 2007. ¹H and ¹⁹F NMR relaxation studies of fleroxacin with *Micrococcus luteus*. *J. Pharm. Biomed. Anal.* 43:1595-1601.

Wang,H., J.L.Dzink-Fox, M.Chen, and S.B.Levy. 2001. Genetic characterization of highly fluoroquinolone-resistant clinical *Escherichia coli* strains from China: role of *acrR* mutations. *J.Antimicrob. Agents Chemother.* 45:1515-1521.

Wang,M., J.H.Tran, G.A.Jacoby, Y.Zhang, F.Wang, and D.C.Hooper. 2003. Plasmid-mediated quinolone resistance in clinical isolates of *Escherichia coli* from Shanghai, China. *J.Antimicrob. Agents Chemother.* 47:2242-2248.

Warren,J.W., E.Abrutyn, J.R.Hebel, J.R.Johnson, A.J.Schaeffer, and W.E.Stamm. 1999. Guidelines for antimicrobial treatment of uncomplicated acute bacterial cystitis and acute pyelonephritis in women. Infectious Diseases Society of America (IDSA). *Clin. Infect. Dis.* 29:745-758.

Watts,A. and P.J.Spooner. 1991. Phospholipid phase transitions as revealed by NMR. *Chem. Phys. Lipids* 57:195-211.

- Wise,R., J.M.Andrews, G.Marshall, and G.Hartman. 1999. Pharmacokinetics and inflammatory-fluid penetration of moxifloxacin following oral or intravenous administration. *J.Antimicrob. Agents Chemother.* 43:1508-1510.
- Wise,R., D.Lister, C.A.M.Mcnulty, D.Griggs, and J.M.Andrews. 1986. The Comparative Pharmacokinetics of 5 Quinolones. *J.Antimicrob. Agents Chemother.* 18:71-81.
- Wittebort,R.J., A.Blume, T.H.Huang, S.K.Dasgupta, and R.G.Griffin. 1982. C-13 Nuclear Magnetic-Resonance Investigations of Phase-Transitions and Phase-Equilibria in Pure and Mixed Phospholipid-Bilayers. *Biochemistry* 21:3487-3502.
- Wolkers,F.W., L.M. Crowe, N.M.Tsvetkova, F. Tablin, and J.H. Crowe. 2002. In Situ assessment of erythrocyte membrane properties during cold storage. *Mol.Membr.Biol.* 19:59-65.
- Yeagle,P.L., W.C.Hutton, C.H.Huang, and R.B.Martin. 1976. Structure in the polar head region of phospholipid bilayers: A ³¹P [1H] nuclear Overhauser effect study. *Biochemistry* 15:2121-2124.
- Yoshida,H., M.Bogaki, M.Nakamura, and S.Nakamura. 1990. Quinolone resistance-determining region in the DNA gyrase gyrA gene of Escherichia coli. *J.Antimicrob. Agents Chemother.* 34:1271-1272.
- Yu,X., G.L.Zipp, and G.W.Davidson, III. 1994. The effect of temperature and pH on the solubility of quinolone compounds: estimation of heat of fusion. *Pharm. Res.* 11:522-527.

- Zhang,L., X.Z.Li, and K.Poole. 2001. Fluoroquinolone susceptibilities of efflux-mediated multidrug-resistant *Pseudomonas aeruginosa*, *Stenotrophomonas maltophilia* and *Burkholderia cepacia*. *J.Antimicrob. Agents Chemother.* 48:549-552.
- Zhang,Y., Y.Chen, and G.Jin. 2010. PEGylated phospholipid membrane on polymer cushion and its interaction with cholesterol. *Langmuir* 26:11140-11144.
- Zhong,Q., D.Inniss, K.Kjoller, and V.B.Elings. 1993. Fractured Polymer Silica Fiber Surface Studied by Tapping Mode Atomic-Force Microscopy. *Surf. Sci.* 290:L688-L692.
- Zidovetzki,R., I.W.Sherman, A.Atiya, and H.De Boeck. 1989. A nuclear magnetic resonance study of the interactions of the antimalarials chloroquine, quinacrine, quinine and mefloquine with dipalmitoylphosphatidylcholine bilayers. *Mol. Biochem. Parasitol.* 35:199-207.

